

RESEARCH TECHNICAL REPORT
*Sprinkler Performance under
Non-Sloped Obstructed
Ceiling Construction*



Sprinkler Performance under Non-Sloped Obstructed Ceiling Construction

Prepared by

Prateep Chatterjee

FM Global

1151 Boston-Providence Turnpike
Norwood, MA 02062

December 2018

Project ID 0003059742

Disclaimer

The research presented in this report, including any findings and conclusions, is for informational purposes only. Any references to specific products, manufacturers, or contractors do not constitute a recommendation, evaluation or endorsement by Factory Mutual Insurance Company (FM Global) of such products, manufacturers or contractors. FM Global does not address life, safety, or health issues. The recipient of this report must make the decision whether to take any action. FM Global undertakes no duty to any party by providing this report or performing the activities on which it is based. FM Global makes no warranty, express or implied, with respect to any product or process referenced in this report. FM Global assumes no liability by or through the use of any information in this report.

Executive Summary

Industrial facilities with obstructed ceiling construction are commonly found worldwide. This type of construction is defined in FM Global Loss Prevention Data Sheet (DS) 2-0, *Installation Guidelines for Automatic Sprinklers*ⁱ, as a ceiling assembly forming channels that cannot hold more than one sprinkler branch line. The hot gases produced during a fire event therefore cannot reach the nearest four ceiling-level sprinklers anywhere within a single channelⁱ. The current guidelines included in DS 2-0ⁱ and NFPA 13ⁱⁱ for the installation of ceiling sprinklers in the presence of obstructed ceiling construction are supported by limited test data. Also, concerns have been raised as to whether sprinklers will activate in a timely fashion providing control of fire spread when they are not installed within every channel formed by the obstructed ceiling construction. Therefore, determining the installation guidelines for ceiling-level sprinklers in the presence of obstructed ceiling construction is needed.

The present study was conducted to understand and quantify the impact of obstructed ceiling construction on sprinkler protection under non-sloped ceilings through both numerical simulations and supporting full-scale fire testing. Several kinds of obstructed ceiling construction are used in warehouses, e.g., beams, metallic purlins and girders, and concrete tees. However, for this study, All Metal Building Structure (AMBS) type construction was considered. In AMBS, purlins and girders are primarily present below the ceiling. AMBS construction is commonly found in North American warehouses. The study considered scenarios involving fast- and slow-growing fires and the use of quick-response, ordinary temperature (QR/OT) and standard-response, high temperature (SR/HT) sprinklers.

Numerical modeling and large-scale testing were conducted in the present study. The parameters considered include the following: the effect of multiple types of ceiling structural members (presence of purlins and girders), as well as various dimensions and separation distances of the ceiling structural members relative to the sprinklers. The study was divided into two parts:

1. A numerical modeling effort using FireFOAMⁱⁱⁱ to evaluate sprinkler activation times and patterns with large-scale fires as plume sources. Results from this part of the study were used to develop a large-scale testing plan.
2. Large-scale fire tests conducted using commonly found warehouse commodities (Cartoned Unexpanded Plastic [CUP] and Unexpanded Uncartoned Plastic [UUP]). The results from the tests and the modeling study are used to develop recommendations for future DS 2-0ⁱ updates.

ⁱ FM Global Data Sheet 2-0, *Installation Guidelines for Automatic Sprinklers*, FM Global, January 2014.

ⁱⁱ NFPA 13: Standard for the Installation of Sprinkler Systems, National Fire Protection Association, 2016.

ⁱⁱⁱ FireFOAM. [Online]. <http://www.fmglobal.com/modeling>

From the range of conditions explored in numerical modeling and large-scale testing, major trends involving the principal parameters were identified. They are summarized below.

- For the CUP commodity, modeling results showed that activations of the central sprinklers (i.e., ones close to the ignition region) are not adversely affected by the presence of purlins of a depth of ≤ 610 mm (24 in.).
- Three large-scale tests were conducted using the CUP commodity with the testing parameters developed from modeling results. Purlin depths of 300–610 mm (12–24 in.) were selected based on the modeling input. Compared to the four sprinkler activations in a CUP baseline test conducted earlier with an unobstructed ceiling, five–six central sprinkler activations occurred in the obstructed ceiling tests (all within 6–11 s intervals) and fire spread was successfully controlled. Sprinkler skipping did not occur unlike in the baseline test and considerably less commodity damage was observed in all three tests.
- To overcome the potential of spray impingement when sprinklers are placed inside deep channels formed by purlins, modeling and testing results recommended lowering the sprinkler links from a DS 2-0 maximum permissible depth of 430 mm (17 in.) for QR/OT sprinklers installed below unobstructed ceilings¹ to a maximum of 760 mm (30 in.) for 610 mm (24 in.) deep purlins (i.e., 150 mm or 6 in. below the bottom edge of the purlins). For the 760 mm (30 in.) link distance, the average activation times were found to be earlier than in the case of sprinklers located 430 mm (17 in.) under unobstructed ceilings. A similar observation was also made for the SR/HT sprinklers. Therefore, for purlin depths >430 mm (17 in.) for QR/OT sprinklers and >330 mm (13 in.) for SR/HT sprinklers, a general recommendation was made for the sprinkler links to be placed on a plane below the bottom of the purlins, up to a distance of 150 mm (6 in.).

Both the modeling results and large-scale tests showed that purlin depths of ≤ 300 mm (12 in.) do not adversely affect the activation times of the central sprinklers for the CUP commodity, which involves fast fire growth rates. No significantly biased sprinkler activation patterns due to flow confinement in the purlin channels (“flow channeling” effect) was observed. Flow channeling was, however, observed in the modeling results and in tests conducted with purlin depths of 460 mm (18 in.) and 610 mm (24 in.). This occurrence could have an adverse effect on the sprinkler activation pattern away from the fire source, a fact that would be of concern for conditions when the central sprinklers are unable to arrest fire spread.

- For the UUP commodity, which involves an initially slow fire growth rate, modeling showed that the flow channeling effect caused biased activation patterns to develop below the central purlin channels. In addition, early perimeter sprinkler activations also occurred due to hot gas accumulation near the outside girders. Flow channeling and early perimeter sprinkler activations were also observed in a large-scale test involving the UUP commodity and 610 mm (24 in.) purlins.

- For purlin depths >300 mm (12 in.), modeling using the UUP commodity showed that closing the purlin channel gaps above the girder locations reduces the flow channeling effect, resulting in symmetric activation patterns.

After analyzing the results from the large-scale tests and the modeling study, the following general recommendations are made toward a future update of the DS 2-0ⁱ sprinkler protection designs for non-sloped ceilings in the presence of obstructed ceiling construction:

1. A ceiling with purlins of ≤ 300 mm (12 in.) depth can be considered of unobstructed type. The existing guidance in the current DS 2-0ⁱ for purlins of 100 mm (4 in.) remains applicable and can be extended to purlins of 300 mm (12 in.) depth.
2. For purlin depths >430 mm (17 in.) in case of QR/OT sprinklers or >330 mm (13 in.) for SR/HT sprinklers, links could be placed on a plane at a maximum distance of 150 mm (6 in.) below the bottom edge of the purlins. This recommendation is valid for a maximum purlin depth of 610 mm (24 in.).
3. For purlin depths ≤ 610 mm (24 in.), sprinklers need not be installed in every purlin channel in contrast to the current guidelines provided in DS 2-0ⁱ. Due to the strong channeling effect observed in the modeling results and the tests for purlin depths ≥ 460 mm (18 in.), it is recommended that vertical barriers be installed to close the purlin channels in order to reduce biased sprinkler activation patterns. Based on modeling results, a maximum closed purlin channel length of 7.6 m (25 ft) is recommended.

Abstract

An investigation based on numerical simulations was conducted to facilitate the understanding of protection challenges associated with the presence of obstructed ceiling construction (purlins and girders) on non-sloped/horizontal ceilings. The simulations were conducted using the FireFOAM computational fluid dynamics (CFD) code. Ceiling jets resulting from growing fires of Cartoned Unexpanded Plastic (CUP) and Unexpanded Uncartoned Plastic (UUP) commodities were simulated to investigate the effect of the obstructed ceiling construction on sprinkler activations. For quick-response, ordinary temperature and standard-response, high temperature sprinklers, simulation results show that purlins of 610 mm (24 in.) depth will not cause significant delays in the activation of the first ring of ceiling sprinklers. However, the same analysis showed that, for purlin depths ≥ 460 mm (18 in.), significant channeling of the ceiling jet occurs. Using modeling, mitigation of the channeling effect was shown to be possible by closing the purlin channel gaps above the girder locations. Large-scale fire tests conducted with the CUP and UUP commodities confirmed the observations from the modeling study: 610 mm (24 in.) purlins were found not to affect the activation time and pattern of the sprinklers closest to the ignition location for the CUP commodity. However, in three tests with the CUP and UUP commodities where purlin depths were ≥ 460 mm (18 in.), a strong channeling of the ceiling jet was observed in the central channels. In the UUP test, biased sprinkler activations occurred below the central purlin channels due to the flow channeling effect. Based on the modeling and large-scale test results, recommendations are made to update FM Global Loss Prevention Data Sheet (DS) 2-0, *Installation Guidelines for Automatic Sprinklers*.

Acknowledgments

Several people contributed toward the successful completion of the study. Mr. Andre Mierzwa is sincerely thanked for providing key technical feedback during the initiation of the project. Mr. Weston Baker provided input toward selection of parameters and continually gave feedback on the modeling and testing results. His contributions are gratefully acknowledged. Thanks are due to Mr. Richard Davis for help in identifying relevant ceiling structural designs. Dr. Yi Wang is sincerely thanked for providing key technical feedback, constant support in making modeling and testing resources available, and for his thorough review of documentation without which the project would not have progressed in a timely manner. Dr. Karl Meredith was available for discussions throughout the duration of the project and provided editorial feedback. His many contributions are greatly appreciated. Messrs. Seth Sienkiewicz, Benjamin Ditch, Stephen D’Aniello, and Dr. Yogish Gopala are thanked for their help with large-scale test preparation. Dr. Yibing Xin is acknowledged for providing free-burn test data subsequently used in selected simulations. The FM Global Research Campus personnel, specifically Mr. Jeff Chaffee and the Large Burn Laboratory crew including Messrs. Michael Racicot and Michael Skidmore, are thanked for their considerable help in conducting the large-scale tests. Drs. Sergey Dorofeev and Francesco Tamanini are acknowledged for providing their technical feedback. Dr. Tamanini is also thanked for his guidance on post-processing the large-scale test data.

Table of Contents

Executive Summary.....	i
Abstract.....	iv
Acknowledgments.....	v
Table of Contents.....	vi
List of Figures	ix
List of Tables	xiv
1. Introduction	1
1.1 Literature Survey.....	4
1.2 Objectives.....	5
1.3 Technical Approach.....	5
2. Numerical Modeling	8
2.1 Model Details	8
2.1.1 FireFOAM Solver	8
2.1.2 Mesh Generation	8
2.2 Fire Growth Model.....	9
2.3 Sprinkler Activation Setup.....	11
3. Numerical Modeling Results and Discussion	13
3.1 CUP Simulations	13
3.1.1 Ceiling Jet in the Presence of Obstructed Ceiling Construction	13
3.1.2 Quick-Response, Ordinary Temperature Sprinklers	18
3.1.2.1 Sprinkler Activation Times.....	18
3.1.2.2 Effect of Sprinkler Link Distance	23
3.1.2.3 Effect of Ceiling Clearance	26
3.1.2.4 Effect of Purlin Separation Distance	28
3.1.2.5 Effect of Girder Separation Distance	28
3.1.2.6 Offset Sprinkler Arrangement	31
3.1.3 Standard-Response, High Temperature Sprinklers.....	33
3.2 UUP Simulations.....	35
3.2.1 Weak Plume Ceiling Jet.....	35
3.2.2 Sprinkler Activation Sequence	36
3.3 Summary	40
3.4 Large-scale Testing Recommendations	42

4.	Large-scale Testing Results and Discussion	45
4.1	Test Parameters	45
4.1.1	Test Commodities	47
4.1.2	Automatic Sprinkler Protection	47
4.1.3	Test Setup	48
4.1.4	Storage Arrangement.....	49
4.1.5	Ignition	49
4.2	Recording and Instrumentation.....	49
4.3	Test Evaluation Criteria.....	51
4.4	Summary of Test Results.....	52
4.5	Test #1 Results	54
4.5.1	Highlights	54
4.5.2	Results and Damage Assessment.....	54
4.6	Test #2 Results	57
4.6.1	Highlights	57
4.6.2	Results and Damage Assessment.....	57
4.7	Test #3 Results	60
4.7.1	Highlights	60
4.7.2	Results and Damage Assessment.....	60
4.8	Test #4 Results	63
4.8.1	Highlights	63
4.8.2	Results and Damage Assessment.....	63
4.9	Ceiling Level Gas Temperatures.....	66
4.10	Comparison against Baseline Test Results.....	71
4.11	Summary	74
5.	Conclusions and Recommendations.....	76
5.1	Conclusions	76
5.2	Recommendations	78
	References	79
	Appendix A. Fire Chronology	81
A.1	Test #1.....	81
A.2	Test #2.....	82
A.3	Test #3.....	83
A.4	Test #4.....	84
	Appendix B. Selected Testing Photographs.....	85

B.1	Test #1.....	85
B.2	Test #2.....	88
B.3	Test #3.....	91
B.4	Test #4.....	94
Appendix C.	FireFOAM Modeling Details	97

List of Figures

1-1: Obstructed ceiling construction (e.g., purlins and girders) in (a) the absence, and (b) the presence of insulation.....	2
1-2: Ceiling structural elements: (a) truss structures that do not provide significant obstruction to flow, and (b) examples of C- and Z-shaped purlins with a girder present below them.	3
1-3: Example of sprinklers installed below obstructed ceiling construction with a depth less than or equal to 530 mm (21 in.) [1].....	4
1-4: Drawings (not to scale) showing a 3-tier-high rack storage array as a fire source, the clearance height above the top of the array (h) and the ceiling height (H) from the floor: (a) front view showing purlins of depth d_p , spaced w_p width apart, and (b) elevation view showing girders below the purlins, of depth d_g , spaced w_g width apart.....	6
2-1: Computational mesh showing a ceiling located 3.0 m (10 ft) above the CUP rack-storage array. Purlins of a depth of 610 mm (24 in.), separated by 1.5 m (5 ft), and a 610 mm (24 in.) deep girder are also shown.....	9
2-2: Fire growth over the CUP rack-storage array. Flames are impinging on a horizontal ceiling with no obstructed ceiling construction present.....	10
2-3: Modeled HRR (chemical and convective) and radiant fraction variation as a function of time for the 2 x 2 x 3 array of CUP commodity.	10
2-4: Prescribed model chemical HRR as a function of time for the UUP commodity.....	11
3-1: Ceiling jet depicted by CO ₂ contours ($Y_{CO_2} = 0.02-0.04$) shown under a ceiling located 3.0 m (10 ft) above the CUP rack-storage array. The ceiling does not have any obstructed construction in the form of girders or purlins.	14
3-2: Ceiling jet depicted by CO ₂ contours ($Y_{CO_2} = 0.02-0.04$) under a ceiling located 3.0 m (10 ft) above the CUP rack-storage array. The ceiling has 100 mm (4 in.) deep purlins separated by 1.5 m (5 ft) and 610 mm (24 in.) deep girders separated by 7.6 m (25 ft).	15
3-3: Ceiling jet depicted by CO ₂ contours ($Y_{CO_2} = 0.02-0.04$) under a ceiling located 3.0 m (10 ft) above the CUP rack-storage array. The ceiling has 300 mm (12 in.) deep purlins separated by 1.5 m (5 ft) and 610 mm (24 in.) deep girders separated by 7.6 m (25 ft).	16
3-4: Ceiling jet depicted by CO ₂ contours ($Y_{CO_2} = 0.02-0.04$) under a ceiling located 3.0 m (10 ft) above the CUP rack-storage array. The ceiling has 610 mm (24 in.) deep purlins separated by 1.5 m (5 ft) and 610 mm (24 in.) deep girders separated by 7.6 m (25 ft).	17
3-5: Activation time contours for QR/OT sprinkler links at 430 mm (17 in.) below a ceiling located 3.0 m (10 ft) above the CUP rack-storage array in (a) the absence of obstructed ceiling construction, and in the presence of 610 mm (24 in.) deep girders separated by 7.6 m (25 ft) and purlins with a separation distance of 1.5 m (5 ft) and depths of (b) 100 mm (4 in.), (c) 200 mm (8 in.), and (d) 300 mm (12 in.). Discrete locations of sprinkler links arranged in a 3.0 m x 3.0 m (10 ft x 10 ft) spacing with one sprinkler centered on the CUP array are also shown with the corresponding activation times.	20

3-6: Activation time contours for QR/OT sprinkler links at 430 mm (17 in.) below a ceiling located 3.0 m (10 ft) above the CUP rack-storage array in the presence of 610 mm (24 in.) deep girders separated by 7.6 m (25 ft) and purlins with a separation distance of 1.5 m (5 ft) and depths of (a) 360 mm (14 in.), (b) 460 mm (18 in.), (c) 530 mm (21 in.), and (d) 610 mm (24 in.).	21
3-7: QR/OT sprinkler activation times at 430 mm (17 in.) below a ceiling located 3.0 m (10 ft) above the CUP rack-storage array as a function of purlin depth along (a) central purlins channel, and (b) in a perpendicular to the purlin direction. Purlins are separated by 1.5 m (5 ft) and girders by 7.6 m (25 ft).	23
3-8: Activation time contours for QR/OT sprinkler links below a ceiling located 3.0 m (10 ft) above the CUP rack-storage array in the presence of 610 mm (24 in.) deep girders separated by 7.6 m (25 ft) and purlins with a separation distance of 1.5 m (5 ft) with a purlin depth of 530 mm (21 in.), sprinkler links at (a) 530 mm (21 in.), and (b) 690 mm (27 in.) below the ceiling, and with a purlin depth of 610 mm (24 in.), sprinkler links at (c) 610 mm (24 in.), and (d) 760 mm (30 in.) below the ceiling.	25
3-9: QR/OT sprinkler activation times at various sprinkler link distances below a ceiling located 3.0 m (10 ft) above the CUP rack-storage array as functions of purlin depth along (a) the central purlins channel, and (b) in a perpendicular to the purlin direction. Purlins are separated by 1.5 m (5 ft) and girders by 7.6 m (25 ft).	26
3-10: Activation time contours for QR/OT sprinkler links in the presence of 610 mm (24 in.) deep girders separated by 7.6 m (25 ft), purlins with a separation distance of 1.5 m (5 ft) and a depth of 360 mm (14 in.), and sprinkler links 430 mm (17 in.) below the ceiling with a ceiling clearance of (a) 3.0 m (10 ft), and (b) 1.5 m (5 ft).	27
3-11: QR/OT sprinkler activation times at 430 mm (17 in.) below a ceiling located 1.5 m (5 ft) and 3.0 m (10 ft) above the CUP rack-storage array as functions of purlin depth along (a) the central purlins channel, and (b) in a perpendicular to the purlins direction. Purlins are separated by 1.5 m (5 ft) and girders by 7.6 m (25 ft).	27
3-12: Activation time contours for QR/OT sprinkler links below a ceiling located 3.0 m (10 ft) above the CUP rack-storage array in the presence of 610 mm (24 in.) deep girders separated by 7.6 m (25 ft) and purlins with a separation distance of 3.0 m (10 ft) and a depth of (a) 100 mm (4 in.), (b) 360 mm (14 in.), and (c) 610 mm (24 in.). Sprinkler links are 430 mm (17 in) below the ceiling.	29
3-13: Effect of purlin separation distance on QR/OT sprinkler activation times at 430 mm (17 in.) below a ceiling located 3.0 m (10 ft) above the CUP rack-storage array as a function of purlin depth along (a) the central purlins channel, and (b) in a perpendicular to the purlins direction. Purlins are separated by 1.5 m (5 ft) and 3.0 m (10 ft) and girders by 7.6 m (25 ft).	30
3-14: Activation time contours for QR/OT sprinkler links below a ceiling located 3.0 m (10 ft) above the CUP rack-storage array in the presence of 610 mm (24 in.) deep girders separated by 12.2 m (40 ft), purlins with a separation distance of 1.5 m (5 ft) and a depth of 360 mm (14 in.), and sprinkler links 430 mm (17 in.) below the ceiling. Discrete locations of sprinkler links arranged in a 3.0 m × 3.35 m (10 ft × 11 ft) spacing.	30
3-15: Effect of girder separation distance on QR/OT sprinkler activation times at 430 mm (17 in.) below a ceiling located 3.0 m (10 ft) above the CUP rack-storage array as a function of purlin depth along (a) central purlins channel, and (b) in a perpendicular to the purlins direction. Purlins are separated by 1.5 m (5 ft) and girders by 7.6 m (25 ft) and 12.2 m (40 ft).	31

3-16: Activation time contours for QR/OT sprinkler links below a ceiling located 3.0 m (10 ft) above the CUP rack-storage array in the presence of 610 mm (24 in.) deep girders separated by 7.6 m (25 ft) and purlins with a separation distance of 1.5 m (5 ft) and a depth of (a) 300 mm (12 in.), (b) 460 mm (18 in.), and (c) 610 mm (24 in.). Sprinkler links are 430 mm (17 in.) below the ceiling. Discrete sprinkler locations correspond to an offset sprinkler arrangement with 3.0 m × 3.0 m (10 ft × 10 ft) spacing.	32
3-17: Activation time contours for SR/HT sprinkler links at 330 mm (13 in.) below a ceiling located 3.0 m (10 ft) above the CUP rack-storage array in (a) the absence of obstructed ceiling construction, and in the presence of 610 mm (24 in.) deep girders separated by 7.6 m (25 ft) and purlins with a separation distance of 1.5 m (5 ft) and a depth of (b) 300 mm (12 in.), (c) 460 mm (18 in.), and (d) 610 mm (24 in.).	34
3-18: Activation time contours for SR/HT sprinkler links below a ceiling located 3.0 m (10 ft) above the CUP rack-storage array in the presence of 610 mm (24 in.) deep girders separated by 7.6 m (25 ft) and purlins with a separation distance of 1.5 m (5 ft) with a purlin depth of 610 mm (24 in.). The sprinkler links are (a) 610 mm (24 in.), and (b) 760 mm (30 in.) below the ceiling.	35
3-19: Ceiling jet at 375 s depicted by CO ₂ contours ($Y_{CO_2} = 0.02-0.04$) under a ceiling located 7.6 m (25 ft) above the UUP fire source in (a) the absence of obstructed ceiling construction, and in the presence of 610 mm (24 in.) deep girders separated by 7.6 m (25 ft) and purlins with a separation distance of 1.5 m (5 ft) and a depth of (b) 200 mm (8 in.), (c) 300 mm (12 in.), and (d) 610 mm (24 in.).	36
3-20: Activation time contours for QR/OT sprinkler links at 430 mm (17 in.) below a ceiling located 3.0 m (10 ft) above a UUP fire source in (a) the absence of obstructed ceiling construction, and in the presence of 610 mm (24 in.) deep girders separated by 7.6 m (25 ft) and purlins with a separation distance of 1.5 m (5 ft) and a depth of (b) 200 mm (8 in.), (c) 300 mm (12 in.), and (d) 610 mm (24 in.). Discrete locations of sprinkler links arranged in a 3.0 m × 3.0 m (10 ft × 10 ft) spacing are also shown with the corresponding activation times.	38
3-21: Ceiling jet at 395 s depicted by CO ₂ contours ($Y_{CO_2} = 0.01-0.04$) under a ceiling located 3.0 m (10 ft) above the UUP fire source with 610 mm (24 in.) deep purlins separated by 1.5 m (5 ft) and girders separated by 7.6 m (25 ft). The purlin channels are (a) open with 610 mm (24 in.) deep girders located below the purlins, and (b) closed by obstructing the top of the 610 mm (24 in.) girders.	39
3-22: Activation time contours for QR/OT sprinkler links at 430 mm (17 in.) below a ceiling located 3.0 m (10 ft) above a UUP fire source. Purlins are separated by 1.5 m (5 ft) and girders by 7.6 m (25 ft) with (a) 300 mm (12 in.), and (b) 460 mm (18 in.) deep purlins. Purlin channels are closed at the girder locations.	40
3-23: Activation time contours for QR/OT sprinkler links below a ceiling located 3.0 m (10 ft) above a UUP fire source in the presence of girders separated by 7.6 m (25 ft). Purlins with a separation distance of 1.5 m (5 ft) and a depth of 610 mm (24 in.) form (a) open channels, and (b) channels closed at the girder locations. Sprinkler links are located 610 mm (24 in.) below the ceiling.	41
3-24: Flowchart for determining the sequence of the CUP large-scale tests.	44

4-1: Testing setup (not to scale) showing a 4-tier-high CUP rack storage array as a fire source with two target arrays (separated by 1.2 m or 4 ft), 610 mm (24 in.) tall girders spaced 7.6 m (25 ft) apart, and purlins of depth d_p separated by 1.5 m (5 ft): (a) front view showing purlins, and (b) side view showing girders present below the purlins.	46
4-2: FM Global standard (a) CUP, and (b) UUP commodities	47
4-3: Plan view of the test array (CUP commodity) with ignition placed between two sprinklers. The sprinklers, piping, purlin, and girder distances relative to the test array are shown.	48
4-4: Photographs of test arrays: (a) CUP Test #3, and (b) UUP Test #4.	50
4-5: Camera locations and types in the three tests.	51
4-6: Sprinkler operation pattern and top view of damage assessment for Test #1.	55
4-7: Damage assessment on the main array for Test #1.....	55
4-8: Temperatures of the ceiling steel angle for Test #1. The thermocouples on the steel angle are named with a prefix of STLTC (Steel Thermocouple), followed by their placement relative to the ignition location (e.g., IGN stands for thermocouple above the ignition location, 06E means the thermocouple was offset by 6 in. toward the east, etc.).....	56
4-9: Water pressure measured at the main water supply header duct for Test #1.	56
4-10: Sprinkler operation pattern and top view of damage assessment for test #2.	58
4-11: Damage assessment on the main array for Test #2.....	58
4-12: Temperatures of the ceiling steel angle for Test #2.	59
4-13: Water pressure for Test #2.	59
4-14: Sprinkler operation pattern and top view of damage assessment for Test #3.	61
4-15: Damage assessment on the main array for Test #3.....	61
4-16: Temperatures of the ceiling steel angle for Test #3.	62
4-17: Water pressure for Test #3.	62
4-18: Sprinkler operation pattern and top view of damage assessment for Test #4.	64
4-19: Damage assessment on the main array for Test #4.....	64
4-20: Temperatures of the ceiling steel angle for Test #4.	65
4-21: Water pressure for Test #4.	65
4-22: Test #1 ceiling temperature contours shown in 15 s increments.....	67
4-23: Test #2 ceiling temperature contours shown in 15 s increments.....	68
4-24: Test #3 ceiling temperature contours shown in 15 s increments.....	69
4-25: Test #4 ceiling temperature contours shown in 60 s increments.....	70
4-26: Activation times plotted as functions of number of activations for tests with and without obstructed ceiling construction for the CUP tests.	71
4-27: Comparison of sprinkler operation patterns for tests conducted with (a) unobstructed ceiling, and (b) obstructed ceiling (average activation times for Tests #1–3: purlin depths were between 300–610 mm or 12–24 in.). The commodity was CUP and the storage arrangements were identical in all tests.	72
4-28: Activation times plotted as functions of number of activations for tests with and without obstructed ceiling construction for the UUP tests.....	74

4-29: Comparison of sprinkler operation pattern for tests conducted with (a) unobstructed ceiling, and (b) obstructed ceiling (610 mm or 24 in. deep purlins). The commodity was UUP and the storage arrangements were identical in the two tests.....	75
B-1: Test #1 array at 1 min after ignition.	85
B-2: Test #1 array at 1 min 15 s after ignition.	85
B-3: Test #1 array at 1 min 30 s after ignition.	86
B-4: Test #1 array at 1 min 45 s after ignition.	86
B-5: Test #1 post-test photograph of the east face of the main array showing fire damage.	87
B-6: Test #2 array at 1 min after ignition.	88
B-7: Test #2 array at 1 min 15 s after ignition.	88
B-8: Test #2 array at 1 min 30 s after ignition.	89
B-9: Test #2 array at 1 min 45 s after ignition.	89
B-10: Test #2 post-test photograph of the east face of the main array showing fire damage.	90
B-11: Test #3 array at 1 min after ignition.	91
B-12: Test #3 array at 1 min 15 s after ignition.	91
B-13: Test #3 array at 1 min 30 s after ignition.	92
B-14: Test #3 array at 1 min 45 s after ignition.	92
B-15: Test #3 post-test photograph of the east face of the main array showing fire damage.	93
B-16: Test #4 array at 5 min after ignition.	94
B-17: Test #4 array at 6 min after ignition.	94
B-18: Test #4 array at 7 min after ignition.	95
B-19: Test #4 array at 8 min after ignition.	95
B-20: Test #4 post-test photograph of the east face of the main array showing fire damage. Close-up of the damage area is shown in the inset.	96

List of Tables

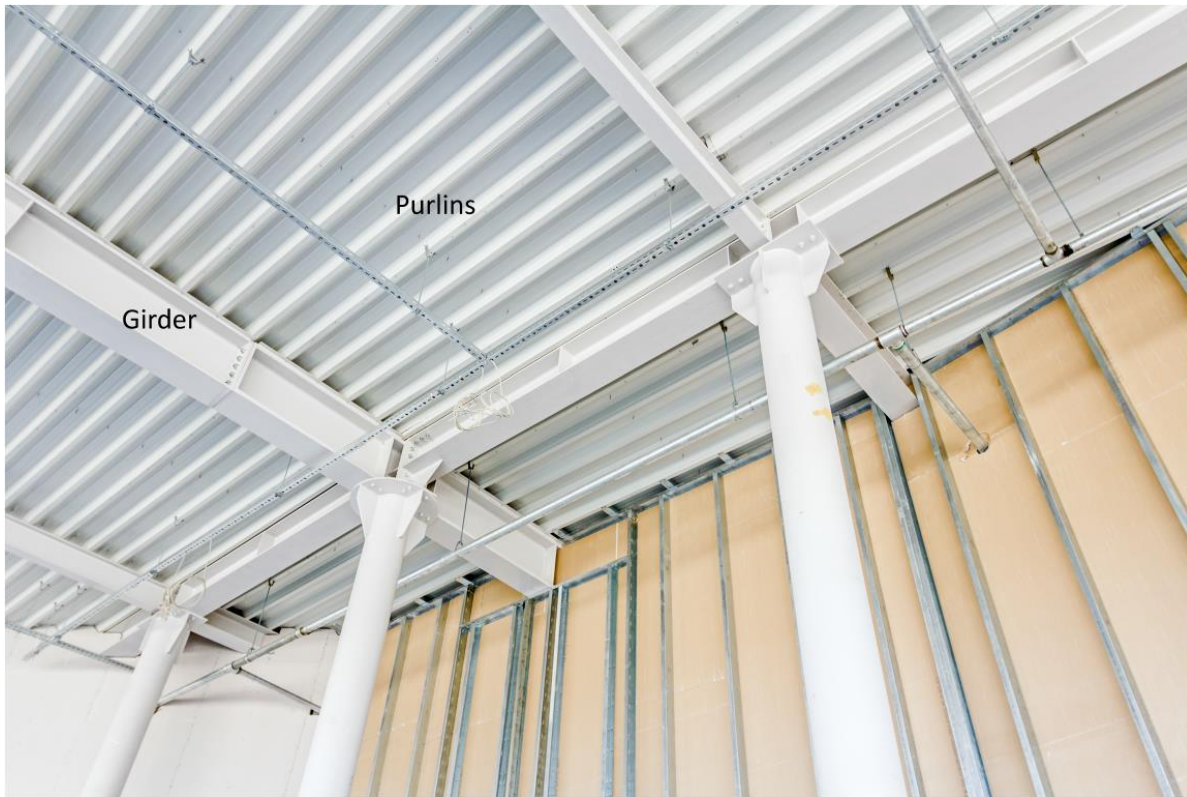
1-1: Parameters for the obstructed ceiling construction simulations.	7
2-1: List of sprinkler activation parameters used in the present study.	12
3-1: Activation times for the eight QR/OT sprinklers surrounding the ignition location. Three times are reported (in s): average for all eight locations, two locations in the central channel, and six locations in the outer two channels.	19
3-2: Activation times for the eight SR/HT sprinklers surrounding the ignition location. Three times are reported (in s): average for all eight locations, two locations in the central channel, and six locations in the outer two channels.	33
4-1: Parameters used in the obstructed ceiling construction tests.	46
4-2: Summary of test parameters and results for the CUP tests.	52
4-3: Summary of test parameters and results for the UUP tests.	53
4-4: Test performance comparison between baseline and obstructed ceiling construction tests (#1–3) for the CUP commodity.	71
4-5: Test performance comparison between baseline and the obstructed ceiling construction test (#4) for the UUP commodity.	73

1. Introduction

Industrial facilities with obstructed ceiling construction are commonly found worldwide (see Figure 1-1 for examples). Obstructed ceiling construction is defined in FM Global Loss Prevention Data Sheet (DS) 2-0, *Installation Guidelines for Automatic Sprinklers* [1], as a ceiling assembly forming channels that cannot hold more than one sprinkler branch line. The hot gases produced during a fire event therefore cannot reach the nearest four ceiling-level sprinklers anywhere within a single channel (see Figure 1-1 (a) for an example of channels formed by purlins). In this context, a channel consists of structural ceiling members that extend down from the ceiling at least 100 mm (4 in.), is less than 70% open in cross-sectional area, and has structural members spaced horizontally that would prevent two sprinkler branch lines from being installed within it. This type of construction is typically caused by the presence of purlins, girders, beams, and other similar types of structural roof supporting materials at the ceiling level. In some cases, the channels formed by the purlins are filled with insulation, as shown in Figure 1-1(b), effectively reducing the channel depth. Other construction elements, like truss structures shown in Figure 1-2(a), do not provide significant obstruction to the hot gas flow. Irrespective of the shape of the purlins popular in the industry, as can be observed in Figure 1-2(b), these structures tend to keep the flow of hot combustion products originating from fires confined in the channels, possibly delaying the activation of sprinklers. Other common ceiling assemblies that are considered obstructed ceiling construction use either steel beams or concrete tees. While the construction industry manufactures purlins in common depths ranging from 150 to 360 mm (6 to 14 in.), other ceiling assemblies, such as steel beams and concrete tees, are commonly deeper than 610 mm (24 in.). Trends in warehouses around the world are also toward using deeper purlins. To address the impact of obstructed ceiling construction on sprinkler operation, DS 2-0 [1] currently recommends that sprinklers be installed within every channel formed by obstructed ceiling construction for the following:

- **Non-storage sprinklers** – in case obstructions extend down more than 530 mm (21 in.) below the ceiling (see Section 2.1.3.2.4.2 in DS 2-0 for details), and
- **Storage sprinklers** – in case obstructions extend down more than 300 mm (12 in.) below the ceiling for quick-response type and more than 530 mm (21 in.) for standard-response type (see Section 2.2.3.4.2 in DS 2-0 for details).

When sprinklers are installed under ceilings with obstructed construction, but where the ceiling structural members do not extend more than 530 mm (21 in.) vertically, sprinklers are installed in a horizontal plane below the ceiling members (see Figure 1-3 for one example of the guidance provided in DS 2-0). The current guidelines included in DS 2-0 and NFPA 13 [2] for the installation of ceiling sprinklers in the presence of obstructed ceiling construction are supported by limited test data. Also, concerns have been raised as to whether sprinklers will activate in a timely fashion providing control of fire spread when they are not installed within every channel formed by obstructed ceiling construction. Therefore, determining the installation guidelines for ceiling-level sprinklers in the presence of obstructed construction is needed through both numerical simulations and supporting full-scale fire testing.



(a) Purlins and girders below the ceiling [3]

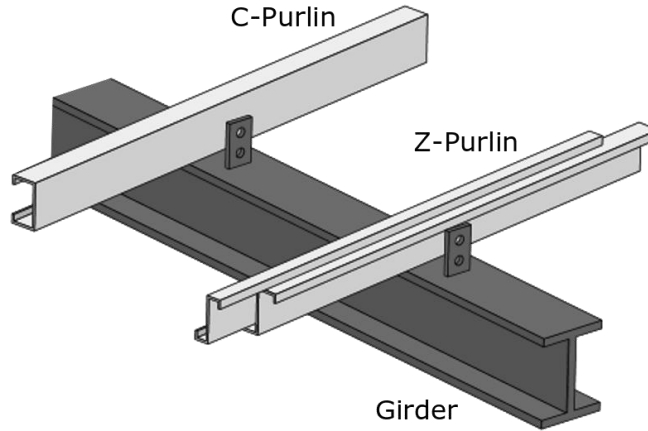


(b) Insulation present below the ceiling reduces the purlin channel depth [4]

Figure 1-1: Obstructed ceiling construction (e.g., purlins and girders) in (a) the absence, and (b) the presence of insulation.



(a) Truss structures present below the ceiling (unobstructed ceiling) [5]



(b) Types of purlins

Figure 1-2: Ceiling structural elements: (a) truss structures that do not provide significant obstruction to flow, and (b) examples of C- and Z-shaped purlins with a girder present below them.

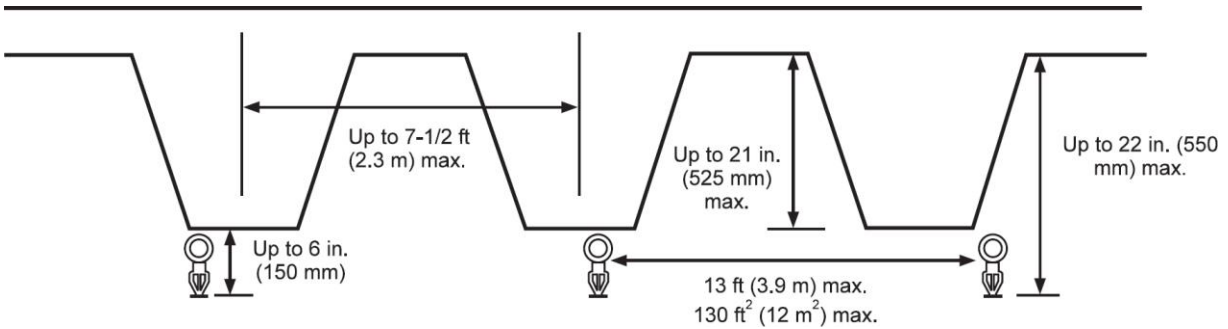


Figure 1-3: Example of sprinklers installed below obstructed ceiling construction with a depth less than or equal to 530 mm (21 in.) [1].

1.1 Literature Survey

FM Global recommendations for obstructions below ceilings have been made primarily from the standpoint of the effect of the obstructions on sprinkler discharge [6]. The effect on sprinkler activation times and patterns have been studied as well. The first study was conducted by Heskestad [7] evaluating thermal response of sprinklers by comparing ceiling jet temperature and velocity profiles for smooth and beamed ceilings. Heskestad observed that sprinkler activations for beamed ceilings would require considerably larger fire sizes. Delichatsios [8] developed a model to describe ceiling flows between adjacent beams and compared predicted temperature and velocity against experimental data. Delichatsios [7] further analyzed the effect of beams on the sprinkler activations and concluded that channeling of the ceiling jet between beams causes skewed activation patterns.

Heskestad conducted a series of reduced-scale (1:12.5) tests to identify beam (purlin) configurations that provided the greatest challenge to sprinkler water demand. A simulated Early Suppression-Fast Response (ESFR) sprinkler system and a fuel array simulating a full-scale array were used in the tests. Full-scale equivalent beam depths of 150–610 mm (6–24 in.) and spacings in the range of 0.38–3.0 m (1.25–10 ft), with or without the presence of girders were selected. The tests showed that the majority of the beamed configurations produced fewer sprinkler operations compared to the smooth ceiling tests. Inclusion of girders to the purlin configurations both increased and decreased the number of activations depending on the purlin depth. A worst-case scenario involving 610 mm (24 in.) deep beams on a 1.5 m (5 ft) spacing was identified.

Bill et al. [9] investigated fast-response residential sprinkler performance and concluded that fire protection is significantly challenged in the presence of beams below sloped ceilings.

Heskestad extended his previous reduced-scale study to investigate ESFR sprinkler response under sloped ceilings with 250 mm (10 in.) deep purlins over girders. Results for sprinkler activations were compared between horizontal and sloped ceiling configurations. Significantly more activations were observed in the presence of purlins compared to the smooth ceiling configurations.

Besides the smaller-scale studies conducted by Heskestad, none of the other studies have concentrated on determining the effect of various depths, separation distances, and geometries of ceiling structural members.

1.2 Objectives

The present study was conducted to understand and quantify the impact of obstructed ceiling construction on sprinkler protection under non-sloped ceilings. Numerical modeling was also conducted for obstructed sloped ceilings and has been documented separately in Ref. [10].

Several kinds of obstructed ceiling construction are used in warehouses, e.g., beams, metallic purlins and girders, and concrete tees (as shown in Figure 1-3). However, for this study, All Metal Building Structure (AMBS) type construction is considered. AMBS construction is commonly found in North American warehouses. In AMBS, purlins and girders are primarily present below the ceiling. The current study considers scenarios involving fast- and slow-growing fires and the use of quick-response, ordinary temperature (QR/OT) and standard-response, high temperature (SR/HT) sprinklers.

The parameters under consideration include the following: the effect of multiple types of ceiling structural members (presence of purlins and girders), as well as various dimensions and separation distances of the ceiling structural members relative to the sprinklers. The study was divided into two parts:

1. A numerical modeling effort using FireFOAM [11] to evaluate sprinkler activation times and patterns with large-scale fires as plume sources. Results from this part of the study were used to develop a fire testing plan.
2. Large-scale fire tests conducted using commonly found warehouse commodities (Cartoned Unexpanded Plastic [CUP] and Unexpanded Uncartoned Plastic [UUP]). The results from the tests and the modeling study are being used to develop recommendations for DS 2-0 updates.

1.3 Technical Approach

A survey of ceiling structural members was conducted with input from FM Global Engineering Standards. Based on the review, geometric details of obstructed ceiling construction (purlins and girders) were selected along with their spacing under non-sloped ceilings. The selected purlin depths ranged between 100 mm (4 in.) and 610 mm (24 in.). The range was chosen based on not only common purlin depths, but the depths of other common ceiling structural members, such as steel beams and concrete tees. The horizontal distance between purlins (the separation distance) was selected to be 1.5 m (5 ft) and 3.0 m (10 ft) as values which represent common separation distances between purlins and other similar ceiling structural members. Again, based on common ceiling structural members found in the industry, the girders depth was kept fixed at 610 mm (24 in.) and their horizontal separation distances were selected to be 7.6 m (25 ft) and 12.2 m (40 ft).

The numerical simulations involved the prediction of sprinkler activations due to ceiling jet development under non-sloped, obstructed ceiling construction resulting from growing fires. A fast fire growth

scenario was considered on a 3-tier-high (4.6 m or 15 ft) rack storage array of the CUP commodity. Ceiling structural members in the form of vertical beams were considered, while other details of the purlin geometries, as shown in Figure 1-2(b), were not included. It was assumed that the vertical sections of the purlins cause the primary obstruction to the ceiling jet. A slower-growing fire with a prescribed heat release rate (HRR) obtained from experimental data, representative of fire growth over UUP commodity, was also considered, replacing the CUP rack-storage array.

Figure 1-4 shows drawings of the computational setup of an unconfined, non-sloped ceiling with purlins and girders, located above a 3-tier-high rack storage arrangement of CUP commodity. Purlins present below the ceiling have depths d_p and are spaced w_p distance apart. The girder depth is d_g , which is fixed at 610 mm (24 in.), and girder separation distance is w_g . The depth, d_g , is measured from the bottom of the purlins since in industrial facilities girders are mostly installed below the purlins.

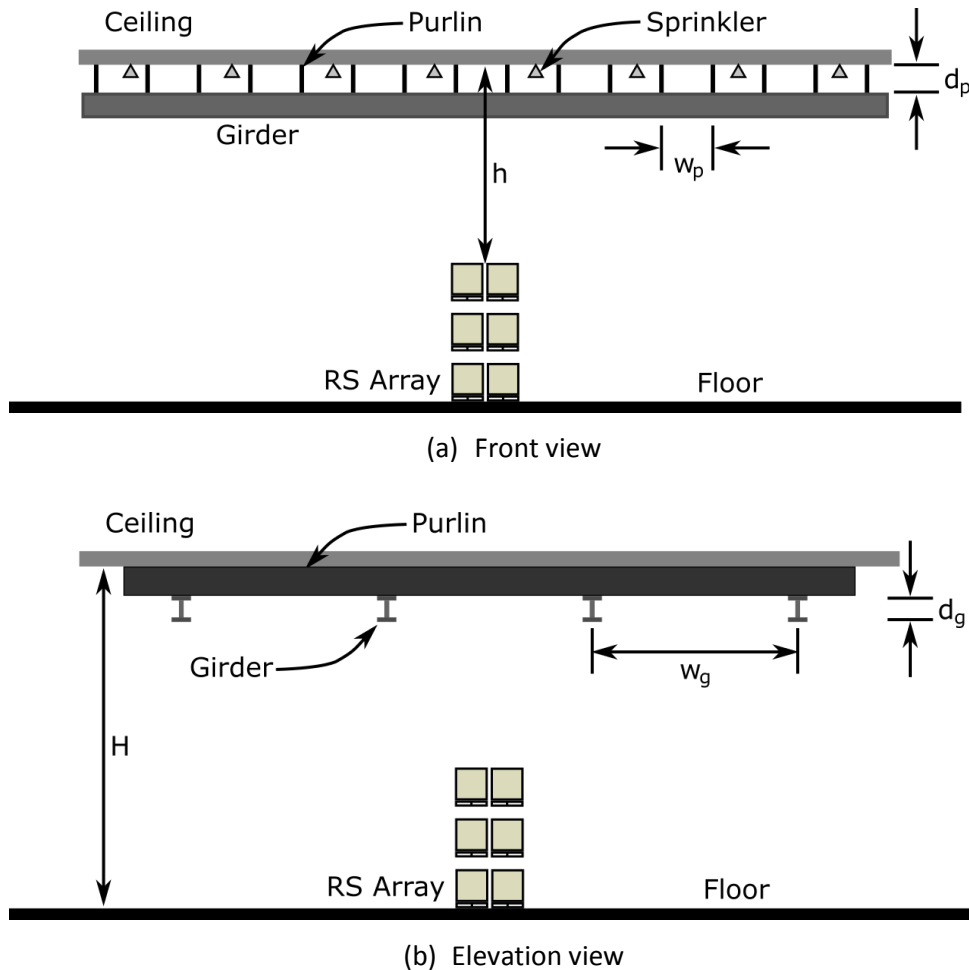


Figure 1-4: Drawings (not to scale) showing a 3-tier-high rack storage array as a fire source, the clearance height above the top of the array (h) and the ceiling height (H) from the floor: (a) front view showing purlins of depth d_p , spaced w_p width apart, and (b) elevation view showing girders below the purlins, of depth d_g , spaced w_g width apart.

A summary of the simulation parameters is included in Table 1-1 below.

Table 1-1: Parameters for the obstructed ceiling construction simulations.

Fire plume source	3-tier-high rack storage of CUP and prescribed HRR UUP fire
Ceiling heights (H)	7.6 m (25 ft) and 9.1 m (30 ft)
Ceiling clearance (h)	1.5 m (5 ft) and 3.0 m (10 ft) for the CUP commodity
Purlin depth (d_p)	100–610 mm (4–24 in.)
Purlin spacing (w_p)	1.5 m (5 ft) and 3.0 m (10 ft)
Girder depth (d_g)	610 mm (24 in.)
Girder spacing (w_g)	7.6 m (25 ft) and 12.2 m (40 ft)
Sprinkler RTI	30 (m-s) ^{0.5} (54 (ft-s) ^{0.5}), quick response and 119 (m-s) ^{0.5} (216 (ft-s) ^{0.5}), standard response
Activation temperatures	74°C (165°F) and 140°C (286°F)

Based on the simulation results, worst-case sprinkler activation scenarios were identified (e.g., skewness of activation patterns and maximum delay) and selection of ceiling height, commodity, and purlin depth and spacing were made for large-scale testing recommendations. A limited number of large-scale suppression tests were conducted to develop protection guidelines for obstructed ceiling construction. Based on the large-scale testing and modeling results, recommendations are made toward an update of DS 2-0.

2. Numerical Modeling

2.1 Model Details

Numerical simulations of fire growth and sprinkler activations below obstructed ceilings were conducted using FireFOAM, a computational fluid dynamics (CFD) code [11]. Details of the code, mesh generation, fire growth model, and sprinkler activation setup are provided below.

2.1.1 FireFOAM Solver

FireFOAM [11], which is based on the open-source framework OpenFOAM [12], is used in the current study. OpenFOAM supports unstructured meshes with cells of arbitrary shapes permitting flexibility in ceiling jet mesh generation [13]. FireFOAM includes models for large eddy simulation (LES) of buoyant turbulent diffusion combustion [14], pyrolysis [15], and radiation heat transfer [16]. Using FireFOAM, ceiling jets have been simulated for unconfined, smooth horizontal, and inclined ceilings. Temperature and velocity predictions in the ceiling jets have also been validated using experimental data [17] [18] [19].

Multiphase-flow aspects of fire suppression are also included in FireFOAM. A Lagrangian transport model is employed to simulate water droplets originating from a sprinkler, transporting through fire plumes, and impinging on burnt and/or unburnt surfaces. A response time index (RTI) model has been included and has been verified to give accurate estimates of sprinkler activation [20]. Actual delivered density (ADD) predictions have been made by the model [21] and suppression of rack-storage commodity has successfully been simulated [20] [22].

In the present study, the combustion, turbulent flow, and radiation models were used to simulate the fire plumes and the resulting ceiling jets. The pyrolysis model was applied to generate the spatiotemporally varying fuel mass loss rates from the CUP commodity (details available in Ref. [17]). Following the approach in Ref. [17], suppression simulations have not been conducted. FireFOAM version 2.2.x [11] has been used for the simulations.

2.1.2 Mesh Generation

The OpenFOAM version 3.0 mesh generation utility, *snappyHexMesh*, was used for mesh generation [13]. The *snappyHexMesh* utility generates three-dimensional meshes primarily composed of hexahedral volumes. The current set of meshes has been generated with the inclusion of Stereolithography (STL) geometries of boxes, pallets, and horizontal ceilings, including the purlins and girders.

The purlin and girder structures have been simplified and details present in the actual structures (e.g., C- and Z-shaped purlins, I-beam structure for girders, see Figure 1-2(b)) have not been included in the study, as such details will not significantly affect the flow dynamics. Instead, simplified vertical obstructions were considered: purlins were assumed to have 100 mm (4 in.) width, and girders were assumed to be 200 mm (8 in.) wide. Vertical depths of 100–610 mm (4–24 in.) for the purlins were considered, whereas the girders were generally kept at a fixed depth of 610 mm (24 in.). In some

simulations, girder depths greater than 610 mm (24 in.) were also considered. Details of the mesh generation steps are available in Ref. [17].

With increasing purlin depth, from 100 mm (4 in.) to 610 mm (24 in.), the total number of cells in the computational domain increased from ~2.6 million to ~4.1 million. The mesh resolution around the CUP rack-storage array was kept constant at 25 mm (1 in.), whereas the uniform mesh below the ceiling (down to 300–610 mm [12–24 in.] perpendicular distance) was kept at a 100 mm (4 in.) resolution. The mesh resolution around the purlins and girders was between 25 mm and 50 mm (1–2 in.). The plume region mesh was kept at a fixed resolution of 100 mm (4 in.).

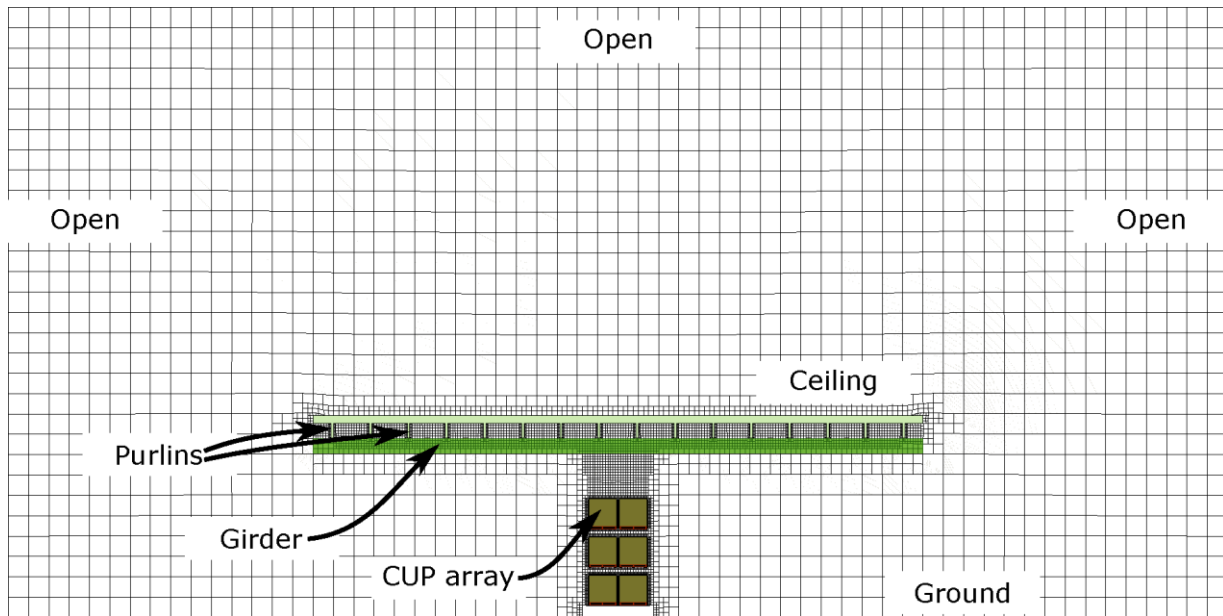


Figure 2-1: Computational mesh showing a ceiling located 3.0 m (10 ft) above the CUP rack-storage array. Purlins of a depth of 610 mm (24 in.), separated by 1.5 m (5 ft), and a 610 mm (24 in.) deep girder are also shown.

2.2 Fire Growth Model

The transient fire growth modeling over the CUP rack-storage array was conducted with the application of a pyrolysis model for the CUP commodity [23] (see Ref. [17] for the model description). Following the approach in Ref. [17], to expedite the simulation process in the current study, the pyrolysis model [23] was not directly applied. Instead, fire growth predictions were carried out using the full pyrolysis model and the resulting pyrolysis model output was saved. Then, for the current simulations a built-in “mapped-boundary” method in OpenFOAM was used to map the stored pyrolysis model output, thus avoiding a repeat calculation using the pyrolysis model. The mapping process is described in detail in Section 2.3.1 of Ref. [17].

Using the mapped boundary condition for pyrolysis, numerical simulations were conducted under various ceiling configurations. In Figure 2-2 the fire at 40 s, 100 s, and 150 s, represented by the

stoichiometric mixture fraction isocontour, is shown impinging on a horizontal ceiling. The fire chemical HRR reaches ~17 MW at 100 s and the peak HRR is ~25 MW at 150 s, as shown in Figure 2-3. Correspondingly, the convective HRR at 100 s is ~12 MW and its peak value is ~15 MW at 150 s. The radiant fraction, also shown in Figure 2-3, varies with time, beginning with a 0.5 value for the igniter, then reducing to ~0.22 for corrugated burning and finally approaching ~0.35 with increased burning of the polystyrene cups inside the cartons.

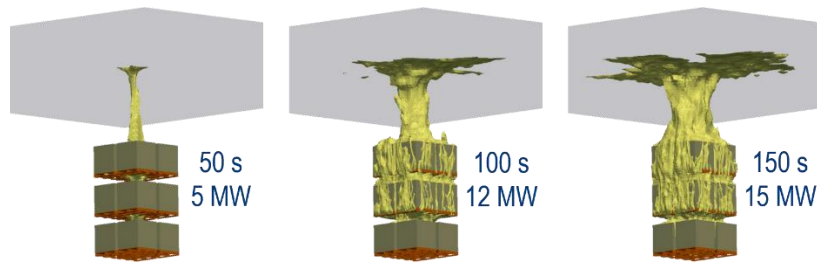


Figure 2-2: Fire growth over the CUP rack-storage array. Flames are impinging on a horizontal ceiling with no obstructed ceiling construction present.

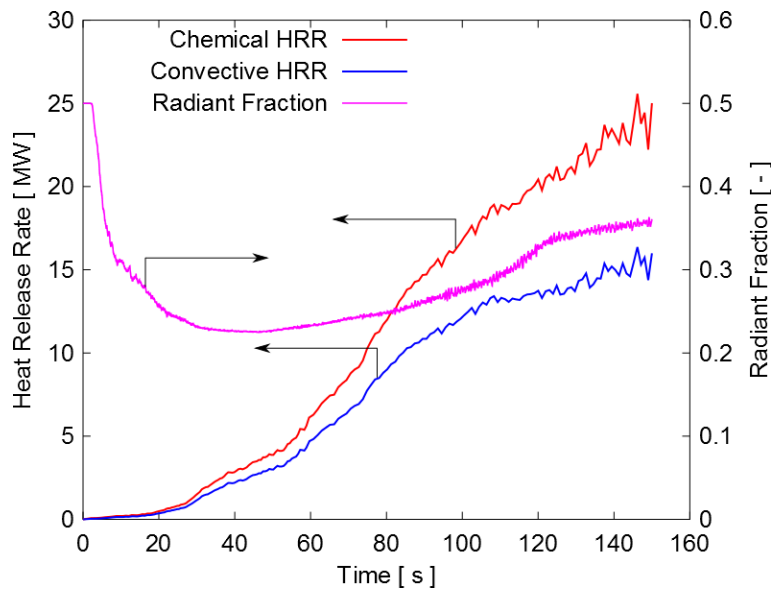


Figure 2-3: Modeled HRR (chemical and convective) and radiant fraction variation as a function of time for the 2 x 2 x 3 array of CUP commodity.

A fire growth model was not available for the UUP commodity. Therefore, a prescribed fuel mass loss rate (MLR) was imposed on a 2.4 m x 2.4 m (8 ft x 8 ft) inlet on the ground level. The MLR data were obtained from a free-burn test conducted with two pallet loads of UUP commodity under the 20 MW fire products collector (FPC) at the FM Global Research Campus. The resulting chemical HRR computed in the simulations is shown in Figure 2-4. A constant radiant fraction of 0.46 was used in the simulations. The maximum convective HRR at 540 s was ~9 MW.

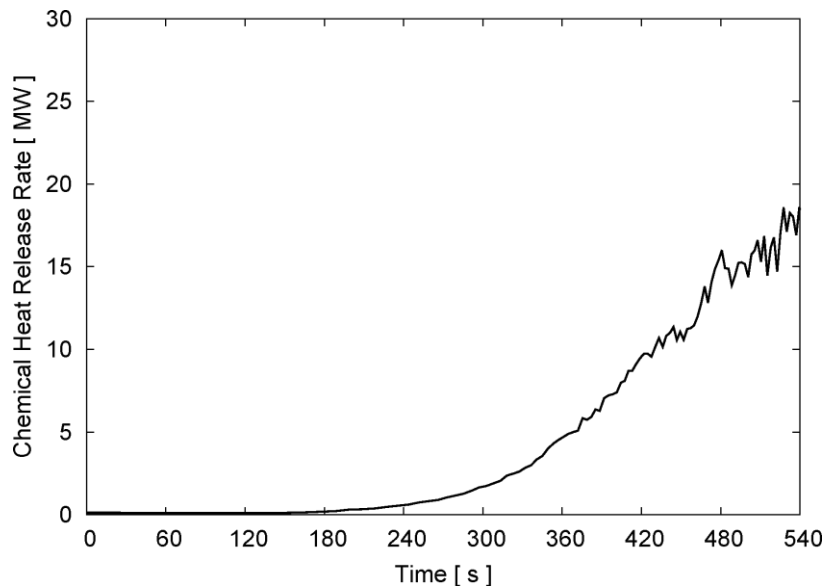


Figure 2-4: Prescribed model chemical HRR as a function of time for the UUP commodity.

For all simulations, the ceiling, including the purlins and girders, were treated as inert walls, with an isothermal temperature boundary (at 25°C or 298.15 K) and a no-slip condition for velocity. As shown in Figure 2-1, the open boundaries on the sides were kept far away from the ceiling and rack-storage locations. The downstream outlet boundary was also kept sufficiently far away from the top of the ceiling locations so as not to affect the flow.

2.3 Sprinkler Activation Setup

Sprinkler activations were simulated with calculations based on the RTI value. A scalar field variable for activation time, t_{act} , was used to record potential activation times at each location in the computational mesh. Activation patterns based on the t_{act} field values were extracted for a plane parallel to the ceiling, located at a perpendicular distance of 430 mm (17 in.) to the flat part of the ceiling. Activation patterns at further distances from the ceiling were also extracted for a few scenarios (e.g., when the purlin depth was greater than 430 mm or 17 in.). These results provide detailed, spatial contours of activation times, as described in Section 3. Activation times for any arbitrary sprinkler layout can be extracted by probing the t_{act} field at specified locations, e.g., ignition below one or among four sprinklers, or other sprinkler spacings (e.g., 2.4 m x 3.7 m or 8 ft x 12 ft).

A quick-response sprinkler with an ordinary activation temperature (henceforth referred to as a QR/OT sprinkler) and a standard-response sprinkler with a high activation temperature (henceforth referred to as a SR/HT sprinkler) were selected for analysis. Details of the sprinklers are given in Table 2-1. Following the concept of isolating the activation patterns from suppression phenomena, as described in Section 2.5 of Ref. [17], sprinkler sprays were not included in the activation simulations.

Table 2-1: List of sprinkler activation parameters used in the present study.

Name	Response	Activation Temperature °C (°F)	RTI (m-s) ^{0.5} ((ft-s) ^{0.5})	C-Factor (m/s) ^{0.5} ((ft/s) ^{0.5})
QR/OT	Quick	74 (165)	30 (54)	0.22 (0.40)
SR/HT	Standard	140 (286)	119 (216)	0.95 (1.72)

3. Numerical Modeling Results and Discussion

Results are presented for both the CUP and UUP commodities. The CUP simulation results provide guidance toward development of a large-scale testing plan (in Section 3.4). The UUP simulation results are used in developing further understanding of ceiling jet characteristics for slower growing fire scenarios.

3.1 CUP Simulations

Sprinkler activation results are presented in this section for the CUP simulations. The ceiling jet influenced by the purlins is first described, followed by discussion on sprinkler activations.

3.1.1 Ceiling Jet in the Presence of Obstructed Ceiling Construction

A ceiling jet is generated by the transient plume originating from the CUP rack-storage fire. In the absence of obstructed ceiling construction (no girders or purlins), the ceiling jet develops almost symmetrically around the ceiling mid-point, as shown in Figure 3-1. The flow below the ceiling in the presence of obstructed ceiling construction (girders and purlins) is next described for increasing purlin depth. Figure 3-2 shows the development of the ceiling jet with 100 mm (4 in.) deep purlins (separation distance of 1.5 m or 5 ft) and 610 mm (24 in.) deep girders (separation distance of 7.6 m or 25 ft). Instantaneous contours of CO₂ mass fractions, $Y_{CO_2} = 0.02-0.04$, are used as a tracer for illustrating the ceiling jet. The contours are colored by temperature in the range of $300\text{ K } (27^\circ\text{C}) \leq T \leq 600\text{ K } (330^\circ\text{C})$. At 40 s after ignition, the ceiling jet remains confined between the two girders. The ceiling jet develops along the channels formed by the girders and to a lesser extent along the channels formed by the purlins. The 100 mm (4 in.) deep purlins do not provide significant obstruction to the flow. The small opening above the girders and the ceiling (caused by the presence of the purlins) allows some flow to move laterally outwards, but most of the flow outside the central girder channel occurs due to spillage under the girders, as can be observed in Figure 3-2 for the 80 s contours. At later times, e.g., at 120 s, the spillage below the girders causes flow to develop along the purlin channels outside of the two central girders.

For a purlin depth of 300 mm (12 in.), the flow at 40 s develops in the purlin channels between the two central girders, as can be seen in Figure 3-3. At 120 s, the ceiling jet develops perpendicular to the purlin channels, but significant flow along the purlin channels can also be observed. Doubling the purlin depth to 610 mm (24 in.) shows that the purlins create deep channels and the core flow region remains confined in the central channels (see Figure 3-4).

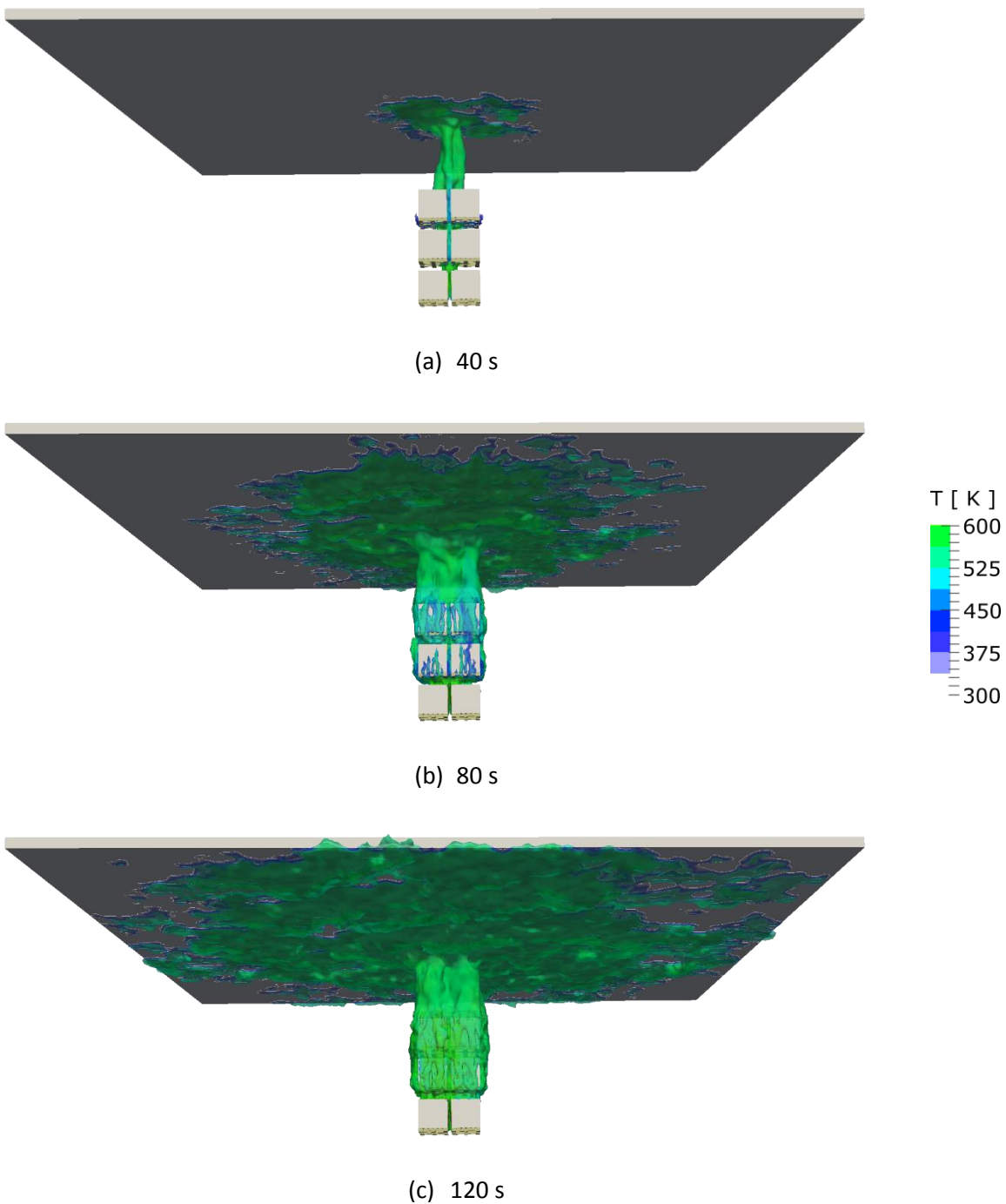


Figure 3-1: Ceiling jet depicted by CO₂ contours ($Y_{CO_2} = 0.02-0.04$) shown under a ceiling located 3.0 m (10 ft) above the CUP rack-storage array. The ceiling does not have any obstructed construction in the form of girders or purlins.

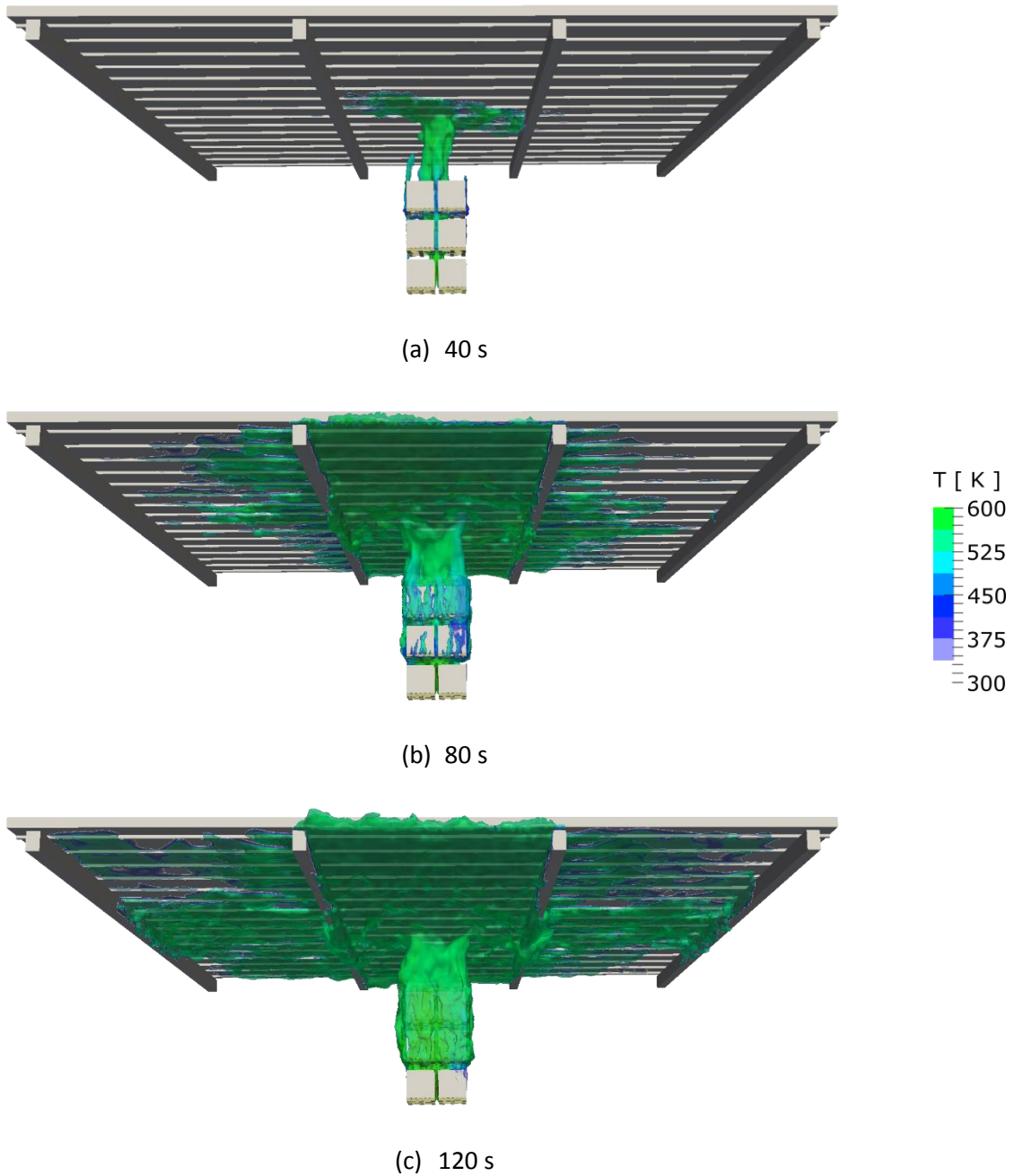


Figure 3-2: Ceiling jet depicted by CO_2 contours ($Y_{\text{CO}_2} = 0.02-0.04$) under a ceiling located 3.0 m (10 ft) above the CUP rack-storage array. The ceiling has 100 mm (4 in.) deep purlins separated by 1.5 m (5 ft) and 610 mm (24 in.) deep girders separated by 7.6 m (25 ft).

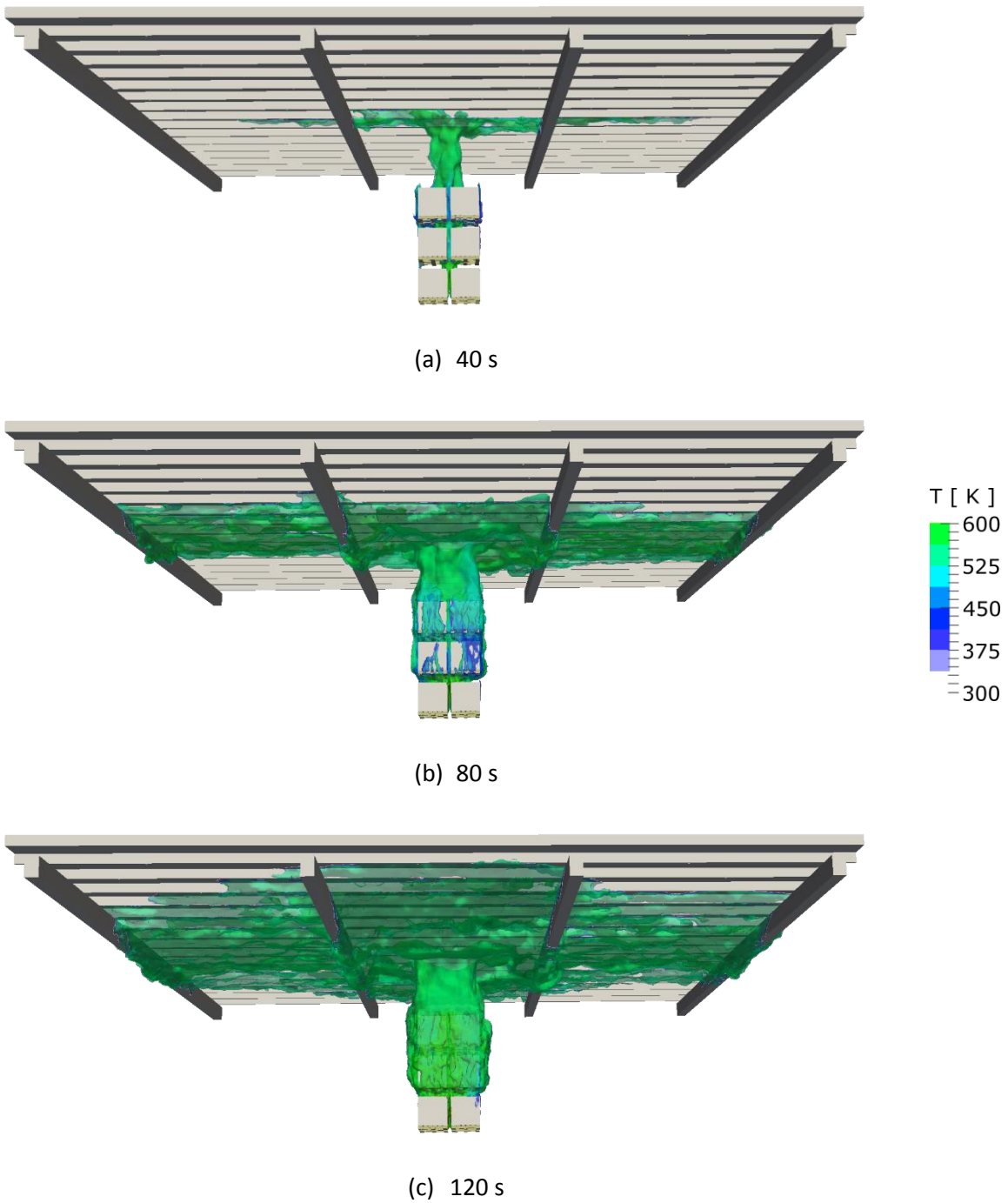


Figure 3-3: Ceiling jet depicted by CO₂ contours ($Y_{CO_2} = 0.02-0.04$) under a ceiling located 3.0 m (10 ft) above the CUP rack-storage array. The ceiling has 300 mm (12 in.) deep purlins separated by 1.5 m (5 ft) and 610 mm (24 in.) deep girders separated by 7.6 m (25 ft).

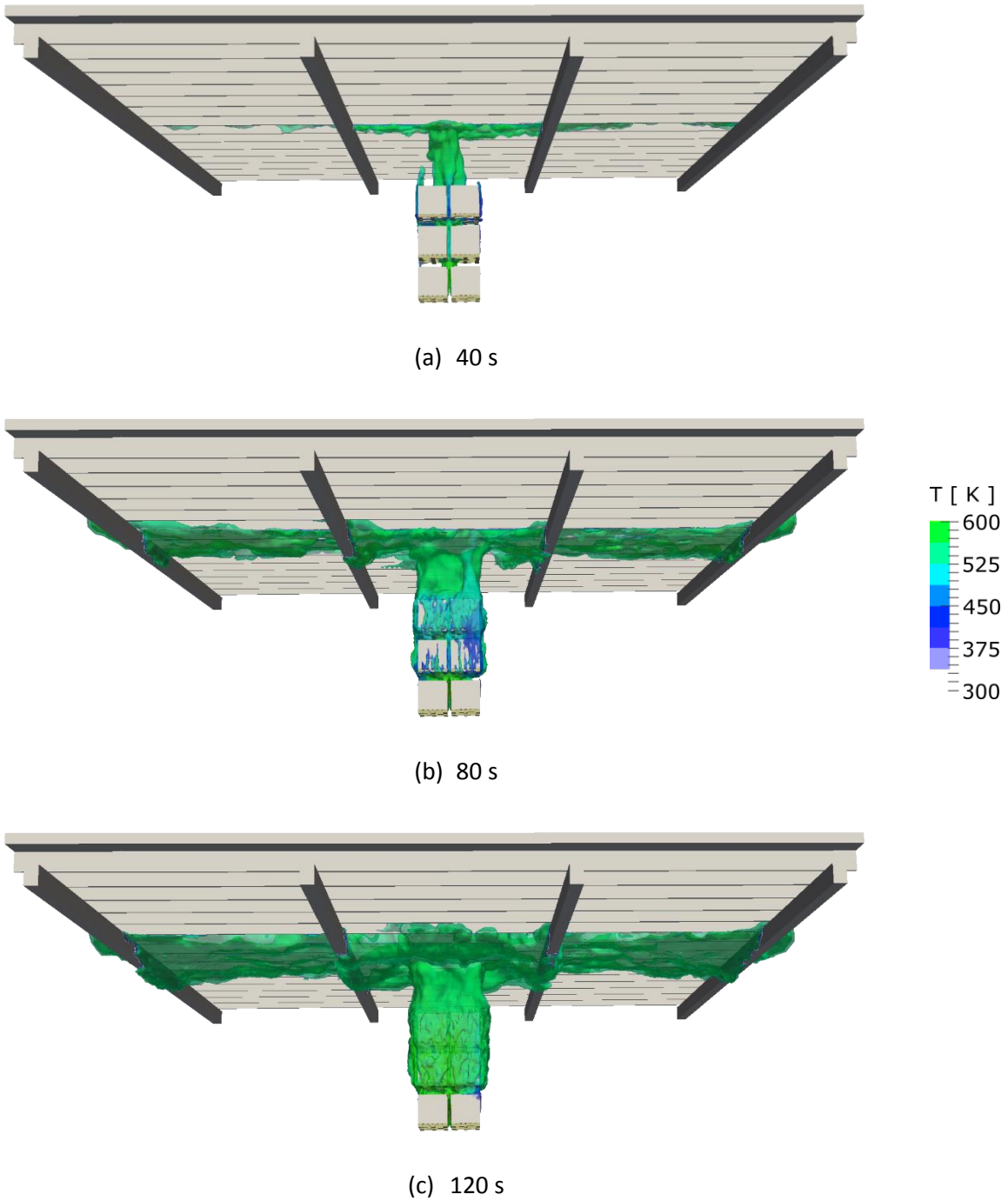


Figure 3-4: Ceiling jet depicted by CO_2 contours ($Y_{\text{CO}_2} = 0.02-0.04$) under a ceiling located 3.0 m (10 ft) above the CUP rack-storage array. The ceiling has 610 mm (24 in.) deep purlins separated by 1.5 m (5 ft) and 610 mm (24 in.) deep girders separated by 7.6 m (25 ft).

3.1.2 Quick-Response, Ordinary Temperature Sprinklers

3.1.2.1 Sprinkler Activation Times

Activation times and patterns are presented in Figures 3-5 and 3-6 for QR/OT sprinklers for an arrangement with a sprinkler located directly above the ignition location. To evaluate the scenario when sprinklers are not present in the purlin channel directly above the ignition location, Section 3.1.2.6 includes a discussion on activation times extracted with an offset sprinkler arrangement. The activation time contours shown are for a plane parallel to and located 430 mm (17 in.) below the ceiling, representing the maximum sprinkler thermal-element offset for sprinklers with K-factor 320 (22.4) and higher. In Figure 3-5(a), activation contours are shown for a ceiling with no obstructed construction. Activation times show symmetry around the ignition location which is at the center of the rack-storage array (the array is depicted by four white boxes in the figures). The slight difference in activation contour development along the top-bottom and left-right directions is due to the orientation of the wood pallets (for a detailed description, refer to Section 2.3.2 in Ref [17]). For the discrete sprinkler location arrangement shown in Figure 3-5, activation time for the sprinkler above the ignition location does not vary significantly (between 25 and 26 s) when purlins and girders are present. However, the activation times of the rest of the sprinklers are affected, as discussed below. Activation times for the eight-sprinkler links surrounding the ignition location (the eight sprinklers together are referred hereon as “first ring sprinklers”) are discussed comparing them to activation times in absence of obstructed ceiling construction. Table 3-1 includes the average activation times of the surrounding eight sprinklers, comparing them to average activation times of the two sprinklers in the central channel and the rest of the six sprinklers.

For a purlin depth of 100 mm (4 in.), with separation distance of 1.5 m (5 ft) and when 610 mm (24 in.) girders are present (separated by 7.6 m or 25 ft), the sprinkler activation contours are shown in Figure 3-5(b) (the purlins and girders are overlaid on the contours). Average activation time for the first ring sprinklers is ~50 s, which is ~31 s earlier compared to when purlins and girders are not present. This indicates that the presence of obstructed ceiling construction can facilitate earlier activations of sprinklers in certain cases, especially for sprinklers located close to the ignition region. The purlin channels do not cause any biased activation pattern, as can be observed from the similar average activation times for the two central channel sprinklers and the other six sprinklers, as reported in Table 3-1. Activation times are primarily affected by the presence of girders that enable channeling of the flow in the direction perpendicular to the purlins.

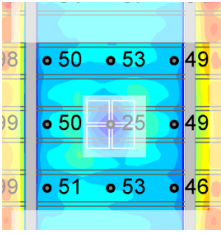
As can be observed in Figure 3-5(c), when doubling the purlin depth to 200 mm (8 in.), the first ring sprinkler average activation time decreases by ~4 s (from ~50 s for the 100 mm or 4 in. deep purlins to ~46 s for the 200 mm or 8 in. deep purlins, as shown in Table 3-1). The open area between the girder and the ceiling doubles for the 200 mm (8 in.) purlins. Flow escapes through this area to the outside of the central girder region causing earlier activations to occur in the purlin channels.

As shown in Figure 3-5(d), for a purlin depth of 300 mm (12 in.), the average activation time for the first ring increases marginally compared to the 200 mm (8 in.) purlin case to ~48 s; however, compared to

the case when obstructed ceiling construction is absent, the average activation time is still considerably earlier. The ceiling jet tends to travel in the channels formed by the purlins (this phenomenon is hereon referred to as a “channeling effect”). A distinct difference between activation patterns for purlin depths <300 mm (12 in.) and for 300 mm (12 in.) purlins can be observed as well. For purlin depths <300 mm (12 in.), the channeling effect is primarily due to the presence of the girders, whereas for the 300 mm (12 in.) purlins the flow predominantly moves in the channels formed by the purlins.

The activation times for deeper purlins, of a depth of 360–610 mm (14–24 in.), are shown in Figure 3-6. The average activation times for the first ring sprinklers are still significantly earlier compared to the case without obstructed ceiling construction. The initial decrease in the first ring average activation time (for purlin depths of 100–300 mm or 4–12 in.) and subsequent increase (for purlin depths ≥360 mm or 14 in.) indicates that the presence of purlins and girders can cause earlier sprinkler activations as discussed above. It should also be noted, as mentioned above, that the skewed activation pattern along the central purlin channel is of greater concern for purlin depths >300 mm (12 in.). The channeling effect for purlin depths ≤300 mm (12 in.) does not cause significant bias in the activation pattern, as can be observed in Table 3-1: the average activation time for the two central channel sprinklers remains almost identical to the average activation time for the rest of the six first ring sprinklers for purlin depths ≤300 mm (12 in.). For a purlin depth of 300 mm (12 in.), on average the two central channel sprinklers activate only ~9 s earlier than the remaining six first ring sprinklers. For purlin depths >300 mm (12 in.), the activation time difference between the central channel and the outer channel sprinklers increases significantly.

Table 3-1: Activation times for the eight QR/OT sprinklers surrounding the ignition location. Three times are reported (in s): average for all eight locations, two locations in the central channel, and six locations in the outer two channels.



	Purlin Depth [in.]					
	0	4	8	12	18	24
Average	81.4	50.1	45.6	47.5	53.4	57.9
Central channel	81.0	49.5	45.0	42.0	40.0	38.0
Outer channels	81.5	50.3	45.8	49.3	57.8	64.5

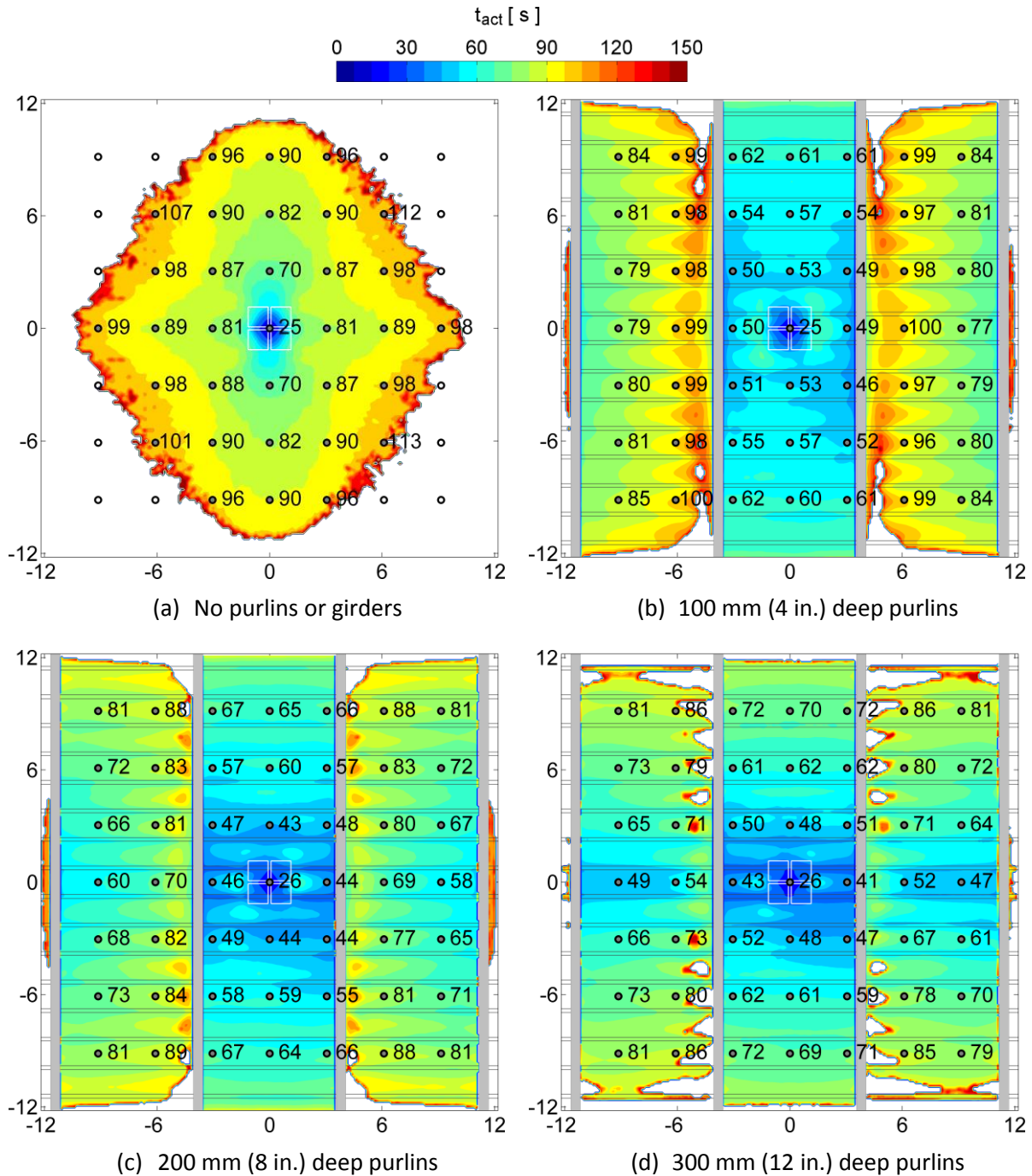


Figure 3-5: Activation time contours for QR/OT sprinkler links at 430 mm (17 in.) below a ceiling located 3.0 m (10 ft) above the CUP rack-storage array in (a) the absence of obstructed ceiling construction, and in the presence of 610 mm (24 in.) deep girders separated by 7.6 m (25 ft) and purlins with a separation distance of 1.5 m (5 ft) and depths of (b) 100 mm (4 in.), (c) 200 mm (8 in.), and (d) 300 mm (12 in.). Discrete locations of sprinkler links arranged in a 3.0 m × 3.0 m (10 ft × 10 ft) spacing with one sprinkler centered on the CUP array are also shown with the corresponding activation times.

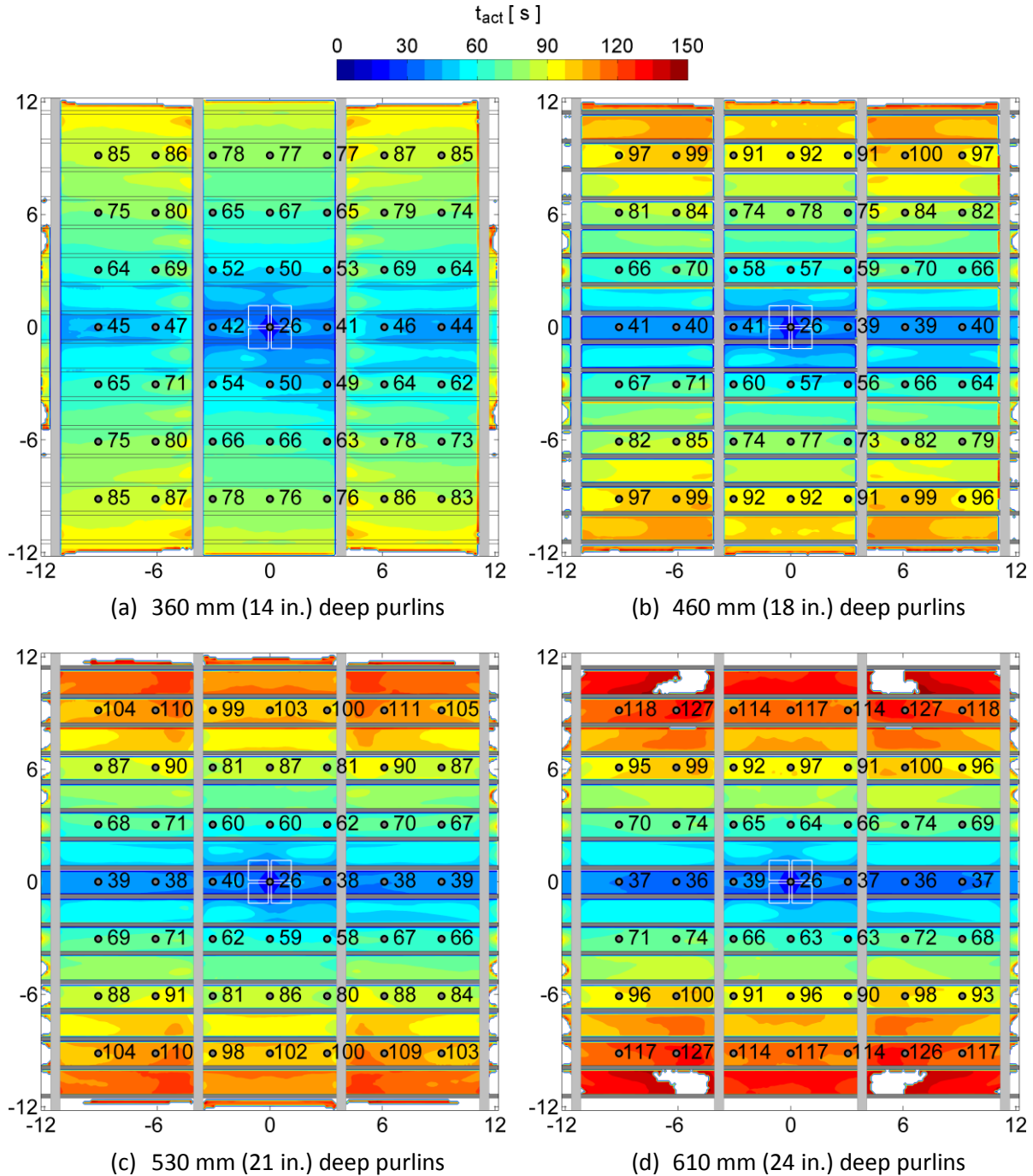


Figure 3-6: Activation time contours for QR/OT sprinkler links at 430 mm (17 in.) below a ceiling located 3.0 m (10 ft) above the CUP rack-storage array in the presence of 610 mm (24 in.) deep girders separated by 7.6 m (25 ft) and purlins with a separation distance of 1.5 m (5 ft) and depths of (a) 360 mm (14 in.), (b) 460 mm (18 in.), (c) 530 mm (21 in.), and (d) 610 mm (24 in.).

For the deepest purlins considered in the study, with depths of 530–610 mm (21–24 in.), the channeling of the ceiling jet along the purlins is also the dominant phenomenon as indicated by the activation patterns in Figure 3-6(c-d). The sprinklers along the central purlin channels beyond the ignition region activate within a few seconds of each other. For sprinkler links beyond the first ring, activation delays in the direction perpendicular to the purlins increase by 33–53 s when compared to purlins of a depth of <300 mm (12 in.). If the sprays from the activated sprinklers above the ignition region and in the first ring cannot slow down the fire growth rate, these activation delays may result in an out of control fire spread situation.

The average activation time for the first ring sprinklers was found to vary between ~45 and 58 s with change in purlin depth. The difference of ~13 s may not severely affect the sprinkler suppression effectiveness. Again, it should be noted that compared to the case where obstructed ceiling construction is absent, the first ring sprinklers activate earlier. However, due to the significant channeling effect along the central purlin channels when the purlin depth is >300 mm (12 in.), several additional sprinkler activations may occur, resulting in the water demand to be exceeded. To evaluate this effect, sprinkler activation times in the central purlin channel are compared with those in the perpendicular direction to the purlins as shown in the contour plot of Figure 3-7. The horizontal arrow indicates the direction of activations along the central channel whereas the vertical arrow represents those in the direction perpendicular to the purlins.

The activation times probed along the two directions are plotted in Figure 3-7(a-b). In the absence of obstructed ceiling construction, the change of activation times in both directions shows a similar trend as indicated by the solid black curves (the small differences in the activation times are caused by non-symmetric fire growth due to the included two-way wood pallet design as discussed in Section 2.3.2 in Ref. [17]). In the presence of the purlins and girders, the activation times for distances ≤ 0.76 m (2.5 ft), i.e., in the plume impingement region, remain similar irrespective of the purlin depth. The presence of purlins and girders causes earlier activation times for distances >0.76 m (2.5 ft) and <3.0 m (10 ft). Along the central channel, the activation times initially increase (up to ~1.8 m or 6 ft) and then decrease as the hot ceiling jet gases tend to accumulate near the girder at 3.8 m (12.5 ft) from the ceiling mid-point causing earlier sprinkler activations. For deeper purlins (≥ 530 mm or 21 in.), activations along the central channel beyond the girder occur almost simultaneously. The activation times in the direction perpendicular to the purlins remain almost similar for purlin depths ≤ 360 mm (14 in.). For deeper purlins, the activation time delay increases with distance. A key observation from Figure 3-7 is that activation times in both directions remain similar up to a distance of ~1.8 m or 6 ft (typical maximum distance between the plume impingement location and the closest sprinkler found in warehouses). This is especially true for purlins with a depth ≥ 300 mm (12 in.). It should be emphasized that the presence of purlins and girders favorably affects sprinkler activation times: up to a distance of ~4 m (13 ft) activation times are earlier compared to when obstructed ceiling construction is absent.

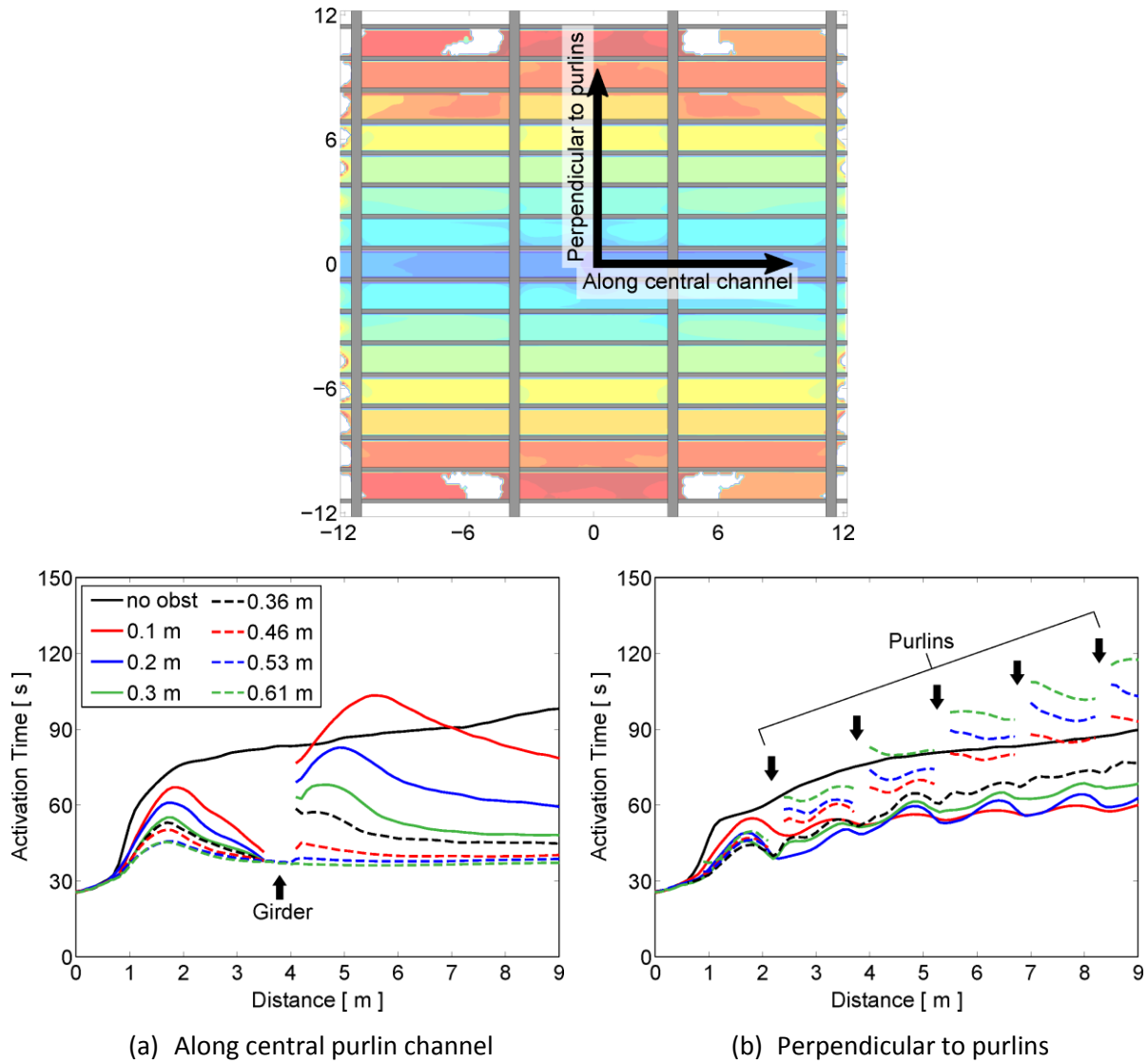


Figure 3-7: QR/OT sprinkler activation times at 430 mm (17 in.) below a ceiling located 3.0 m (10 ft) above the CUP rack-storage array as a function of purlin depth along (a) central purlins channel, and (b) in a perpendicular to the purlin direction. Purlins are separated by 1.5 m (5 ft) and girders by 7.6 m (25 ft).

3.1.2.2 Effect of Sprinkler Link Distance

For deeper purlins (depth >460 mm or 18 in.), as observed in Figure 3-7, due to the significant channeling of flow many simultaneous sprinkler activations could occur when the sprinkler links are located 430 mm (17 in.) below the ceiling. To evaluate the effect of the link distance, activation patterns and times are presented for links present at two planes: aligned with the bottom of the purlins and 150 mm (6 in.) below the bottom edge of the purlins. Activation time contours for two purlin depths, 530 mm (21 in.) and 610 mm (24 in.), are presented in Figure 3-8.

When the sprinkler links are located on the plane aligned with the bottom of the purlins, the average first ring activation time increases by 2–3 s compared to when the purlins are located 430 mm (17 in.) below the ceiling. From Figure 2-3 we can observe that, for the 530 mm (21 in.) purlins, the convective HRR increases from ~5.3 MW to ~5.9 MW in 2 s, whereas for the 610 mm (24 in.) purlins the increase is from ~6.3 MW to ~7.2 MW in 3 s. This indicates that keeping the sprinkler links aligned with the bottom of the purlins does not cause significant activation delays and, in the case of the 3-tier-high CUP array and 3.0 m (10 ft) ceiling clearance, small increases to the HRR are correspondingly observed. When the links are located 150 mm (6 in.) below the bottom edge of the purlins, the activation delays increase to 5–6 s, also indicating that it may be acceptable to locate the sprinkler links below the purlins provided the fire HRR does not increase significantly during this time causing challenges to the protection design. In the case of the CUP fire used in the current study, the convective HRR increases from ~5.3 MW to ~6.9 MW for the 530 mm (21 in.) purlins and from ~6.3 MW to ~8.1 MW for the 610 mm (24 in.) purlins. The HRR increases between 29 and 30% for both purlin depths. It should, however, be noted that for the unobstructed ceiling case, the convective HRR for the first ring activations is considerably higher. This indicates that, in the presence of obstructed ceiling construction, keeping the sprinkler link further away from the ceiling does not adversely affect activation times compared to the unobstructed ceiling case.

To evaluate the issue of water demand being exceeded due to an excessive number of activations in the purlin channels, as shown above in Figure 3-7, activation times along the central channel and perpendicular to the purlins are again compared. Figure 3-9 shows the activation time variation along the two directions. For distances ≤ 1.8 m (6 ft), the activation time variation with distance in the two directions remains almost identical when the sprinkler links are located on a plane passing through the bottom of the purlins. It can be concluded from this analysis that the sprinkler links can be lowered from the 430 mm (17 in.) depth to align them with a plane passing through the bottom of the purlins without significant effect on the activation times. This assessment is based on the convective HRR increase observed in the modeled 3-tier-high CUP fire applied in the current study. Also, compared to the unobstructed ceiling first ring average activation time, aligning the sprinkler links with the bottom of the purlins causes earlier average activation times. Lowering of the sprinklers beyond their maximum allowable vertical distance below the ceiling may become necessary to ensure spray impingement does not take place onto the deeper purlins.

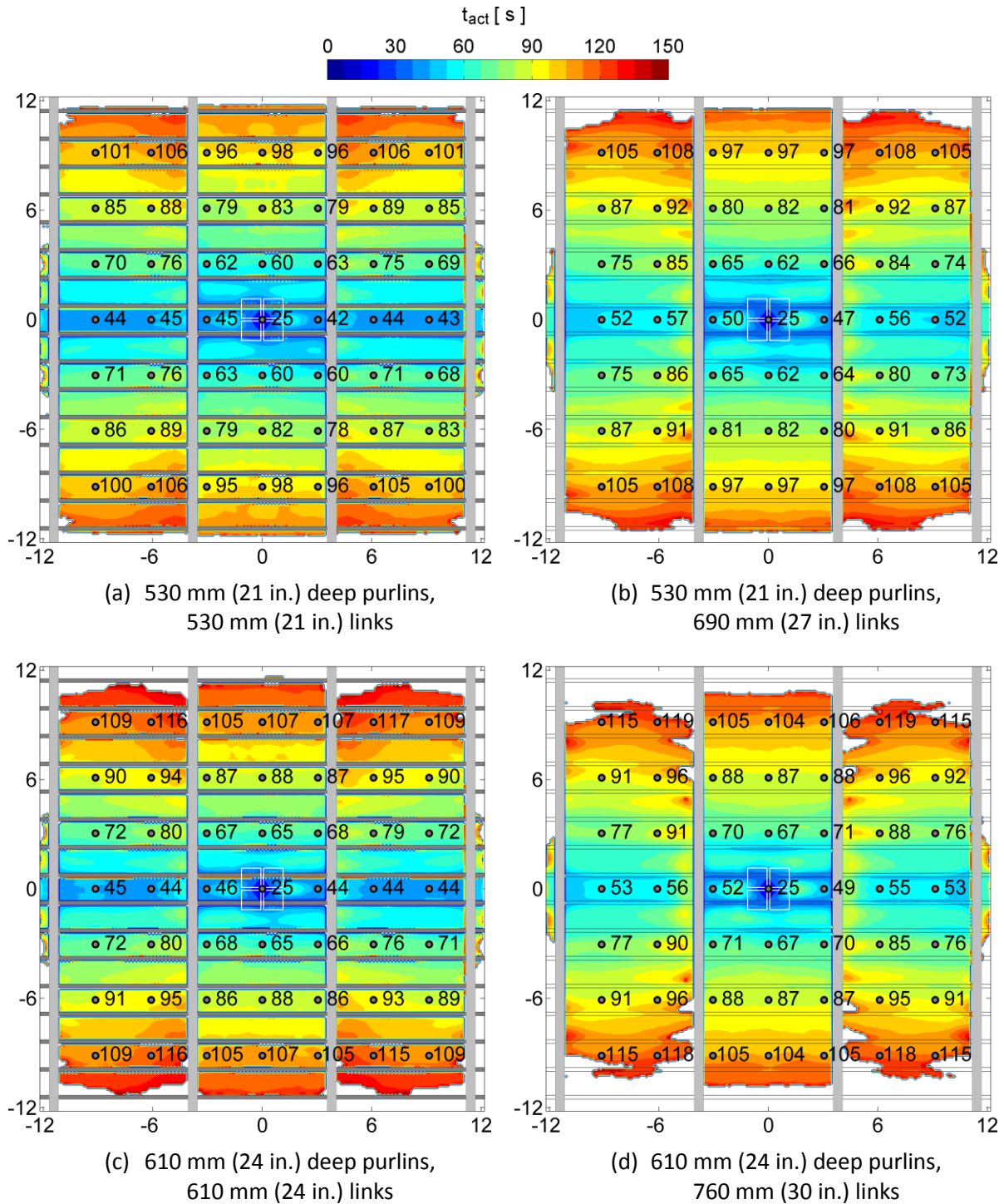


Figure 3-8: Activation time contours for QR/OT sprinkler links below a ceiling located 3.0 m (10 ft) above the CUP rack-storage array in the presence of 610 mm (24 in.) deep girders separated by 7.6 m (25 ft) and purlins with a separation distance of 1.5 m (5 ft) with a purlin depth of 530 mm (21 in.), sprinkler links at (a) 530 mm (21 in.), and (b) 690 mm (27 in.) below the ceiling, and with a purlin depth of 610 mm (24 in.), sprinkler links at (c) 610 mm (24 in.), and (d) 760 mm (30 in.) below the ceiling.

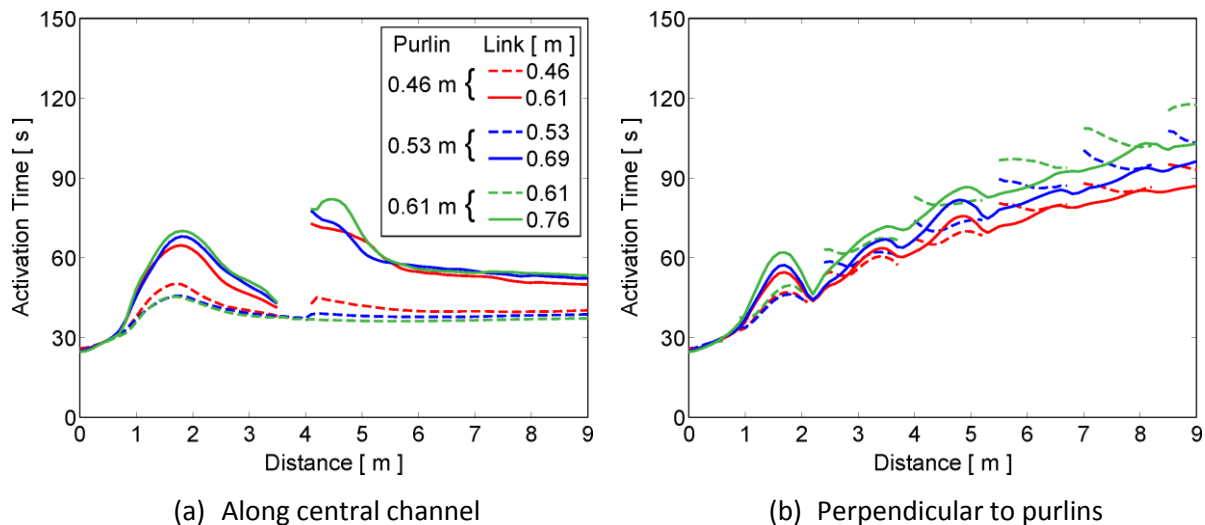


Figure 3-9: QR/OT sprinkler activation times at various sprinkler link distances below a ceiling located 3.0 m (10 ft) above the CUP rack-storage array as functions of purlin depth along (a) the central purlins channel, and (b) in a perpendicular to the purlin direction. Purlins are separated by 1.5 m (5 ft) and girders by 7.6 m (25 ft).

3.1.2.3 Effect of Ceiling Clearance

The effect of ceiling clearance on the activation times and patterns is next evaluated. The ceiling clearance is halved from 3.0 m (10 ft) to 1.5 m (5 ft). Figure 3-10(a) shows the activation pattern and times for the case with a ceiling clearance of 3.0 m (10 ft) and Figure 3-10(b) is when the ceiling clearance is 1.5 m (5 ft). Comparisons are shown for purlin depth and separation distances of 360 mm (14 in.) and 1.5 m (5 ft), respectively. The average time of activation for the first ring sprinklers is found to increase marginally by ~2 s compared to when the ceiling clearance was 3.0 m (10 ft). This could be attributed to the greater channeling effect observed in the three central purlin channels (the central channel and the two on its sides) for the 1.5 m (5 ft) ceiling clearance. The greater channeling of the ceiling jet occurs due to the smaller plume width at the impingement region. The smaller plume width results from reduced entrainment rate for the shorter distance the plume travels (1.5 m or 5 ft instead of 3.0 m or 10 ft) and the higher plume temperatures encountered at the ceiling level. The smaller plume width and higher temperatures result in the development of a narrower ceiling jet. Even though the maximum activation delay along the central channel for the 3.0 m (10 ft) case is ~10 s for distances ≤ 1.8 m (6 ft), as seen in Figure 3-11, the average activation time difference perpendicular to the purlins remains within ~3–4 s. In summary, for lower ceiling clearance, a greater channeling effect is observed, and lower ceiling clearance can therefore be viewed as a worst-case scenario when obstructed ceiling construction is present.

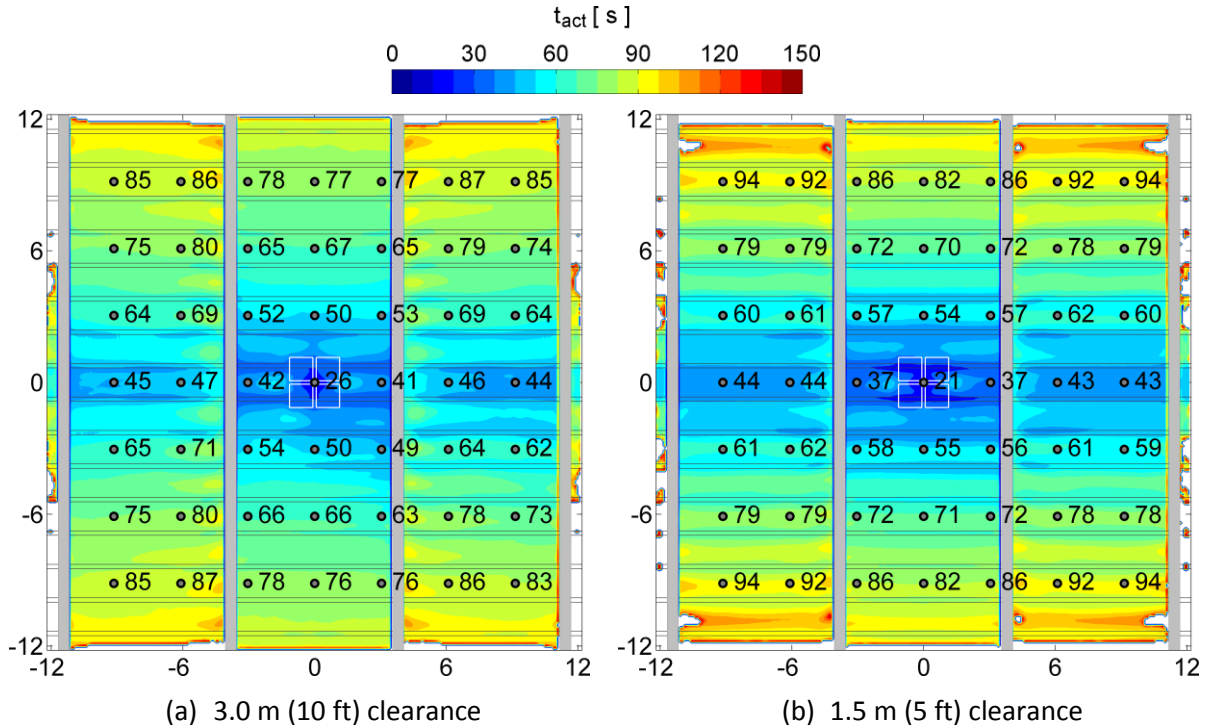


Figure 3-10: Activation time contours for QR/OT sprinkler links in the presence of 610 mm (24 in.) deep girders separated by 7.6 m (25 ft), purlins with a separation distance of 1.5 m (5 ft) and a depth of 360 mm (14 in.), and sprinkler links 430 mm (17 in.) below the ceiling with a ceiling clearance of (a) 3.0 m (10 ft), and (b) 1.5 m (5 ft).

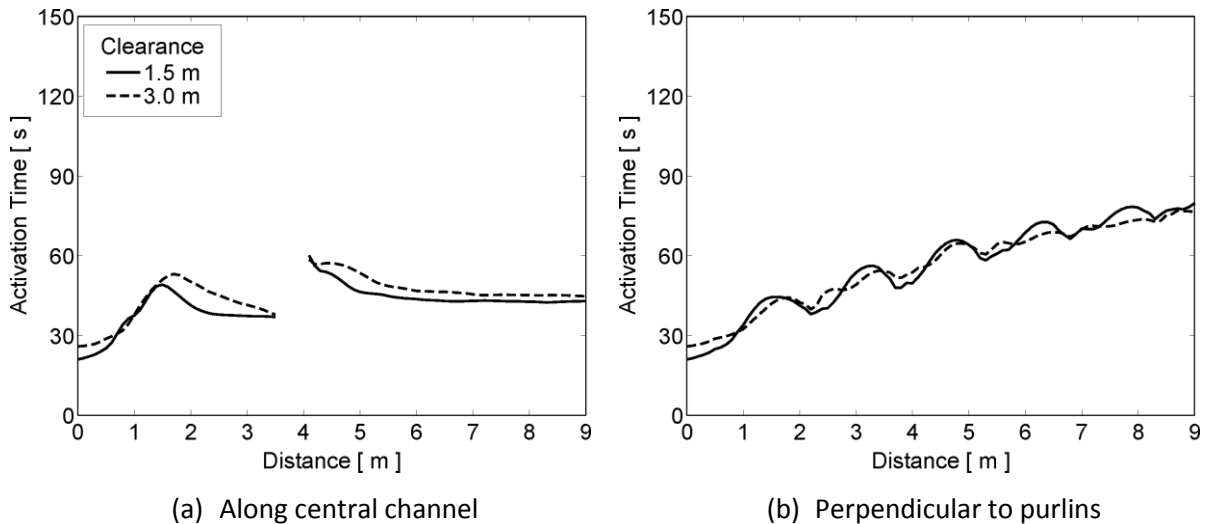


Figure 3-11: QR/OT sprinkler activation times at 430 mm (17 in.) below a ceiling located 1.5 m (5 ft) and 3.0 m (10 ft) above the CUP rack-storage array as functions of purlin depth along (a) the central purlins channel, and (b) in a perpendicular to the purlins direction. Purlins are separated by 1.5 m (5 ft) and girders by 7.6 m (25 ft).

3.1.2.4 Effect of Purlin Separation Distance

Another effect investigated is that of purlin separation distance on sprinkler activation times. The purlin separation distance is doubled from 1.5 m (5 ft) to 3.0 m (10 ft) while keeping the ceiling clearance constant at 3.0 m (10 ft) and the girder separation distance at 7.6 m (25 ft). Figure 3-12 shows the variation of sprinkler activation times and patterns as functions of purlin depth. As in the case of the 1.5 m (5 ft) separation distance results, for the 3.0 m (10 ft) separation distance, by increasing the purlin depth the flow channeling along the central purlin channels increases and earlier activation times are observed for the central channel. The average activation time for the first ring of sprinklers increases by ~3–8 s for purlin depths of 100–610 mm (4–24 in.) when the purlin separation distance is doubled. It should be noted that compared to the case with no obstructed ceiling construction, the average activation times are still quite earlier when the purlin separation distance is doubled. The channeling effect for the wider separation distance of 3.0 m (10 ft) reduces for the same purlin depth. The effect reduces most for the deepest purlins of 610 mm (24 in.) as shown in Figure 3-13(a) and no change is observed for the 100 mm (4 in.) deep purlins. Differences in activation times of the order of ~10 s are observed in the direction perpendicular to the purlins (see Figure 3-13(b)) with the 610 mm (24 in.) deep purlins case showing consistently earlier activations for the 3.0 m (10 ft) purlin separation distance. It can be concluded that greater purlin separation distance would cause less channeling effect wherein the average activation difference between the two central sprinklers adjacent to the ignition location and the remaining six first ring sprinklers decreases.

3.1.2.5 Effect of Girder Separation Distance

Similar to the changing of the purlin separation distance, one case with a girder separation distance of 12.2 m (40 ft) was simulated for a purlin depth of 360 mm (14 in.) and separation distance of 1.5 m (5 ft). Figure 3-14 shows the activation time contours when the girders are separated by 12.2 m (40 ft). The average first ring sprinkler activation time was found to be 54 sⁱ as compared to 49 s for the case with girders separated by 7.6 m (25 ft). Compared to the case with no obstructed ceiling construction, the average activation time for the first ring sprinklers is favorable. Increasing the girder separation distance also did not influence the purlin channeling effect significantly as can be observed in Figure 3-15(a) with maximum delays <3 s observed until a 3.0 m (10 ft) distance from the ceiling mid-point when the girder separation distance is increased. For the same distance from the ignition location, the activation time variation perpendicular to the purlins remains almost identical, as seen in Figure 3-15(b). It can therefore be concluded that girder separation distance has a weak effect on activation times in the region of interest (i.e., within ~1.8 m or 6 ft distance).

ⁱ The sprinkler spacing used was 3 m × 3.35 m (10 ft × 11 ft) to facilitate extraction of activation times.

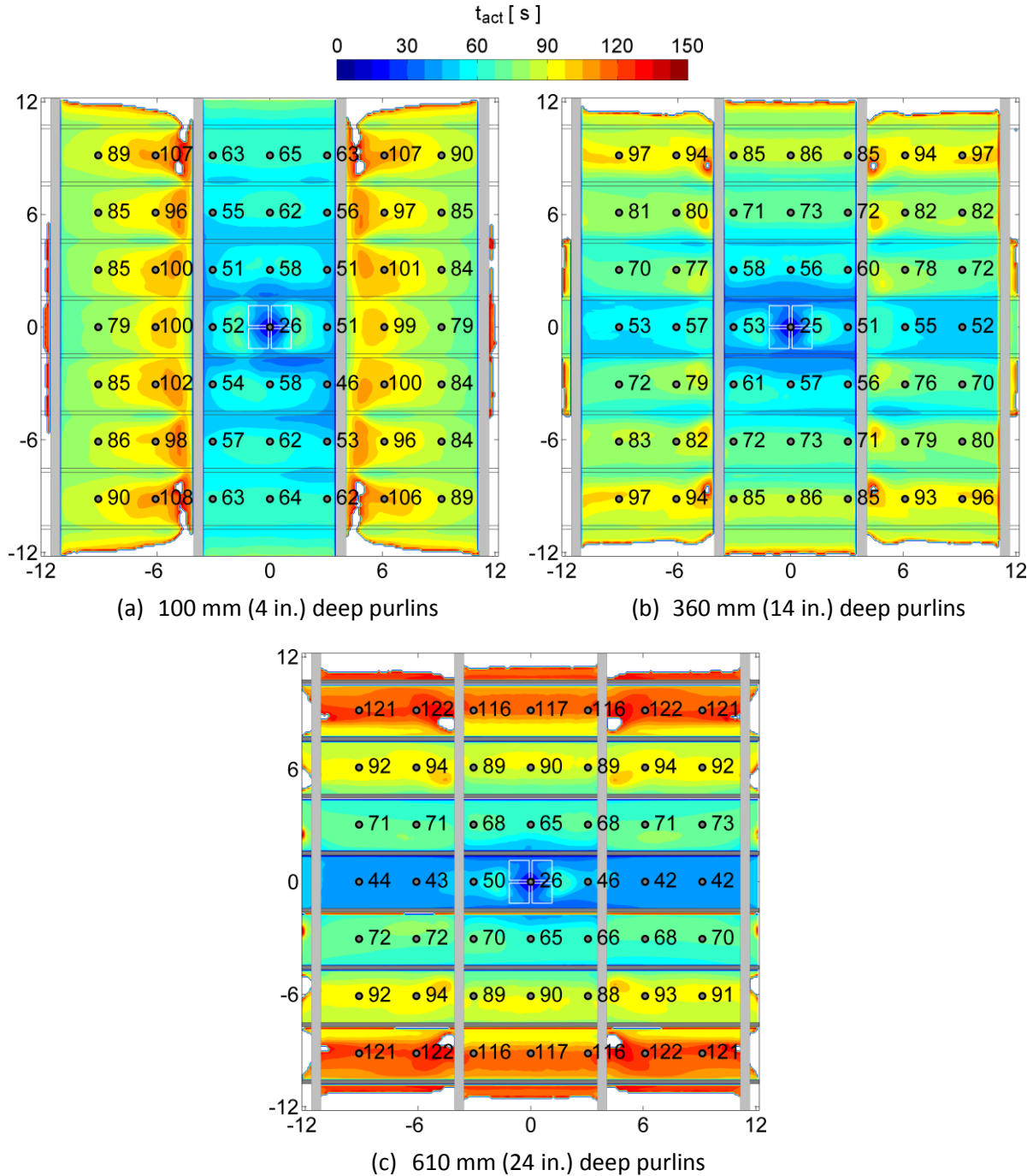


Figure 3-12: Activation time contours for QR/OT sprinkler links below a ceiling located 3.0 m (10 ft) above the CUP rack-storage array in the presence of 610 mm (24 in.) deep girders separated by 7.6 m (25 ft) and purlins with a separation distance of 3.0 m (10 ft) and a depth of (a) 100 mm (4 in.), (b) 360 mm (14 in.), and (c) 610 mm (24 in.). Sprinkler links are 430 mm (17 in) below the ceiling.

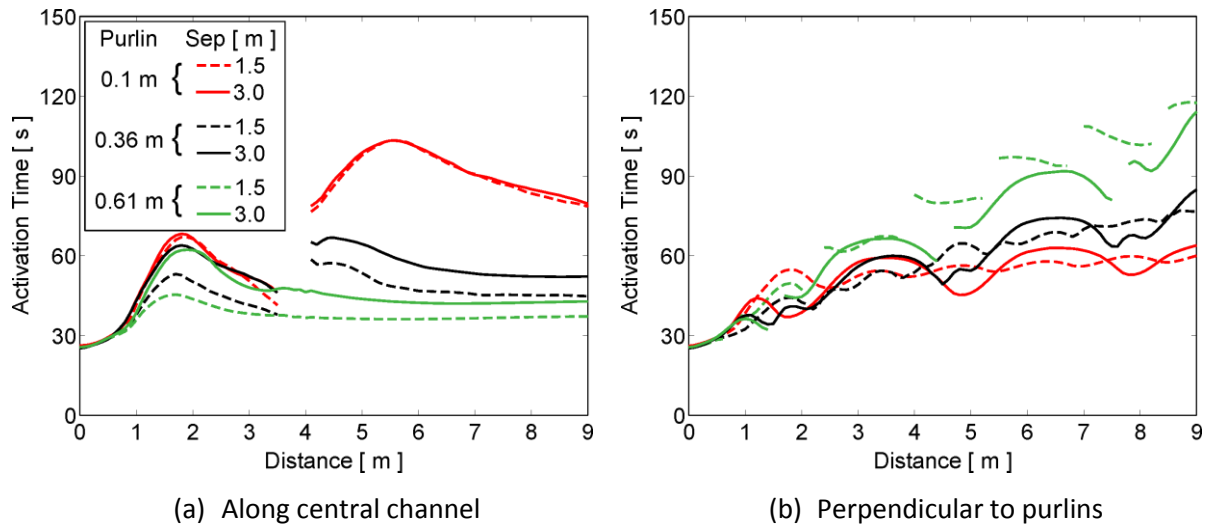


Figure 3-13: Effect of purlin separation distance on QR/OT sprinkler activation times at 430 mm (17 in.) below a ceiling located 3.0 m (10 ft) above the CUP rack-storage array as a function of purlin depth along (a) the central purlins channel, and (b) in a perpendicular to the purlins direction. Purlins are separated by 1.5 m (5 ft) and 3.0 m (10 ft) and girders by 7.6 m (25 ft).

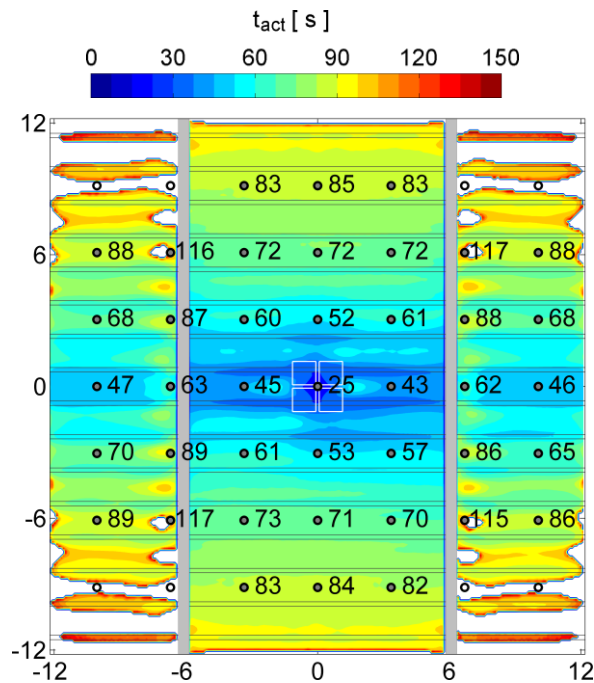


Figure 3-14: Activation time contours for QR/OT sprinkler links below a ceiling located 3.0 m (10 ft) above the CUP rack-storage array in the presence of 610 mm (24 in.) deep girders separated by 12.2 m (40 ft), purlins with a separation distance of 1.5 m (5 ft) and a depth of 360 mm (14 in.), and sprinkler links 430 mm (17 in.) below the ceiling. Discrete locations of sprinkler links arranged in a 3.0 m \times 3.35 m (10 ft \times 11 ft) spacing.

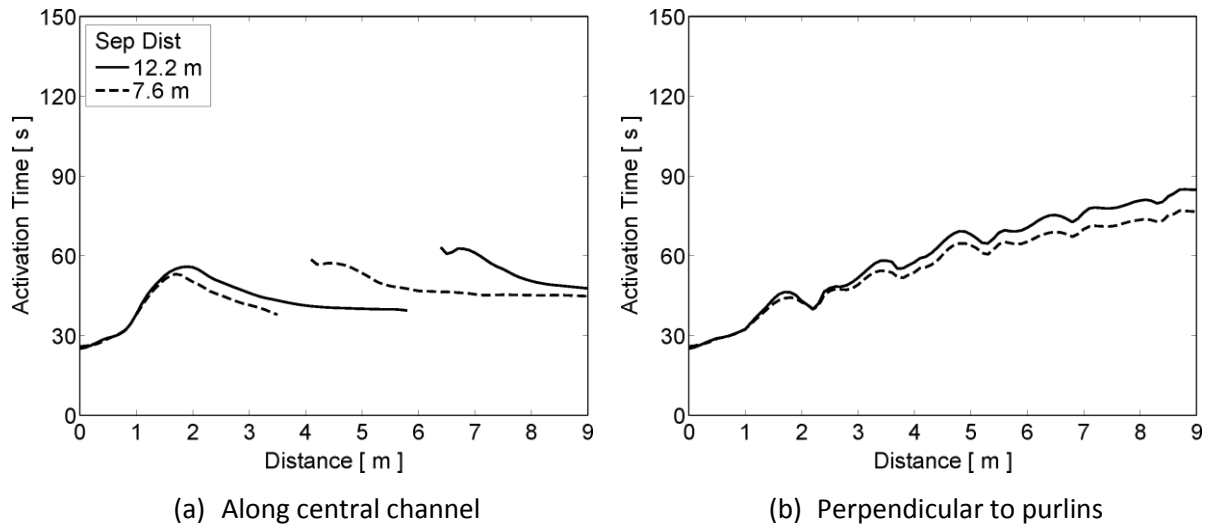


Figure 3-15: Effect of girder separation distance on QR/OT sprinkler activation times at 430 mm (17 in.) below a ceiling located 3.0 m (10 ft) above the CUP rack-storage array as a function of purlin depth along (a) central purlins channel, and (b) in a perpendicular to the purlins direction. Purlins are separated by 1.5 m (5 ft) and girders by 7.6 m (25 ft) and 12.2 m (40 ft).

3.1.2.6 Offset Sprinkler Arrangement

The analysis presented above used an arrangement with a sprinkler directly above the ignition location with the remaining sprinkler links arranged in a 3.0 m × 3.0 m (10 ft × 10 ft) spacing. In Figure 3-16, activation times for an offset arrangement are shown for the discrete sprinkler link locations. It should be kept in mind that actual sprinkler links were not included in the simulations. Instead, as in Sections 3.1.2.1–3.1.2.5, activation data are extracted from the activation time distributions on the plane parallel to and located 430 mm (17 in.) below the ceilings. Compared to the average activation times for the two central channel sprinklers adjacent to the ignition location (in the centered arrangement), the four nearest sprinklers to the ignition location in the offset arrangement on average activate with 7–17 s delays as can be observed in Figure 3-16. It should be noted that the average activation times reported above are earlier compared to the unobstructed ceiling activation time for the offset arrangement. For large-scale testing, using an offset sprinkler arrangement would challenge the protection design due to the later activations compared to the case when the centered arrangement is selected.

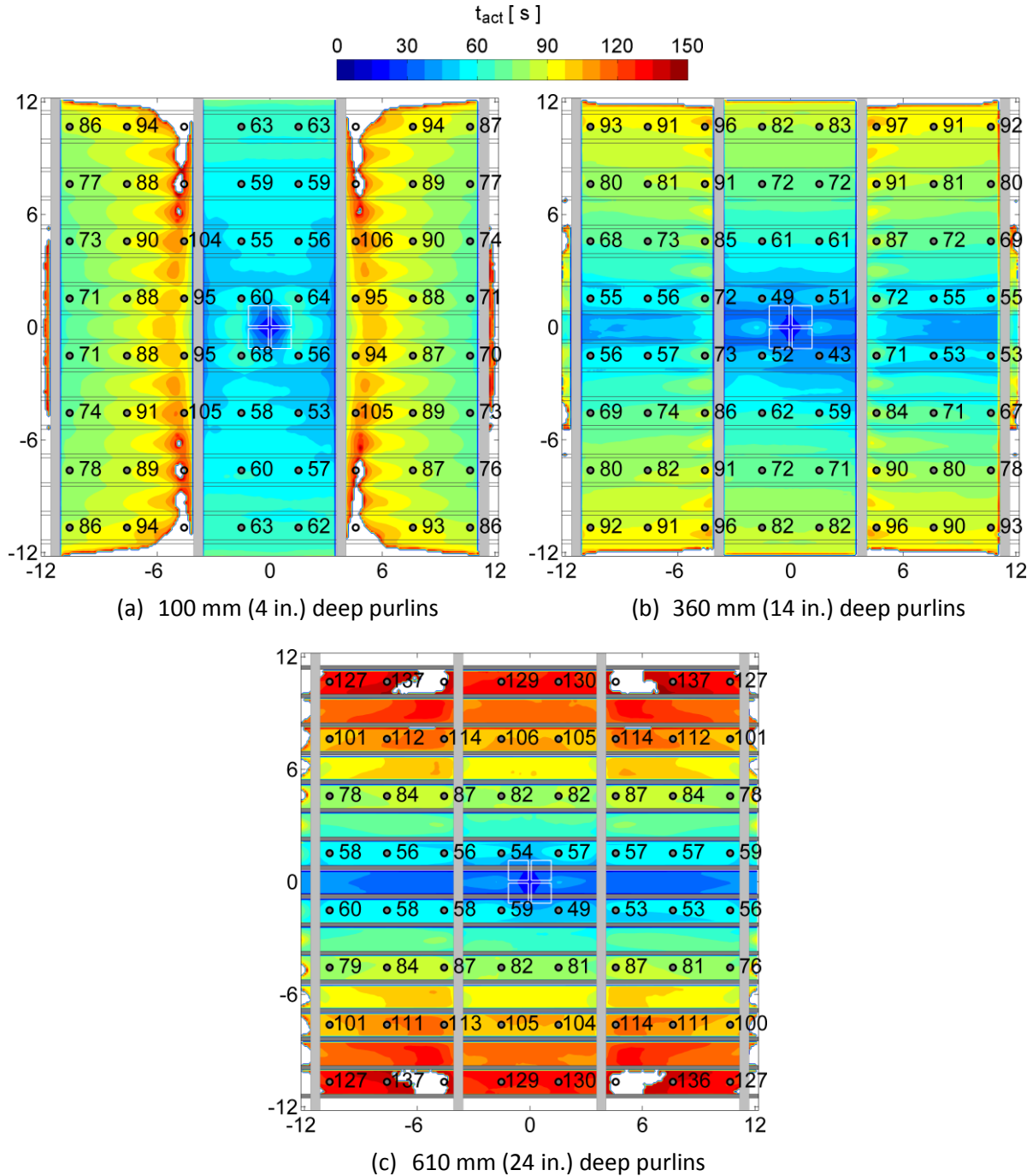


Figure 3-16: Activation time contours for QR/OT sprinkler links below a ceiling located 3.0 m (10 ft) above the CUP rack-storage array in the presence of 610 mm (24 in.) deep girders separated by 7.6 m (25 ft) and purlins with a separation distance of 1.5 m (5 ft) and a depth of (a) 300 mm (12 in.), (b) 460 mm (18 in.), and (c) 610 mm (24 in.). Sprinkler links are 430 mm (17 in.) below the ceiling. Discrete sprinkler locations correspond to an offset sprinkler arrangement with 3.0 m \times 3.0 m (10 ft \times 10 ft) spacing.

3.1.3 Standard-Response, High Temperature Sprinklers

Changing the sprinkler link from QR/OT to SR/HT introduces delays in activation times. For the SR/HT sprinkler link, activation patterns and times are shown in Figure 3-17 for a sprinkler link distance of 330 mm (13 in.). In DS 2-0 [1], the maximum permissible distance for SR/HT sprinkler links is 330 mm (13 in.). For an unobstructed ceiling, the average first ring activation time is 111.4 s, which is 30 s delayed compared to the QR/OT sprinklers. Figure 3-17(a) shows the activation patterns and times for the unobstructed ceiling. As was the case for the QR/OT sprinklers, the presence of obstructed ceiling construction causes on average earlier activations. This can be seen for the 300 mm (12 in.) purlins case in Figure 3-17(b). The average first ring activation time reduces to 88.9 s. The average activation times for purlin depths up to 610 mm (24 in.) are earlier compared to the unobstructed ceiling case. However, as can be observed in Figure 3-17(c-d), flow channeling along the central purlin channels causes skewed activation patterns for the deeper purlins (460–610 mm or 18–24 in.). Table 3-2 provides the comparison of average activation times for the first ring with the central and outer channel sprinkler average activation times.

As demonstrated earlier for the QR/OT sprinklers, for deeper purlins, lowering the sprinkler location helps reduce the skewed sprinkler activation patterns. This is also true for the SR/HT sprinklers located on a plane aligned with the bottom of 610 mm (24 in.) purlins and 150 mm (6 in.) lower than the plane, as can be observed in Figure 3-18. While the average first ring activation time increases marginally to 104.8–107.8 s depending on whether the links are aligned with the bottom of the 610 mm (24 in.) purlins or are 150 mm (6 in.) lower, the average central channel activation times increase to 89.5–97 s. Overall, the biased activation pattern observed for the 330 mm (13 in.) plane below the ceiling is reduced by lowering the sprinkler links. It should be observed, however, that even with lowering the sprinkler links the average activation times remain earlier than in the unobstructed ceiling case.

Table 3-2: Activation times for the eight SR/HT sprinklers surrounding the ignition location. Three times are reported (in s): average for all eight locations, two locations in the central channel, and six locations in the outer two channels.

	Purlin Depth [in.]			
	0	12	18	24
Average	111.4	88.9	95.1	103.4
Central channel	109.0	81.0	76.0	73.5
Outer channels	112.2	91.3	101.5	113.3

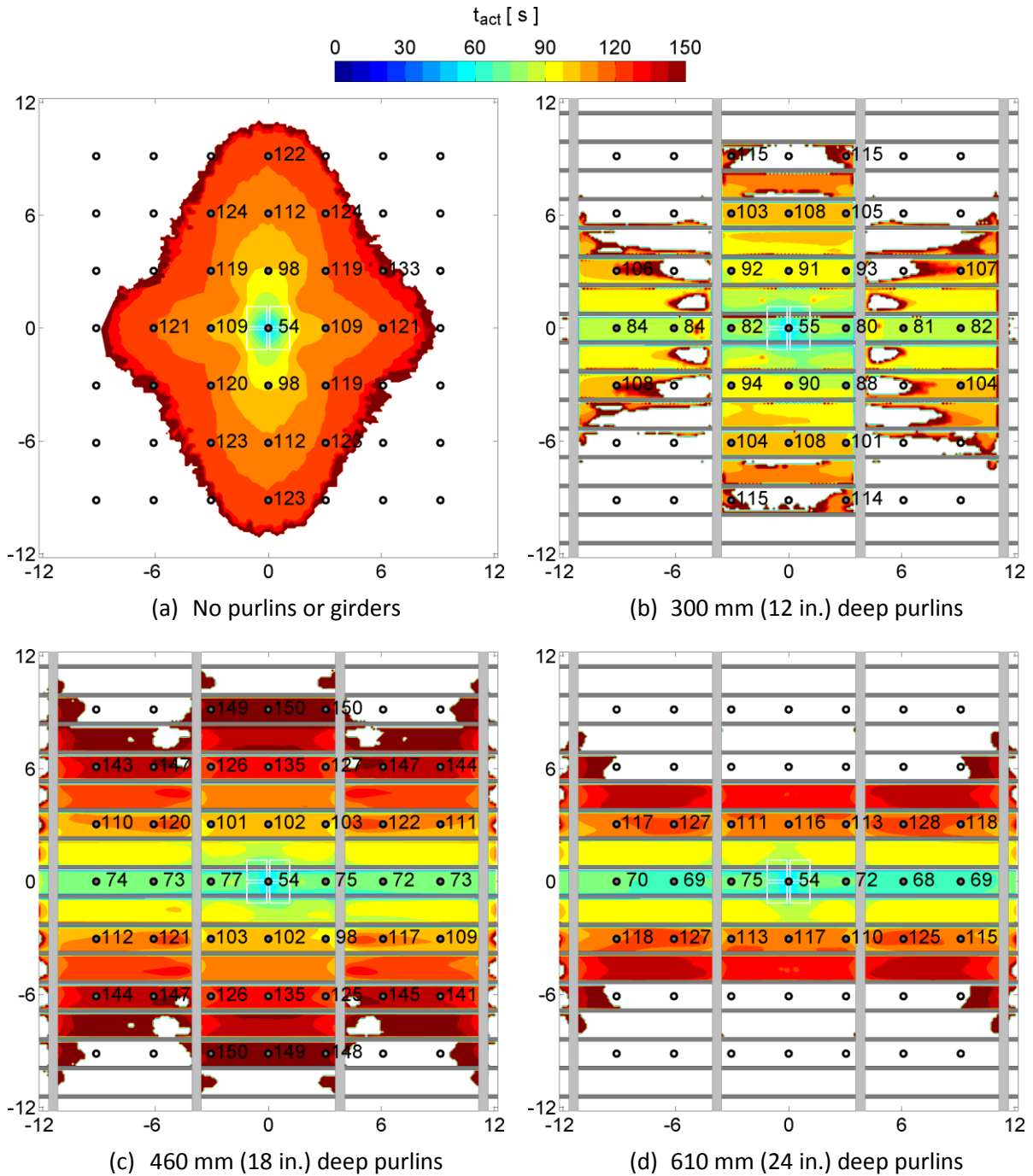


Figure 3-17: Activation time contours for SR/HT sprinkler links at 330 mm (13 in.) below a ceiling located 3.0 m (10 ft) above the CUP rack-storage array in (a) the absence of obstructed ceiling construction, and in the presence of 610 mm (24 in.) deep girders separated by 7.6 m (25 ft) and purlins with a separation distance of 1.5 m (5 ft) and a depth of (b) 300 mm (12 in.), (c) 460 mm (18 in.), and (d) 610 mm (24 in.).

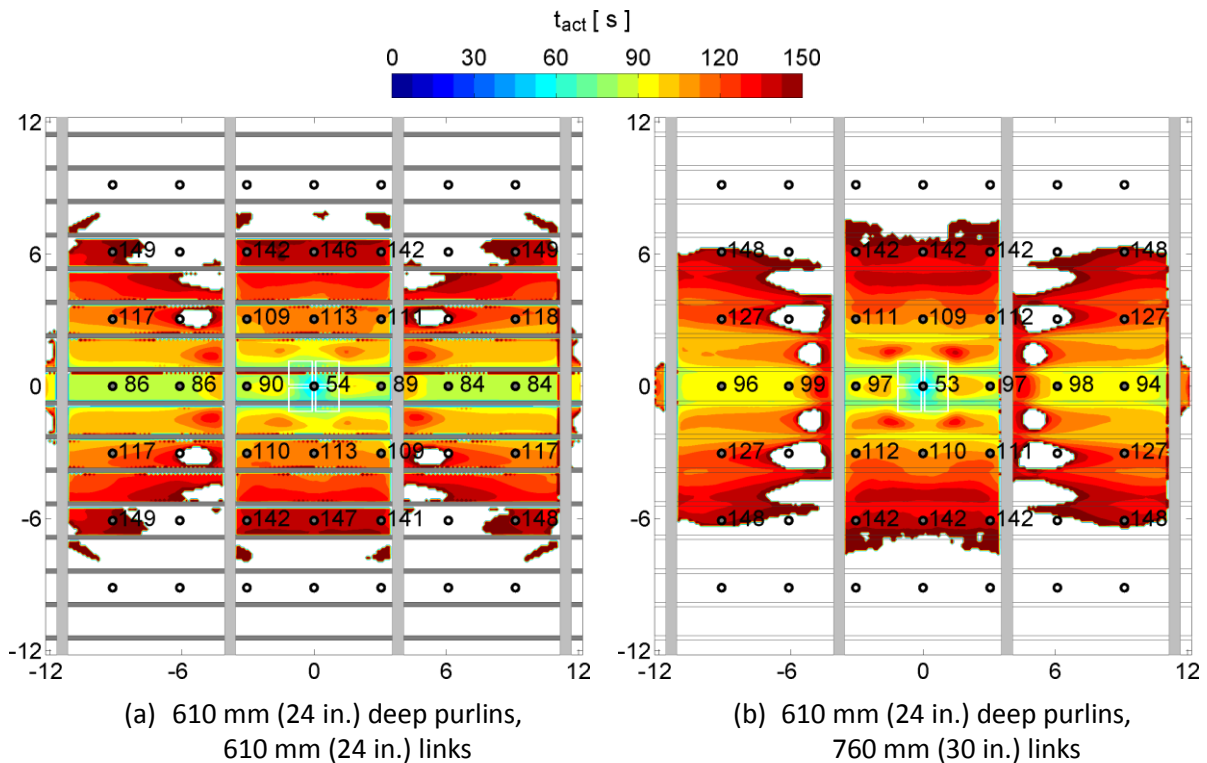


Figure 3-18: Activation time contours for SR/HT sprinkler links below a ceiling located 3.0 m (10 ft) above the CUP rack-storage array in the presence of 610 mm (24 in.) deep girders separated by 7.6 m (25 ft) and purlins with a separation distance of 1.5 m (5 ft) with a purlin depth of 610 mm (24 in.). The sprinkler links are (a) 610 mm (24 in.), and (b) 760 mm (30 in.) below the ceiling.

3.2 UUP Simulations

Sprinkler activation results are presented for the UUP simulations. The ceiling jet influenced by the purlins is first described, followed by discussion on sprinkler activations.

3.2.1 Weak Plume Ceiling Jet

For determining the effect of obstructed ceiling construction on sprinkler activations resulting from an initially weak-plume ceiling jet, the model used the slow fire growth rate of 1.5 m (5 ft) high plastic pallets stored on the floor. The flat part of the ceiling is 7.6 m (25 ft) from the floor in these simulations. The fire chemical HRR was obtained from experimental measurements conducted under the FM Global Research Campus 20 MW Fire Products Collector (FPC). At 375 s, the chemical HRR is ~6 MW and the corresponding ceiling jet is illustrated in Figure 3-19. Instantaneous contours of CO₂ mass fractions, $Y_{CO_2} = 0.02-0.04$, are used as a tracer for illustrating the ceiling jet (colored by temperature in the range of $300\text{ K} \leq T \leq 600\text{ K}$). The unconfined ceiling jet when no obstructed construction is present is shown in Figure 3-19(a). When purlins of a depth of 200 mm (8 in.) are present, the ceiling jet is primarily confined between the central girders, even though significant flow channeling through the purlin

channels is observable in Figure 3-19(b). Increasing the purlin depth to 300 mm (12 in.) causes the channeling effect to increase; however, the flow perpendicular to the purlins is also observed to occur in Figure 3-19(c). For the deepest purlin investigated (610 mm or 24 in.), the ceiling jet is primarily confined to the central channels, as shown in Figure 3-19(d).

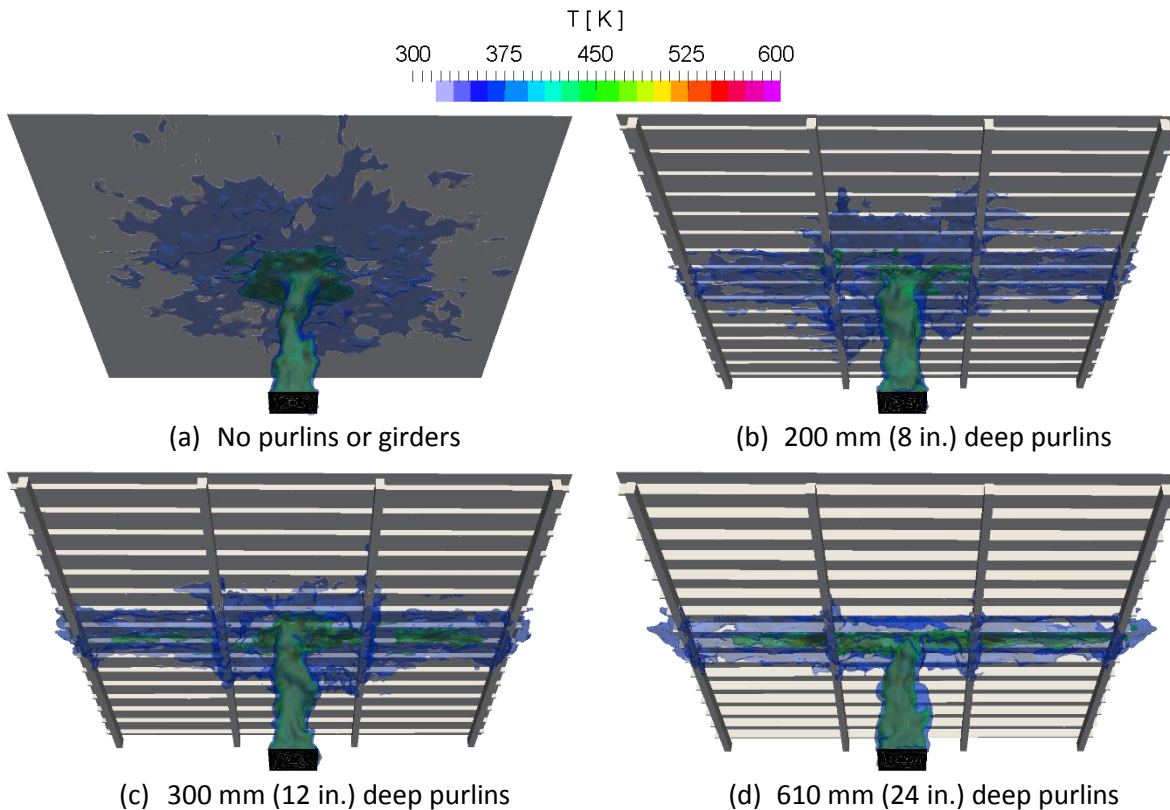


Figure 3-19: Ceiling jet at 375 s depicted by CO₂ contours ($Y_{CO_2} = 0.02-0.04$) under a ceiling located 7.6 m (25 ft) above the UUP fire source in (a) the absence of obstructed ceiling construction, and in the presence of 610 mm (24 in.) deep girders separated by 7.6 m (25 ft) and purlins with a separation distance of 1.5 m (5 ft) and a depth of (b) 200 mm (8 in.), (c) 300 mm (12 in.), and (d) 610 mm (24 in.).

3.2.2 Sprinkler Activation Sequence

For the case of a ceiling with no obstructed construction, the QR/OT sprinkler activation contours are shown in Figure 3-20(a). A symmetric activation pattern around the ceiling mid-point is observed. The average activation time for the first sprinkler ring (excluding the central sprinkler location) is found to be 419 s. The activation patterns and times with purlins of a depth of 200 mm (8 in.) are shown in Figure 3-20(b). Sprinkler links activate in the region between the two central girders with an average first ring activation time of 350 s (the central sprinkler is excluded from the central ring averages, as was the case in the CUP simulations). The presence of purlins causes earlier sprinkler activations around the ignition region, as was the case for the CUP commodity. Increasing the purlin depth to 300 mm (12 in.) results in a lesser number of activations occurring between the central girders. Due to the accumulation

of hot gases near the outer girders, early activations are observed for the outermost sprinkler links in the central channel (at ~364 s) as can be seen in Figure 3-20(c). The average first ring sprinkler activation time is 357 s, which is 62 s earlier compared to the case with the unobstructed ceiling. For the deepest purlin investigated (610 mm or 24 in. depth), due to the strong flow channeling effect, only the sprinklers located in the central and the neighboring two channels will activate within 540 s, as is evident from Figure 3-20(d). The majority of the first ring sprinklers will not activate in the time simulated (540 s). Earlier sprinkler activation times near the outer girders are expected in the two channels adjacent to the central channel, again due to the accumulation of the hot ceiling jet gases. It should be noted that the activation trends and the flow channeling effect observed for the 610 mm (24 in.) purlins were also observed in the simulation using 460 mm (18 in.) purlins.

The flow channeling effect is greater for slower growing fires for commodities like UUP as compared to the faster fire growth observed for the CUP commodity. This is because the weak plume from the UUP fire results in a thin ceiling jet, which tends to remain confined in the channels formed by the deeper purlins (for purlin depths >300 mm or 12 in.). The hot gases tend to escape the ignition region through the gaps above the girders in the central purlin channels, as shown in the close-up image in Figure 3-21(a). A possible remedy for stopping the hot gases from escaping would be the creation of closed purlin channels, as shown in Figure 3-21(b). The channels are closed by obstructing the gap above the 610 mm (24 in.) deep girders. The closing of the purlin channels forces the flow to go in the direction perpendicular to the purlins. Part of the ceiling jet escapes outward by flowing under the girders. In the present study, closed purlin channels of 11.4 m² (125 ft²) are formed with the length of the channels being 7.6 m (25 ft).

For purlins of a depth of 300 mm (12 in.) and 460 mm (18 in.), closing the gaps above the girders causes symmetric activation patterns to develop around the central ignition region, as shown in Figure 3-22. The average activation time for the first sprinkler link decreases marginally from 357 s to 349 s for the 300 mm (12 in.) purlins, whereas for the 460 mm (18 in.) purlins the average activation time is 351 s when the purlin channels are closed. The effect of the closed channels is greater for purlin depths >300 mm (12 in.). For deeper purlins, other remedial measures for achieving near symmetric activation patterns in the first ring, like lowering the sprinkler links and aligning them on a plane passing through the bottom of the purlins, do not have a significant effect for weak-plume-driven ceiling jets. This is demonstrated in Figure 3-23(a): for the 610 mm (24 in.) deep purlins and open channels, lowering the sprinkler links from a 430 mm (17 in.) to a 610 mm (24 in.) distance from the ceiling does not remedy the flow channeling effect. However, in addition to lowering the links, if the purlin channels are closed, the average first ring activation time is found to be 352 s; a symmetric activation pattern also develops around the ignition location as can be observed in Figure 3-23(b).

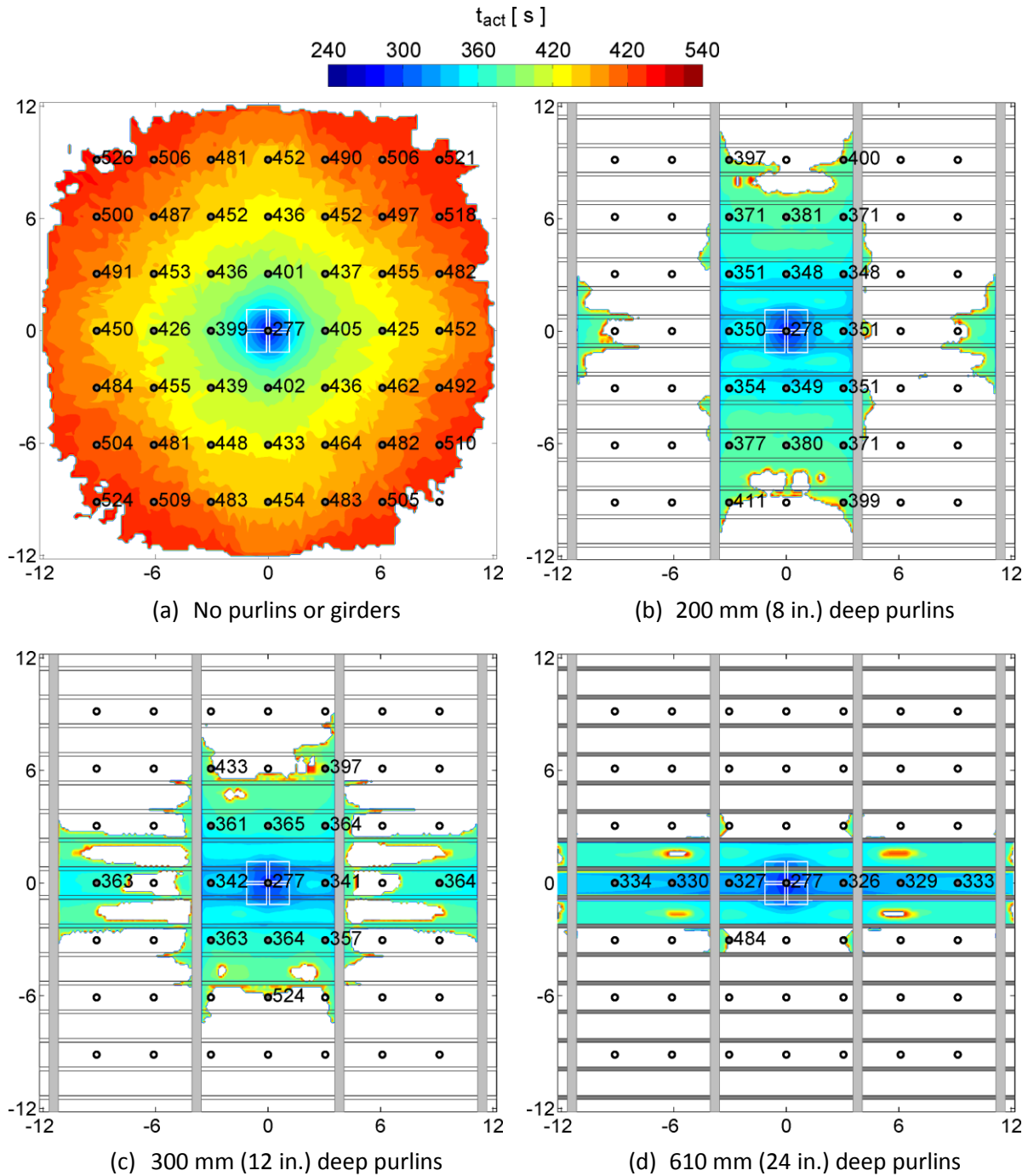


Figure 3-20: Activation time contours for QR/OT sprinkler links at 430 mm (17 in.) below a ceiling located 3.0 m (10 ft) above a UUP fire source in (a) the absence of obstructed ceiling construction, and in the presence of 610 mm (24 in.) deep girders separated by 7.6 m (25 ft) and purlins with a separation distance of 1.5 m (5 ft) and a depth of (b) 200 mm (8 in.), (c) 300 mm (12 in.), and (d) 610 mm (24 in.). Discrete locations of sprinkler links arranged in a 3.0 m × 3.0 m (10 ft × 10 ft) spacing are also shown with the corresponding activation times.

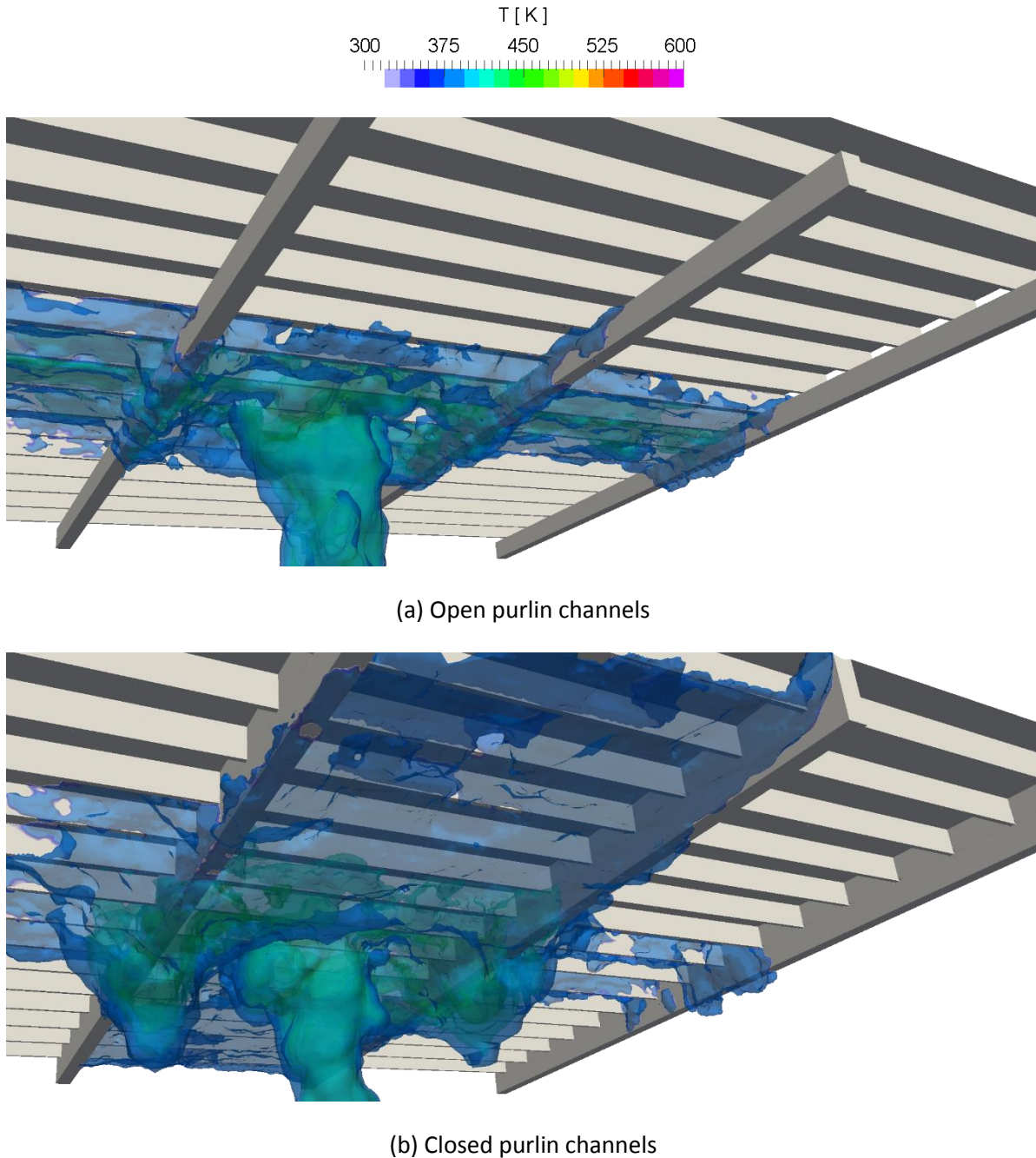


Figure 3-21: Ceiling jet at 395 s depicted by CO₂ contours ($Y_{CO_2} = 0.01-0.04$) under a ceiling located 3.0 m (10 ft) above the UUP fire source with 610 mm (24 in.) deep purlins separated by 1.5 m (5 ft) and girders separated by 7.6 m (25 ft). The purlin channels are (a) open with 610 mm (24 in.) deep girders located below the purlins, and (b) closed by obstructing the top of the 610 mm (24 in.) girders.

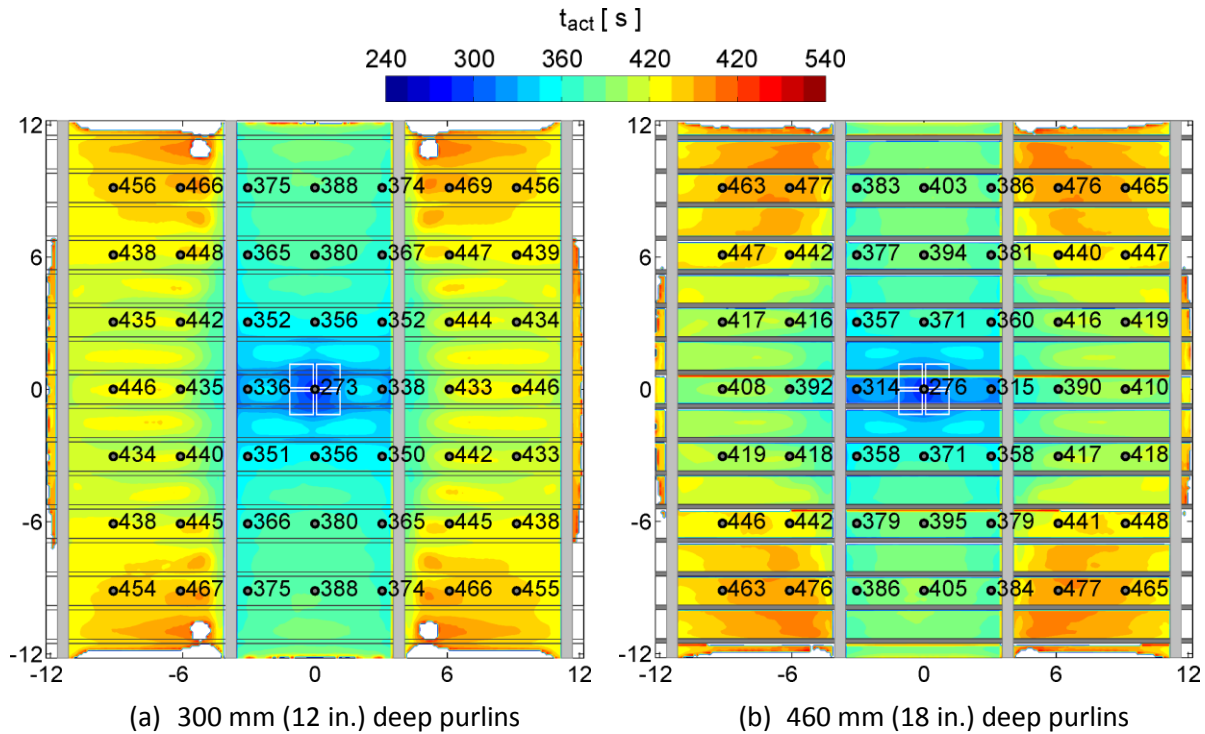


Figure 3-22: Activation time contours for QR/OT sprinkler links at 430 mm (17 in.) below a ceiling located 3.0 m (10 ft) above a UUP fire source. Purlins are separated by 1.5 m (5 ft) and girders by 7.6 m (25 ft) with (a) 300 mm (12 in.), and (b) 460 mm (18 in.) deep purlins. Purlin channels are closed at the girder locations.

3.3 Summary

Based on the sprinkler activation simulations for the CUP rack-storage array fire involving QR/OT sprinklers, the results show that:

- First ring average sprinkler activation time varies between 45 s and 58 s with purlin depth increasing from 100 mm (4 in.) to 610 mm (24 in.). Compared to the case with no obstructed ceiling construction, the average activation times are significantly shorter (23–35 s) indicating that, in most cases, the presence of obstructed ceiling construction could result in early activation of sprinklers.
- Significant channeling of flow along the central purlin channels is observed for purlin depths ≥ 460 mm (18 in). This effect could result in excessive sprinkler activations along the purlin channels and water demand being exceeded.
- For deeper purlins (depths of 530 mm and 610 mm or 21 in. and 24 in.), lowering the sprinkler links from the maximum DS 2-0 permissible depth of 430 mm (17 in.) [1] and locating them on a plane aligned with the bottom of the purlins causes insignificant delays in the average first ring activation time (~ 2 – 3 s). When the links are located at a further distance, 150 mm (6 in.) below the bottom edge of the purlins, the activation delays are 5–6 s. The average activation times are still favorable compared to the unobstructed ceiling case.

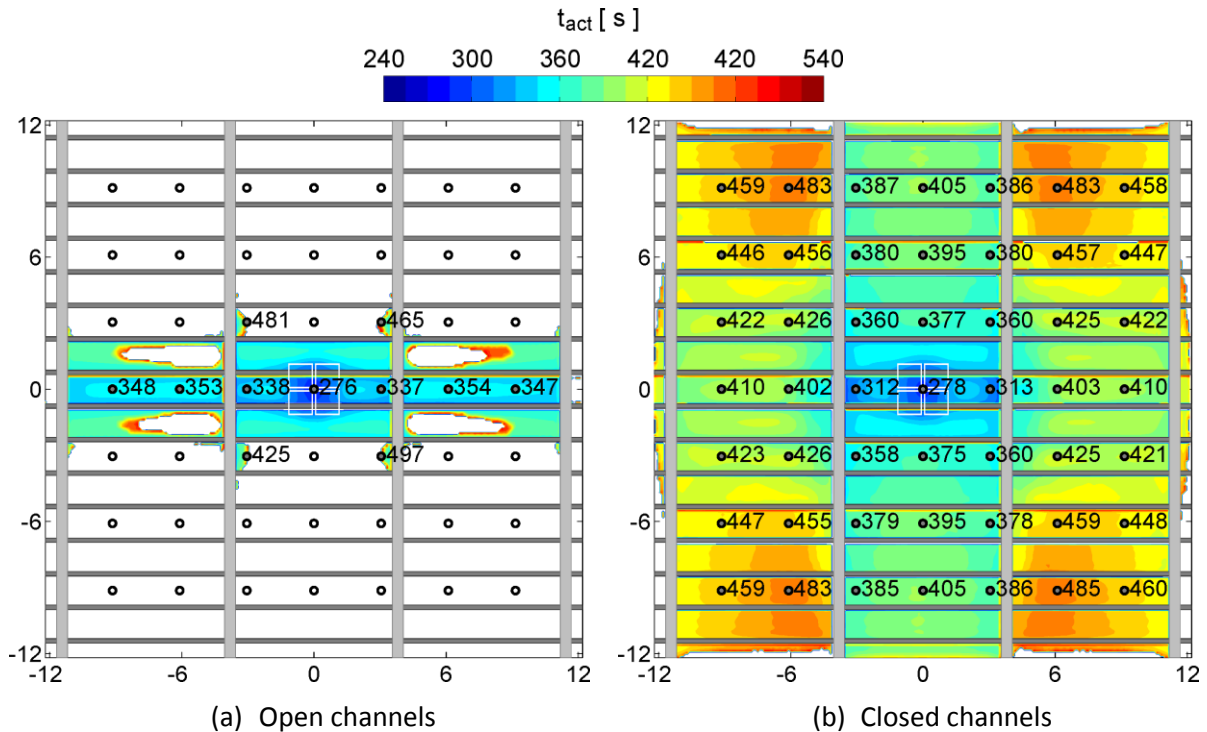


Figure 3-23: Activation time contours for QR/OT sprinkler links below a ceiling located 3.0 m (10 ft) above a UUP fire source in the presence of girders separated by 7.6 m (25 ft). Purlins with a separation distance of 1.5 m (5 ft) and a depth of 610 mm (24 in.) form (a) open channels, and (b) channels closed at the girder locations. Sprinkler links are located 610 mm (24 in.) below the ceiling.

- Decreasing the ceiling clearance from 3.0 m (10 ft) from the top of the CUP rack-storage array to 1.5 m (5 ft), the average first ring activation time increases marginally (~2 s), but stronger flow channeling along the central purlin channels is observed.
- Increasing the purlin separation distance from 1.5 m (5 ft) to 3.0 m (10 ft) causes delays of ~3-8 s for purlin depths up to 610 mm (24 in.), which is still earlier compared to the unobstructed ceiling average activation time. Greater purlin separation distance causes less flow channeling.
- Girder separation distance is found to have a weak effect on sprinkler activation times for distances ≤ 1.8 m (6 ft) from the ceiling mid-point.

For the CUP rack-storage array and SR/HT sprinklers, the results show that:

- As was the case for QR/OT sprinklers, first ring sprinkler activation times for SR/HT sprinklers are shorter by 8–30 s compared to the case with an unobstructed ceiling for purlin depths of 300 mm (12 in.) to 610 mm (24 in.). This supports the observation made for QR/OT sprinklers, that the presence of obstructed ceiling construction could result in early activation of SR/HT sprinklers.
- For deeper purlins (depths up to 610 mm or 24 in.), lowering the sprinkler links from the maximum DS 2-0 permissible depth of 330 mm (13 in.) [1] and locating them on a plane aligned

with the bottom of the purlins causes insignificant delays in the average first ring activation time (~1 s). As for the QR/OT sprinklers, the average SR/HT activation times are also favorable compared to the unobstructed ceiling case.

Based on the sprinkler activation simulations for a UUP source fire involving QR/OT sprinklers, the results show that:

- For a slow growing fire, like in the case of UUP rack-storage fire growth, a weak plume initially develops causing a thin ceiling jet to exist until the HRR becomes large (on the order of 9 MW chemical or 4 MW convective). Due to the weak ceiling jet development, significant flow channeling along the central purlin channels is observed.
- For purlin depths ≤ 300 mm (12 in.), the channeling effect does not disrupt symmetric activations of the first ring sprinklers.
- For purlin depths > 300 mm (12 in.), activations occur primarily in the central purlin channels. Symmetric activations around the ignition region are not observed.
- Mitigation of the flow channeling effect is possible by closing the purlin channel gaps above the girders. By creating closed purlin channels of 11.4 m^2 (125 ft^2) cross-sectional area (corresponding to purlin channel length of 7.6 m or 25 ft), symmetric sprinkler activations are observed for purlin depths > 300 mm (12 in.).

3.4 Large-scale Testing Recommendations

Based on the numerical simulation results and prior large-scale testing experience in the absence of obstructed ceiling construction, the following recommendations were made for conducting the large-scale fire tests:

- Although the numerical simulations were conducted using a 3-tier-high array, a 4-tier CUP array is to be used as previous testing results (in the absence of obstructed ceiling construction) are available for comparison of test performance.
- Purlin depths up to 610 mm (24 in.) should be considered for testing with a separation distance of 1.5 m (5 ft). Girders of a 610 mm (24 in.) depth separated by 7.6 m (25 ft) should be used.
- Ceiling clearance should be kept at 1.5 m (5 ft) based on the greater channeling effect on sprinkler activations observed in the simulation results.
- Sprinkler link location should be kept at 430 mm (17 in.) for purlin depths up to 460 mm (18 in.). For greater purlin depths, the sprinkler links should be in a plane passing through the bottom of the purlins.
- As observed from the numerical simulation results, using an offset sprinkler arrangement would cause greater activation delays. Therefore, an offset arrangement is recommended for the tests. Following DS 8-9 recommendations [24], the sprinkler spacing could be a maximum of $2.4 \text{ m} \times 3.7 \text{ m}$ ($8 \text{ ft} \times 12 \text{ ft}$). This arrangement would also ensure that two central purlin channels are devoid of sprinklers, which would cause greater challenges to protection design, especially for the deeper purlins.

- The main rack-storage array is recommended to be aligned with the purlin channels. In the absence of sprinklers in the two central purlin channels, in this arrangement, control of lateral fire spread could be difficult. The arrangement is also selected as in the case of warehouses with sloped ceilings, the purlins are arranged perpendicular to the slope and the racks are generally aligned with the purlins.
- In addition to the CUP tests, a single test using the UUP commodity is proposed to confirm the greater ceiling jet channeling effect predicted by the model. The purlin channels are to be kept open for all the tests.

The flowchart shown in Figure 3-24 explains the test plan for the CUP commodity based on whether a certain test is deemed to pass or fail.

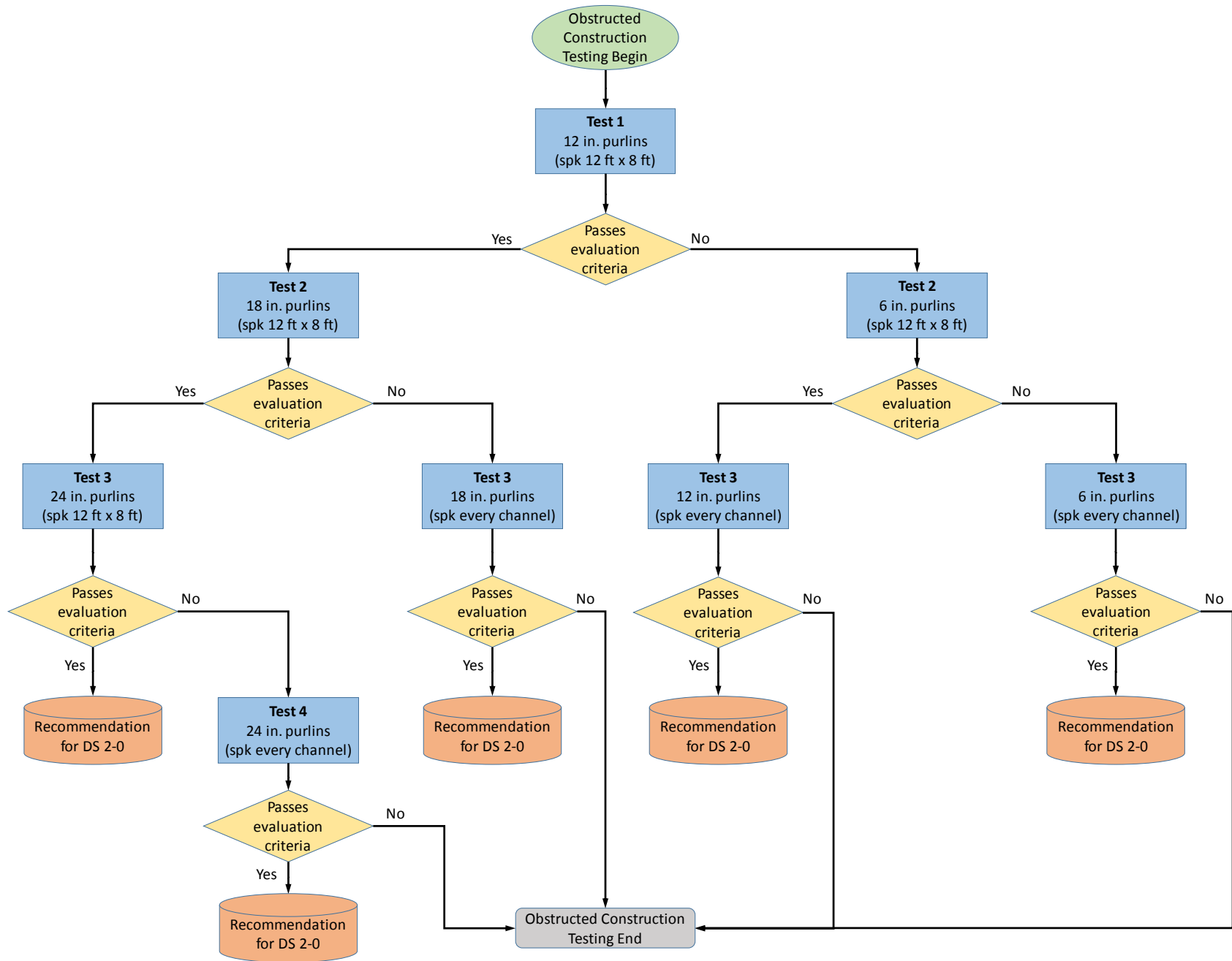


Figure 3-24: Flowchart for determining the sequence of the CUP large-scale tests.

4. Large-scale Testing Results and Discussion

Large-scale tests were designed based on the results from the numerical modeling study and following previous testing conducted under unobstructed ceilings. The test parameters, environmental conditions and instrumentation, test evaluation criteria, and results are presented below.

4.1 Test Parameters

Three tests were conducted for 4-tier-high rack storage of the CUP commodity under ceilings with obstructed ceiling construction. A fourth test was also conducted for 4-tier-high rack storage of the UUP commodity to evaluate the flow channeling effect caused by the initial presence of a weak-momentum ceiling jet confined in the deep purlin channels. The obstructed ceiling construction attached to the south moveable ceiling at the FM Global Research Campus consisted of 0.61 m (2 ft) deep girders and purlins of a depth of 300–610 mm (12–24 in.). The girders (separated by 7.6 m or 25 ft) and purlins (separated by 1.5 m or 5 ft) were constructed using sheet metal.

The methodology followed two previous tests conducted using the CUP and UUP commodities under non-obstructed ceilings [7]. The previously conducted CUP test involved fire growth over a 4-tier rack storage array of 6.1 m (20 ft) height located under a 7.6 m (25 ft) ceiling, and protection using K360 lpm/bar^{0.5} (K25.2 gpm/psi^{0.5}) quick-response, pendent sprinklers with 74°C (165°F) links operating at ~0.97 barg (14 psig) pressure and arranged in a 2.4 m × 3.7 m (8 ft × 12 ft) spacing. Four sprinklers operated during the test and controlled the fire. The fire did not spread to the ends of the main array and target arrays were not ignited. Perimeter sprinklers were not activated during the test. The peak measured steel temperature was within acceptable limits. The sprinkler design was determined to be adequate to protect the commodity.

In the UUP baseline test, the rack storage and ceiling heights were identical to the CUP test described above and the same sprinkler protection design was applied. Fifteen sprinklers operated during the test. The fire did not spread to the ends of the main array and the target arrays were not ignited. The peak measured steel temperature was within acceptable limits.

Figure 4-1 shows the test setup with the obstructed ceiling located above a 4-tier-high rack storage arrangement of the CUP commodity. Purlin depths (d_p) considered for testing were 300 mm (12 in.), 460 mm (18 in.), and 610 mm (24 in.). These depths cover the range of conditions investigated using the numerical model. Table 4-1 provides details of the dimensions and sprinklers.

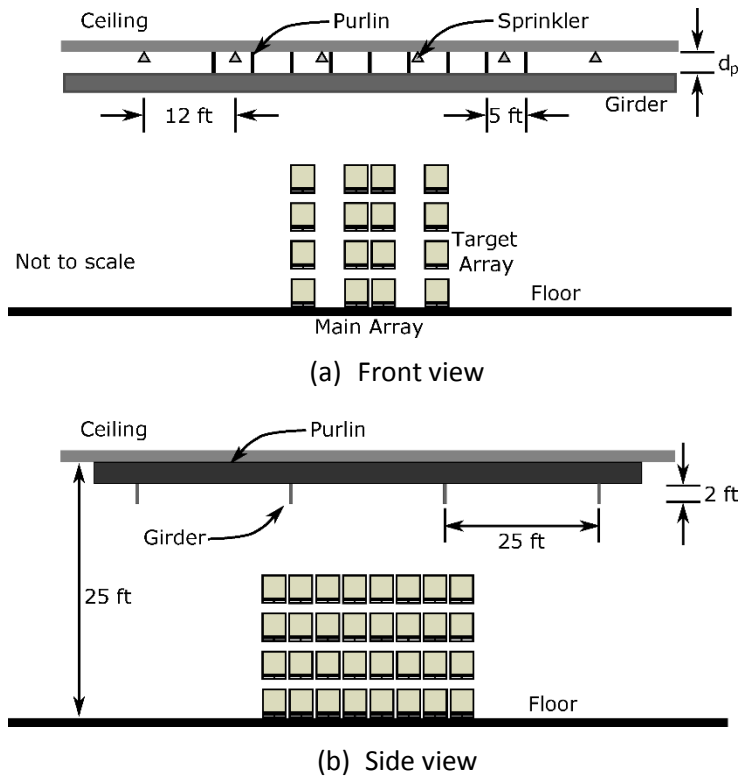


Figure 4-1: Testing setup (not to scale) showing a 4-tier-high CUP rack storage array as a fire source with two target arrays (separated by 1.2 m or 4 ft), 610 mm (24 in.) tall girders spaced 7.6 m (25 ft) apart, and purlins of depth d_p separated by 1.5 m (5 ft): (a) front view showing purlins, and (b) side view showing girders present below the purlins.

Table 4-1: Parameters used in the obstructed ceiling construction tests.

Fire plume source		4-tier-high rack storage of CUP and UUP
Ceiling height (H)		7.6 m (25 ft)
Purlin	depth (d_p)	300 mm (12 in.), 460 mm (18 in.), and 610 mm (24 in.)
	spacing	1.5 m (5 ft)
Girder	depth	0.61 m (2 ft)
	spacing	7.6 m (25 ft)
Sprinklers	type	Pendent, quick-response
	link temperature	74°C (165°F)
	K-factor	K360 lpm/bar ^{0.5} (K25.2 gpm/psi ^{0.5})
	pressure, flow rate	~0.97 barg (14 psig), 380 lpm (100 gpm) per sprinkler
	spacing	2.4 m × 3.7 m (8 ft × 12 ft)
	link clearance	430-580 mm (17-23 in.) from ceiling

4.1.1 Test Commodities

FM Global standard CUP and UUP commodities were used in the tests, as described above. The CUP commodity consists of rigid crystalline polystyrene cups (empty, 0.46 l or 16 oz.), packaged, face down and in a single-wall corrugated containerboard box. The cups are individually compartmented, each layer separated by a corrugated containerboard pad arranged in five layers of 25 cups per layer, yielding a total of 125 cups per box. Eight 530 mm (21 in.) cubic cartons are arranged in a 2 × 2 × 2 arrangement for a total dimension of 1.07 m × 1.07 m × 1.07 m (3.5 ft × 3.5 ft × 3.5 ft), supported on an ordinary, two-way, slatted deck hardwood pallet. Total combustible weight of one pallet load is approximately ~73.8 kg (165.8 lb) – corrugated containerboard (~19.8 kg or 44.8 lb), plastic cups (~31.6 kg or 110.8 lb), and hardwood pallet supporting the commodity (~22.4 kg or 49.4 lb). A photograph of the CUP commodity is shown in Figure 4-2(a). The UUP commodity consists of seven pallets made of high-density polyethylene stacked on top of a two-way slatted deck hardwood pallet resulting in an overall dimension of 1.07 m × 1.22 m × 1.11 m (3.5 ft × 4 ft × 3.7 ft). The plastic pallets weigh ~177.9 kg (392.2 lb) and the hardwood pallet weighs ~22.4 kg (49.4 lb). A photograph of the UUP commodity is shown in Figure 4-2(b).



(a) CUP



(b) UUP

Figure 4-2: FM Global standard (a) CUP, and (b) UUP commodities

4.1.2 Automatic Sprinkler Protection

An FM Approved QR pendent sprinkler with a link rated temperature of 74°C (165°F) was used in this series of tests. Details of the sprinkler properties are summarized in Table 4-1. The sprinkler was installed on a nominal 63.5 mm (2.5 in.) diameter steel piping at a spacing of 2.4 m × 3.7 m (8 ft × 12 ft). The water pressure was set to ~0.97 barg (14 psig) providing a nominal water design density of 41 mm/min (1.0 gpm/ft²) for all tests. The ceiling to sprinkler link distance was set to 430 mm (17 in.) in Tests #1 and 2, and to 580 mm (23 in.) in Tests #3 and 4.

4.1.3 Test Setup

Figure 4-3 shows a plan view of the locations of purlins and girders relative to the sprinkler, piping and the CUP commodity. Nine purlins and four girders were attached to the south moveable ceiling. The sprinkler branch lines were oriented perpendicular to the purlins. For the deeper purlins ($d_p \geq 460$ mm or 18 in.), slots were cut into the sheet metal to accommodate the sprinkler pipes. Tests were carried out with ignition between two sprinklers with an offset distance of 0.61 m (2 ft) from the center of the main array (shown by the red star in Figure 4-3). In this configuration, two central channels do not have sprinklers present, making it a worst-case scenario from a protection standpoint.

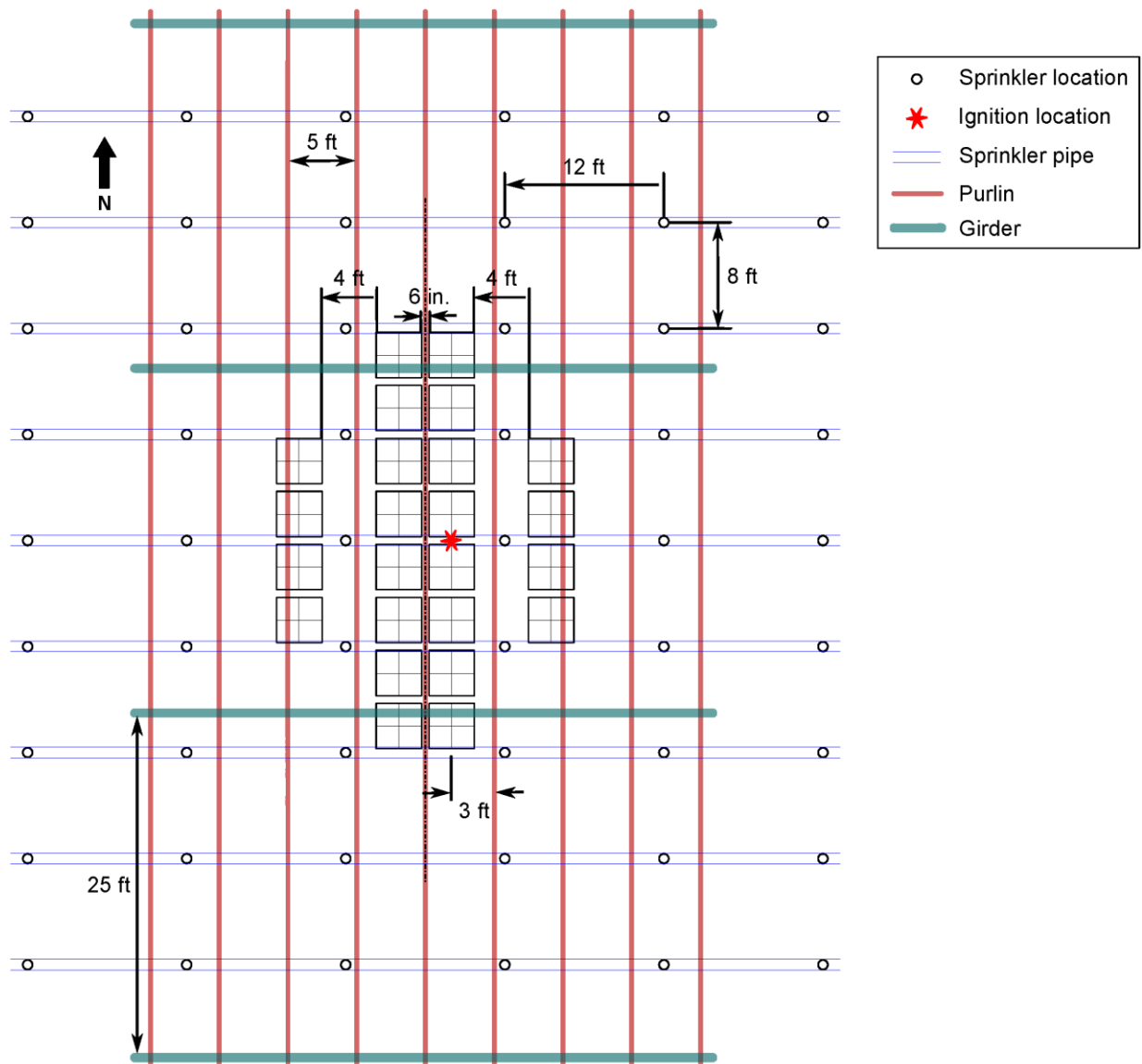


Figure 4-3: Plan view of the test array (CUP commodity) with ignition placed between two sprinklers. The sprinklers, piping, purlin, and girder distances relative to the test array are shown.

4.1.4 Storage Arrangement

The storage arrangement for all four tests consisted of a double row, open frame rack main array and two single row open frame target arrays. The main array ran north-south and was two pallet loads' wide and eight pallet loads' long. The main array was aligned with the purlin channels as this was believed to be a challenging arrangement that would allow for the fire to reach the end of the array if significant channeling effect was experienced. This arrangement, therefore, could be considered to provide a worst-case scenario for protection. The target arrays were one pallet load wide and four pallet loads' long. They were placed to the east and west of the main array with an aisle width of 1.2 m (4 ft). All the longitudinal and transverse flues were a nominal 150 mm (6 in.). The horizontal part of the ceiling was set to a height of 7.6 m (25 ft) for all the tests. The storage height was nominal 6.1 m (20 ft) for all the tests. Figure 4-4 shows photographs of the CUP and UUP test arrays from Tests #3 and 4, respectively. The 610 mm (24 in.) deep purlins and girders are also visible in the photograph.

4.1.5 Ignition

For all the tests, ignition was achieved using two standard FM Global half igniters, which are cylinders made of rolled cellucotton soaked in 113 ml (4 oz.) of gasoline. The igniters were positioned at the base of the lower tier, in the center of the flue space separating two pallets. The ignition location was between two sprinklers, offset within the rack, 0.61 m (2 ft) from the centerline of the longitudinal flue.

4.2 Recording and Instrumentation

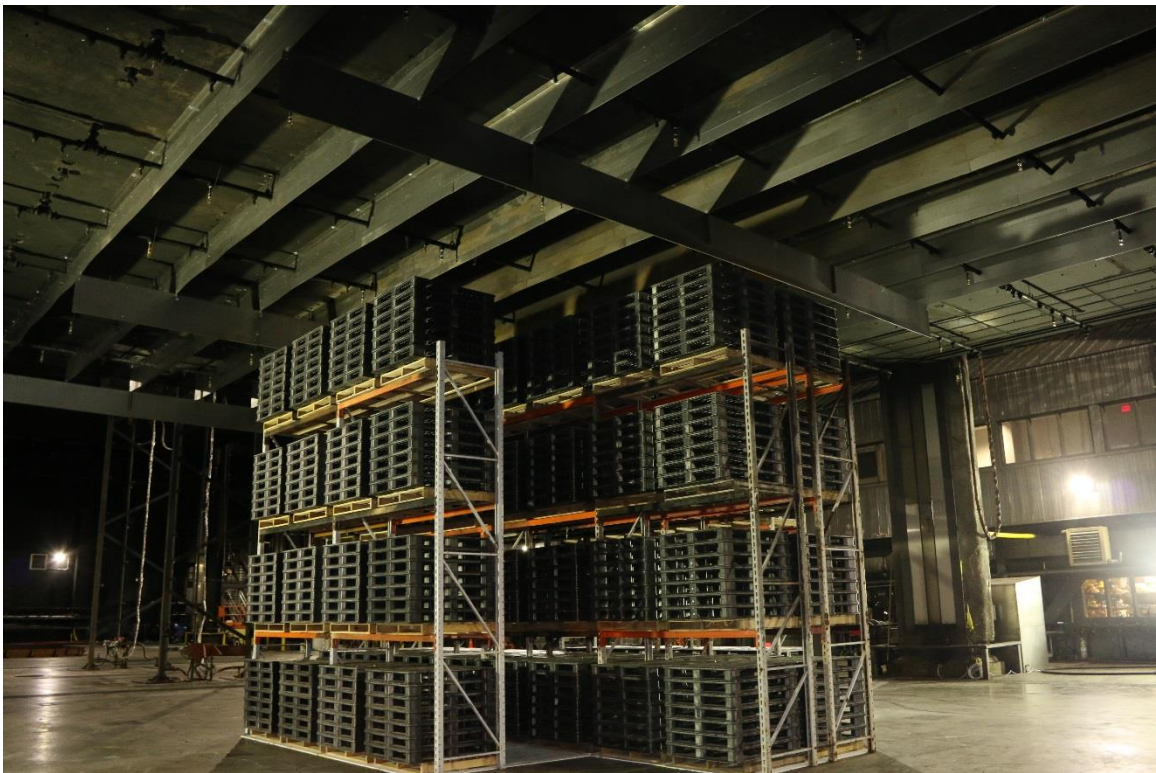
Documentation for the tests included video, still photographs, and audio recordings of the visual observations. The video documentation included four High-Definition (HD) digital video cameras, two "bullet" video cameras, one elevated GoPro video camera, and an infrared (IR) camera for qualitative assessments of the fire. The camera layout for the tests is shown in Figure 4-5.

The following instrumentation was included during the tests:

- Bare-bead, 0.8 mm (20 gauge), Chromel-Alumel (K-type) thermocouples installed 165 mm (6.5 in.) below the ceiling at ceiling center and numerous locations radially outward. The thermocouples have an RTI of $8.0 \pm 1.5 \text{ (m-s)}^{0.5}$ ($14.5 \pm 2.7 \text{ (ft-s)}^{0.5}$).
- Thermocouples embedded in a cross-shaped steel angle at the ceiling center measured steel temperatures. Thermocouples are embedded at the center of the cross and at 150 mm (6 in.) intervals along the length of each of the four legs (total cross-leg length of 0.61 m or 2 ft).
- Flow meters and pressure controllers to monitor and control the sprinkler system.
- Electrical circuits on each sprinkler to determine individual sprinkler activation times.



(a) CUP Test #3



(b) UUP Test #4

Figure 4-4: Photographs of test arrays: (a) CUP Test #3, and (b) UUP Test #4.

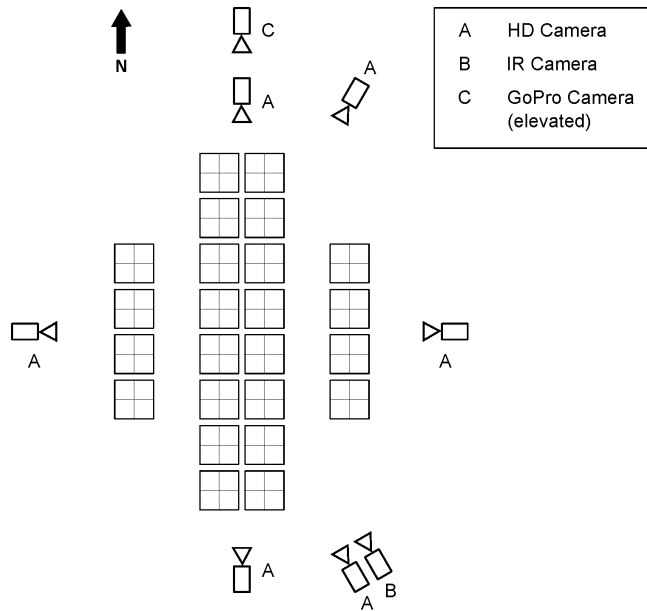


Figure 4-5: Camera locations and types in the three tests.

4.3 Test Evaluation Criteria

The results of large-scale fire tests are evaluated using the following conditions:

- Ideally, the same number of sprinkler operations should occur in the presence of obstructed ceiling construction compared to the baseline tests. In practical terms, the total number of activations on the same order of magnitude (within 2–3 operations) would be acceptable. In the CUP baseline test, four sprinklers operated, whereas in the UUP baseline test, 15 sprinkler operations were observed. Therefore, an ideal scenario for a successful test in the present series would be if sprinkler operations are restricted to a maximum of six–seven for the CUP and 17–18 for the UUP tests, respectively.
- No perimeter sprinkler activations, indicating that further activation of sprinklers would not occur if the ceiling were larger and additional sprinklers were present.
- Extent of fire spread – ideally, the fire spread should be similar to the observed spread in the baseline tests. At worst, the fire should not spread to either end of the main array. Target ignition is permitted but the fire should not propagate to the back of the target commodity.
- Temperatures of steel angle on the ceiling – temperatures encountered in the tests should be in the range observed during the baseline tests and the peak temperature of the steel angle should not exceed 538°C (1000°F).

4.4 Summary of Test Results

Results from the four tests are summarized in this section. A general overview of each test is provided with detailed data presented below. Baseline test results are also included for reference. Test chronologies of the fire events can be found in Appendix A. Summaries of test parameters and results are provided below in Table 4-2 for the CUP tests and in Table 4-3 for the UUP tests, respectively. All times stated are from the start of the fire (i.e., ignition) and are expressed as min:s unless otherwise noted.

Table 4-2: Summary of test parameters and results for the CUP tests.

	Test #	Baseline	1	2	3
	Test date	01/21/2015	02/01/2017	02/10/2017	02/17/2017
	Test site	South moveable ceiling of LBL			
TEST PARAMETERS	Test commodity	CUP			
	Purlin depth [mm (in.)]	0 (0)	300 (12)	460 (18)	610 (24)
	Purlin separation distance [m (ft)]	0 (0)	1.5 (5)		
	Girder depth [mm (in.)]	0 (0)	610 (24)		
	Girder separation distance [m (ft)]	0 (0)	7.6 (25)		
	Array size (main)	2 × 8 × 4			
	Array size (target)	1 × 4 × 4			
	Number of storage levels	4			
	Nominal storage height [m (ft)]	6.1 (20)			
	Nominal ceiling clearance [m (ft)]	1.5 (5)			
	Ceiling height [m (ft)]	7.6 (25)			
	Aisle width [m (ft)]	1.2 (4)			
	Ignition location	Offset, between two			
	Sprinkler orientation	Pendent			
	Sprinkler K-factor [lpm/bar ^{0.5} (gpm/psi ^{0.5})]	360 (25.2)			
	Sprinkler temperature rating [°C (°F)]	74 (165)			
	Nominal RTI [(m-s) ^{0.5} ((ft-s) ^{0.5})]	22 (40) - QR			
	Sprinkler spacing [m (ft)]	2.4 × 3.7 (8 × 12)			
	Discharge pressure [barg (psig)]	0.97 (14)			
	Discharge density [mm/min (gpm/ft ²)]	41 (1.0)			
	Distance of sprinkler link from ceiling [mm (in.)]	430 (17)	430 (17)	430 (17)	580 (23)
	TEST RESULTS	First sprinkler operation (min:s)	01:26	01:28	01:32
Last sprinkler operation (min:s)		02:30	01:37	01:43	01:31
Total number of sprinkler actuations		4	5	6	5
Perimeter sprinkler operations		No	No	No	No
Peak ceiling gas temperature [°C (°F)]		837 (1538)	720 (1329)	890 (1626)	880 (1615)
Peak steel temperature [°C (°F)]		115 (239)	84 (183)	100 (212)	100 (214)
Fire to ends of main array		No	No	No	No
Aisle jump		No	No	No	No
Total duration (min)		30	30	30	30

Table 4-3: Summary of test parameters and results for the UUP tests.

	Test #	Baseline	4
	TEST PARAMETERS	Test date	09/14/2012
Test site		South moveable ceiling of LBL	
Test commodity		UUP	
Purlin depth [mm (in.)]		0 (0)	610 (24)
Purlin separation distance [m (ft)]		0 (0)	1.5 (5)
Girder depth [mm (in.)]		0 (0)	610 (24)
Girder separation distance [m (ft)]		0 (0)	7.6 (25)
Array size (main)		2 × 8 × 4	
Array size (target)		1 × 4 × 4	
Number of storage levels		4	
Nominal storage height [m (ft)]		6.1 (20)	
Nominal ceiling clearance [m (ft)]		1.5 (5)	
Ceiling height [m (ft)]		7.6 (25)	
Aisle width [m (ft)]		1.2 (4)	
Ignition location		Offset, between two	
Sprinkler orientation		Pendent	
Sprinkler K-factor [lpm/bar ^{0.5} (gpm/psi ^{0.5})]		360 (25.2)	
Sprinkler temperature rating [°C (°F)]		74 (165)	
Nominal RTI [(m-s) ^{0.5} ((ft-s) ^{0.5})]		22 (40) - QR	
Sprinkler spacing [m (ft)]		2.4 × 3.7 (8 × 12)	
Discharge pressure [barg (psig)]		0.97 (14)	
Discharge density [mm/min (gpm/ft ²)]		41 (1.0)	
Distance of sprinkler link from ceiling [mm (in.)]		430 (17)	580 (23)
TEST RESULTS		First sprinkler operation (min:s)	06:08
	Last sprinkler operation (min:s)	11:34	20:23
	Total number of sprinkler actuations	15	14
	Perimeter sprinkler operations	Yes (1)	Yes (2)
	Peak ceiling gas temperature [°C (°F)]	524 (976)	880 (1618)
	Peak steel temperature [°C (°F)]	107 (225)	220 (422)
	Fire to ends of main array	No	No
	Aisle jump	No	No
Total duration (min)	30	30	

4.5 Test #1 Results

The purpose of Test #1 was to determine if the presence of the obstructed ceiling construction had a significant impact on the performance of the ceiling sprinklers compared to the CUP baseline test. Obstructed ceiling construction was present below the horizontal ceiling in the form of 300 mm (12 in.) deep purlins separated by 1.5 m (5 ft) and 610 mm (24 in.) deep girders separated by 7.6 m (25 ft). FM Approved K360 (K25.2) pendent QR sprinklers were installed such that the distance between the links and the ceiling was 430 mm (17 in.).

4.5.1 Highlights

A detailed description of fire chronology and a few selected photographs from the test are provided in Sections A.1 and B.1 of Appendix A and Appendix B, respectively. The flame reached the ceiling level 53 s after ignition. The first sprinkler operated at 1 min 28 s. White smoke descended to the floor partially obscuring the array. Four additional sprinklers operated by 1 min 37 s. By 1 min 47 s, flames were reduced to below the third tier. The fire gradually became less intense and ceiling temperatures decreased to 93°C (200°F) at approximately 3 min. At 7 min, peak ceiling temperatures were below 38°C (100°F). The test was terminated at 30 min.

4.5.2 Results and Damage Assessment

Figure 4-6 shows the sprinkler operation pattern and the plan view of the damage assessment. A total of five sprinklers operated during the test. None of the perimeter sprinklers operated. The fire neither reached the ends of the main array nor the target arrays. Figure 4-7 shows the damage to the east and west faces of the main array. The peak steel temperature was 83°C (182°F) and was within acceptable limits (see Figure 4-8 for details). Water pressure in the sprinkler pipes was maintained within acceptable bounds as shown in Figure 4-9. Compared to the baseline test (four sprinkler activations), one additional sprinkler activated. The skipping observed in the baseline test was not observed in this test and considerably reduced commodity damage was noticed.

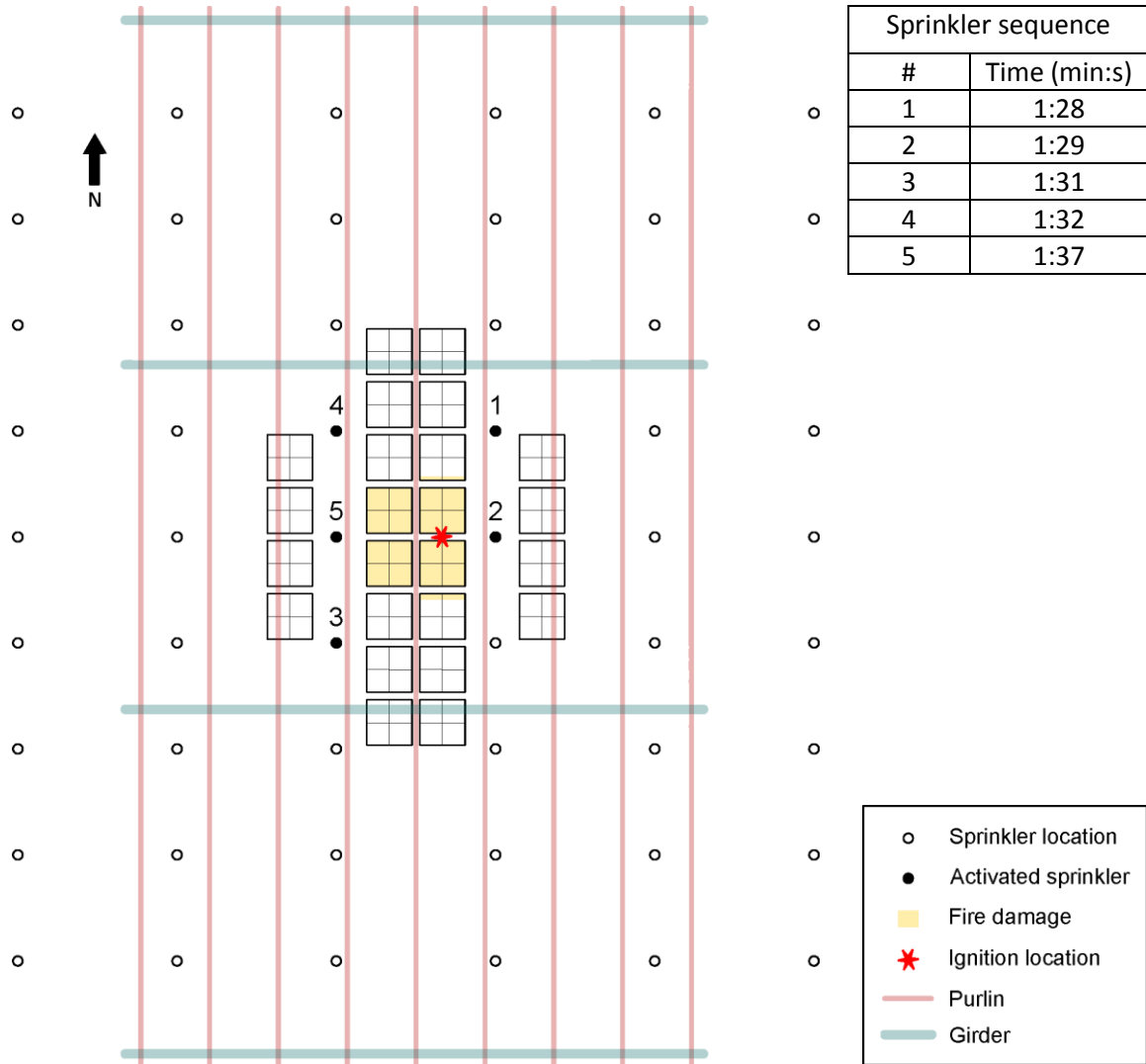


Figure 4-6: Sprinkler operation pattern and top view of damage assessment for Test #1.

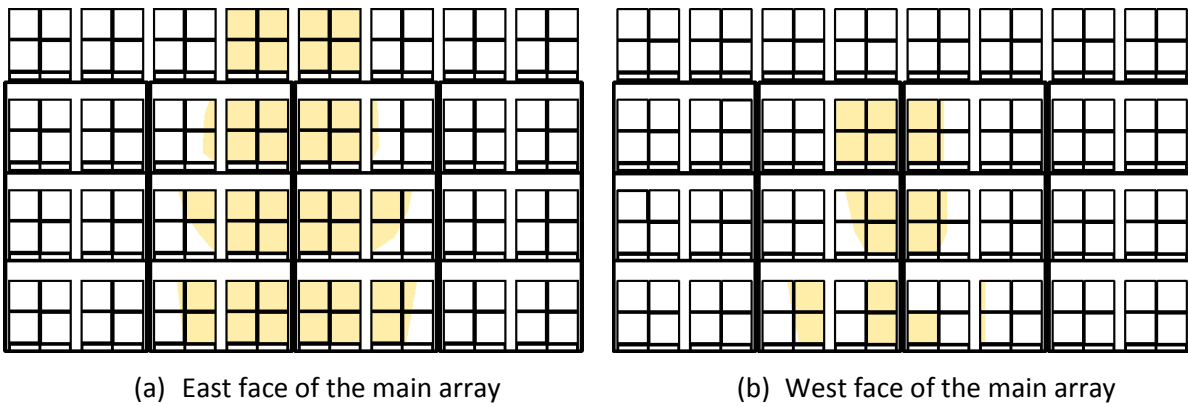


Figure 4-7: Damage assessment on the main array for Test #1.

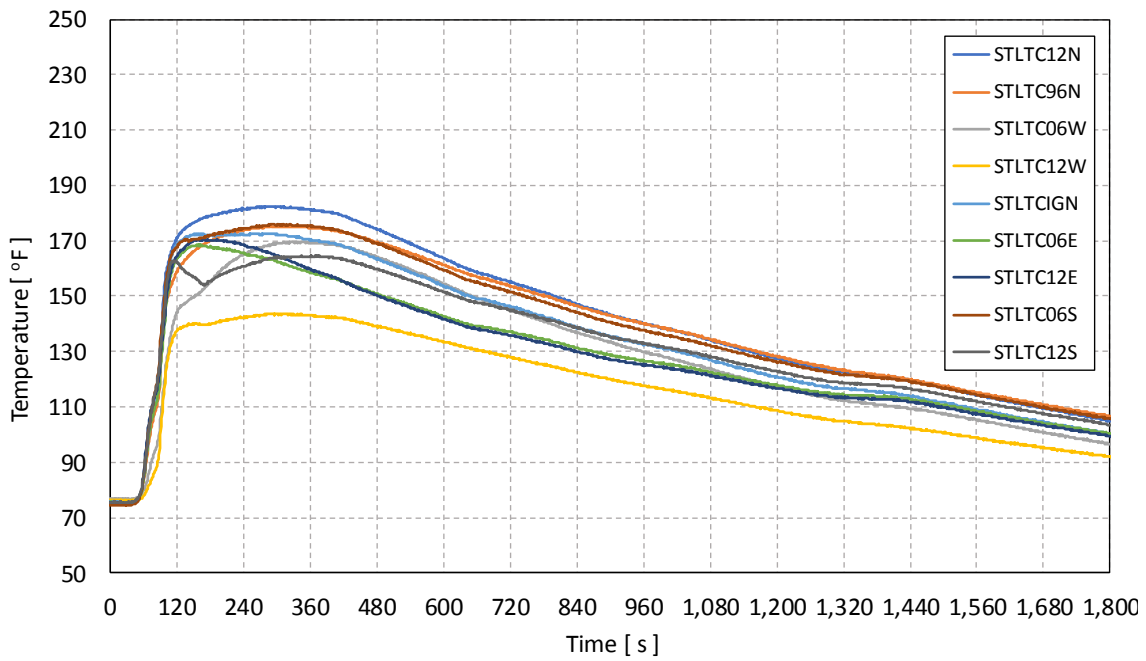


Figure 4-8: Temperatures of the ceiling steel angle for Test #1. The thermocouples on the steel angle are named with a prefix of STLTC (Steel Thermocouple), followed by their placement relative to the ignition location (e.g., IGN stands for thermocouple above the ignition location, 06E means the thermocouple was offset by 6 in. toward the east, etc.)

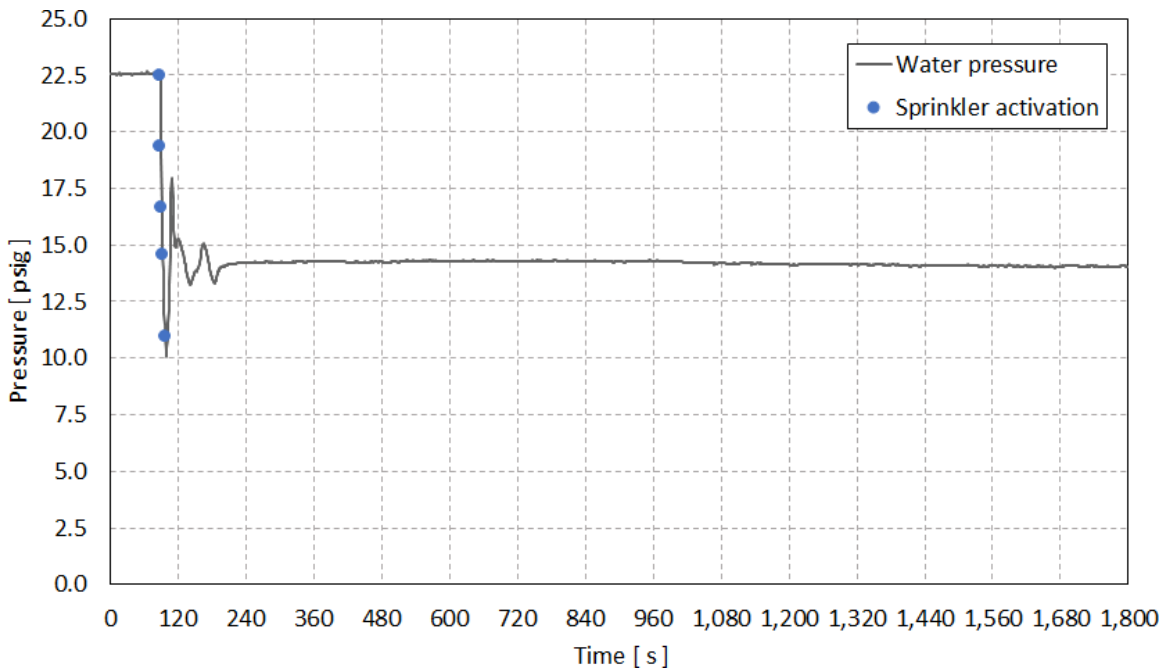


Figure 4-9: Water pressure measured at the main water supply header duct for Test #1.

4.6 Test #2 Results

Test #2 used the same configuration as Test #1 (see Section 4.5 for details), except the purlin depth was increased to 460 mm (18 in.). The sprinklers were again installed such that the distance between the links and the ceiling was 430 mm (17 in.).

4.6.1 Highlights

A detailed description of fire chronology and a few selected photographs from the test are provided in Sections A.2 and B.2 of Appendix A and Appendix B, respectively. The flames reached the ceiling level 59 s after ignition. The first sprinkler operated at 1 min 32 s. Five additional sprinklers operated by 1 min 43 s. By 1 min 49 s, flames were reduced to below the third tier. White smoke descended to the floor partially obscuring the array. The fire gradually became less intense and ceiling temperatures decreased to 93°C (200°F) at approximately 2 min 40 s. After 4 min 10 s, peak ceiling temperatures were below 38°C (100°F). The test was terminated at 30 min.

4.6.2 Results and Damage Assessment

Figure 4-10 shows the sprinkler operation pattern and the plan view of the damage assessment. A total of six sprinklers operated during the test. None of the perimeter sprinklers operated. The fire neither reached the ends of the main array nor the target arrays. Figure 4-11 shows the damage to the east and west faces of the main array. The peak steel temperature was 99°C (211°F) and was within acceptable limits (see Figure 4-12 for details). Water pressure in the sprinkler pipes was maintained within acceptable bounds as shown in Figure 4-13. Compared to the baseline test, two extra sprinklers activated (six total). The skipping in the baseline test was also not observed in this test (symmetric activations around the ignition location) and significantly reduced commodity damage was noticed.

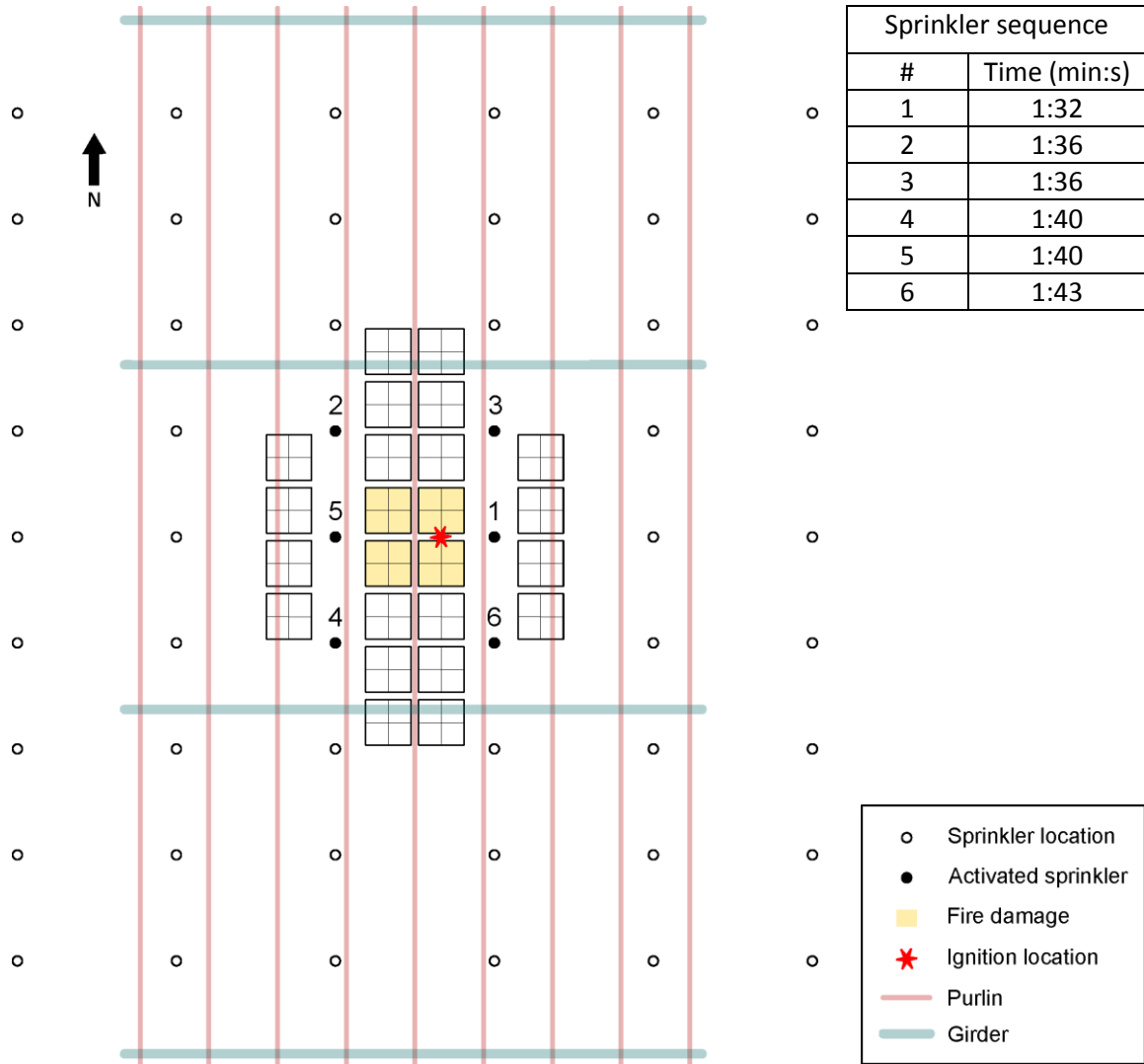


Figure 4-10: Sprinkler operation pattern and top view of damage assessment for test #2.

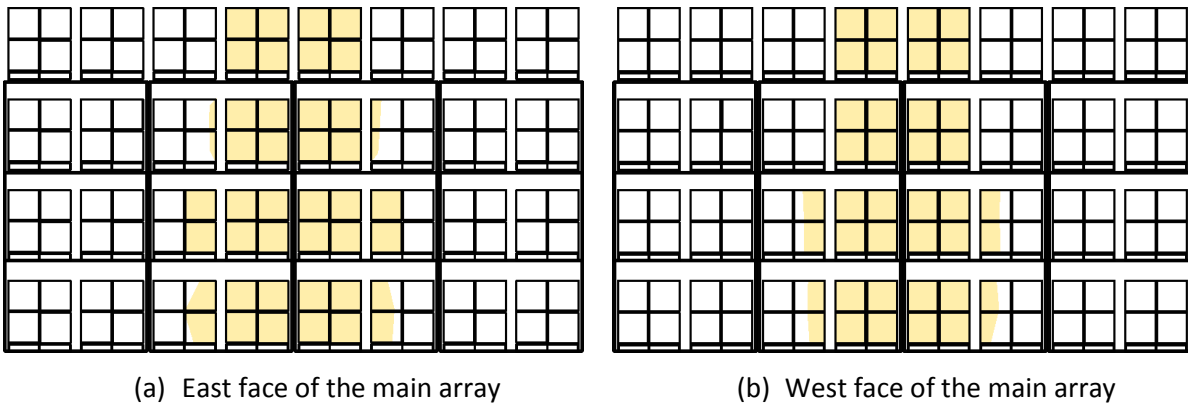


Figure 4-11: Damage assessment on the main array for Test #2.

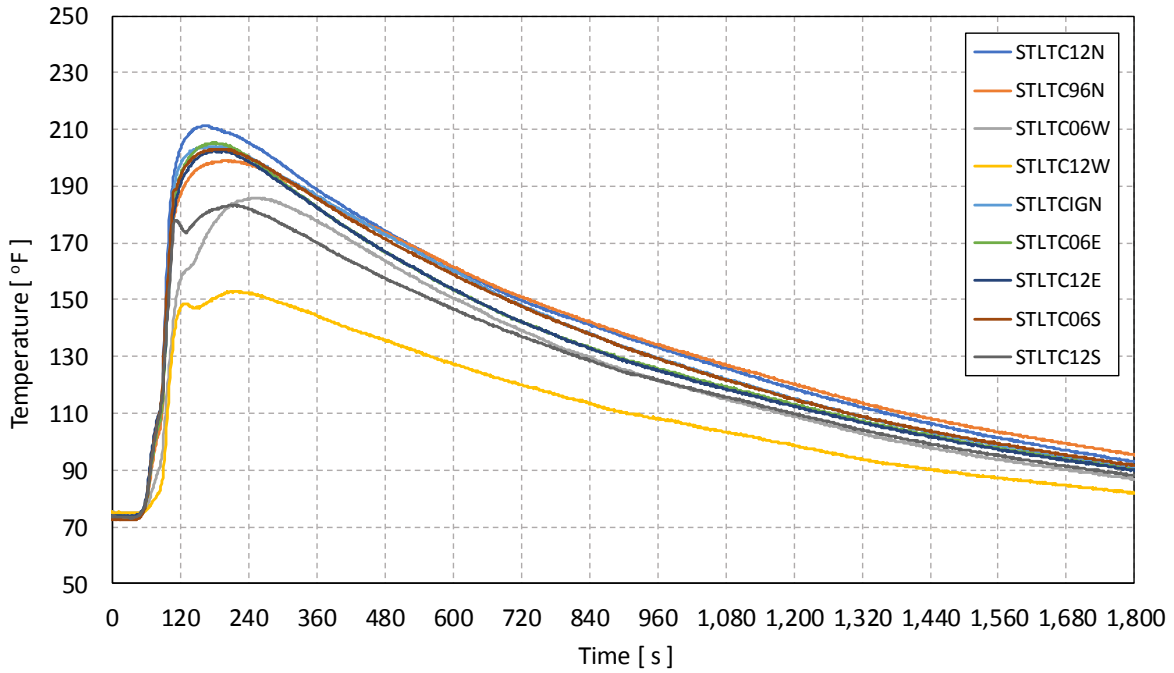


Figure 4-12: Temperatures of the ceiling steel angle for Test #2.

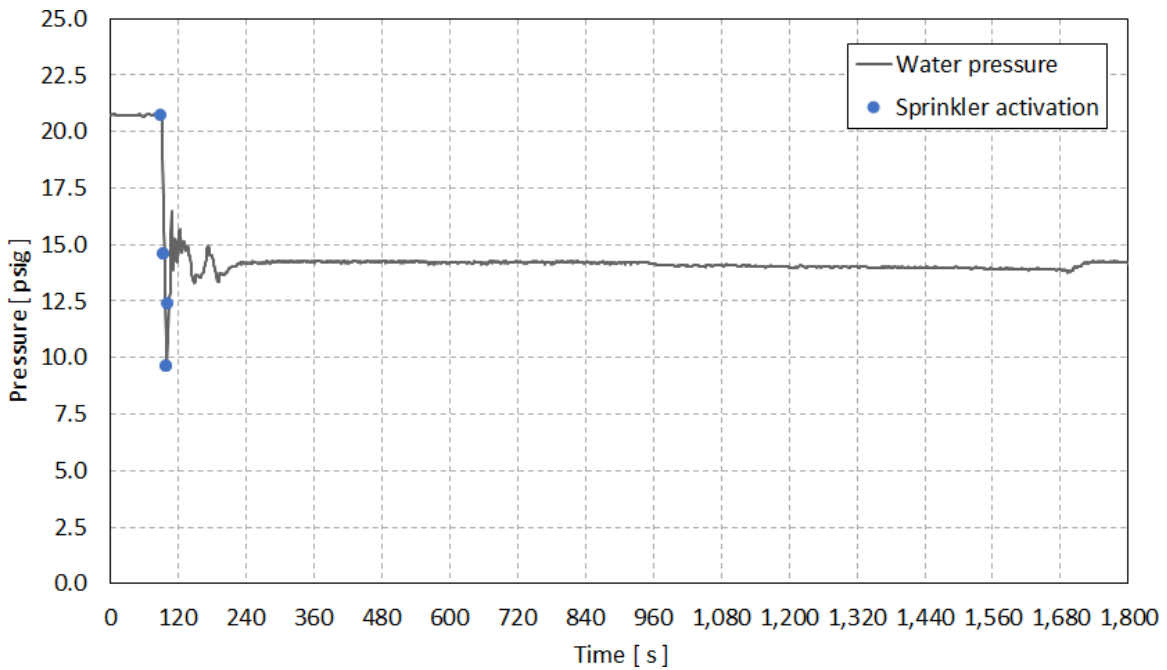


Figure 4-13: Water pressure for Test #2.

4.7 Test #3 Results

Test #3 used the same configuration as Test #1 (see Section 4.5 for details), except the purlin depth was increased to 610 mm (24 in.). However, unlike Tests #1 and 2, the sprinklers were installed such that the distance between the links and the ceiling was 580 mm (23 in.).

4.7.1 Highlights

A detailed description of fire chronology and a few selected photographs from the test are provided in Sections A.3 and B.3 of Appendix A and Appendix B, respectively. The flames reached the ceiling level 51 s after ignition. The first sprinkler operated at 1 min 25 s. By 1 min 46 s, flames were reduced to below the third tier. White smoke descended to the floor partially obscuring the array. Four additional sprinklers operated by 1 min 31 s. The fire gradually became less intense and ceiling temperatures decreased to 93°C (200°F) at approximately 2 min 27 s. At 8 min 50 s, peak ceiling temperatures were below 38°C (100°F). The test was terminated at 30 min.

4.7.2 Results and Damage Assessment

Figure 4-14 shows the sprinkler operation pattern and the plan view of the damage assessment. A total of five sprinklers operated during the test. None of the perimeter sprinklers operated. The fire neither reached the ends of the main array nor the target arrays. Figure 4-15 shows the damage to the east and west faces of the main array. The peak steel temperature was 100°C (212°F) and was within acceptable limits (see Figure 4-16 for details). Water pressure in the sprinkler pipes was maintained within acceptable bounds as shown in Figure 4-17. Similar to Test #1, five sprinklers activated, which is one additional activation compared to the baseline case. The skipping in the baseline test did not occur in this test and considerably reduced commodity damage was observed.

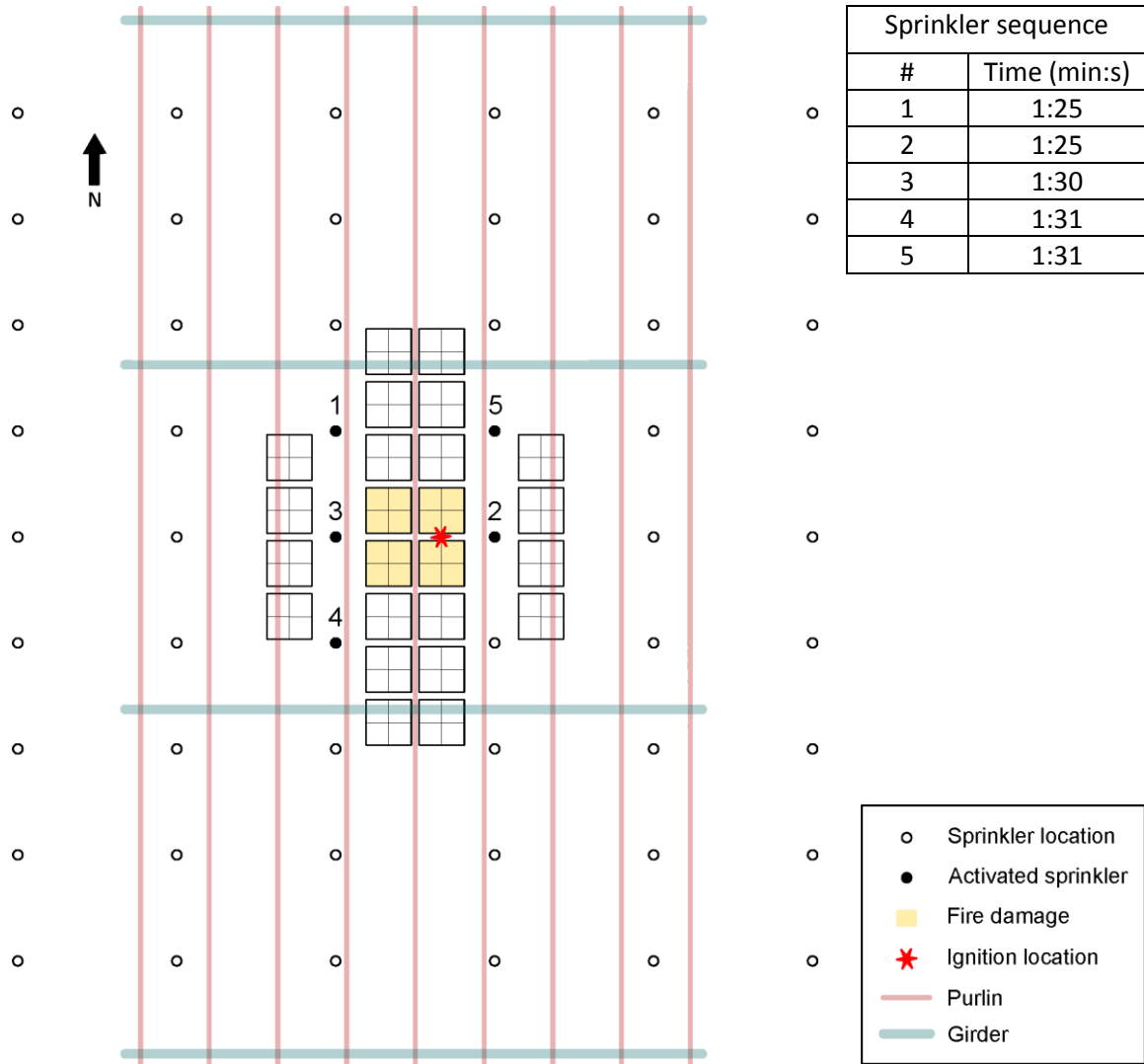


Figure 4-14: Sprinkler operation pattern and top view of damage assessment for Test #3.

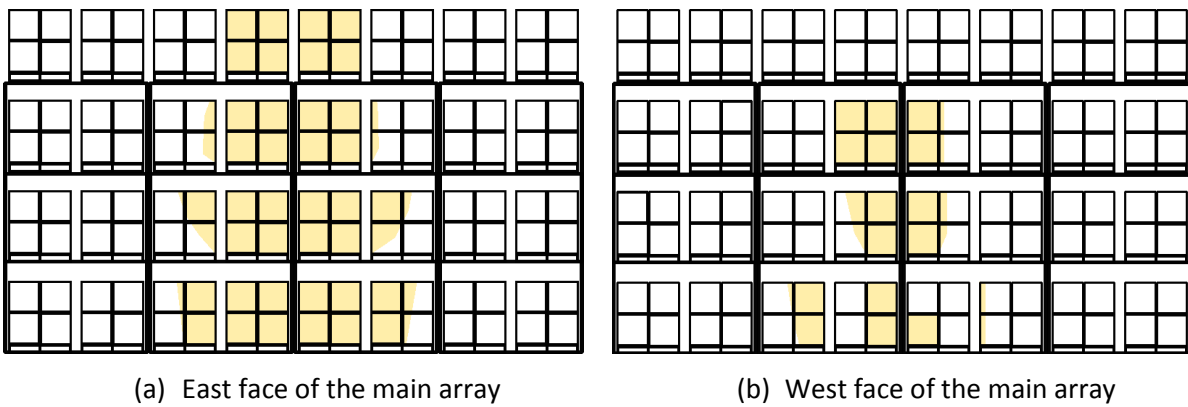


Figure 4-15: Damage assessment on the main array for Test #3.

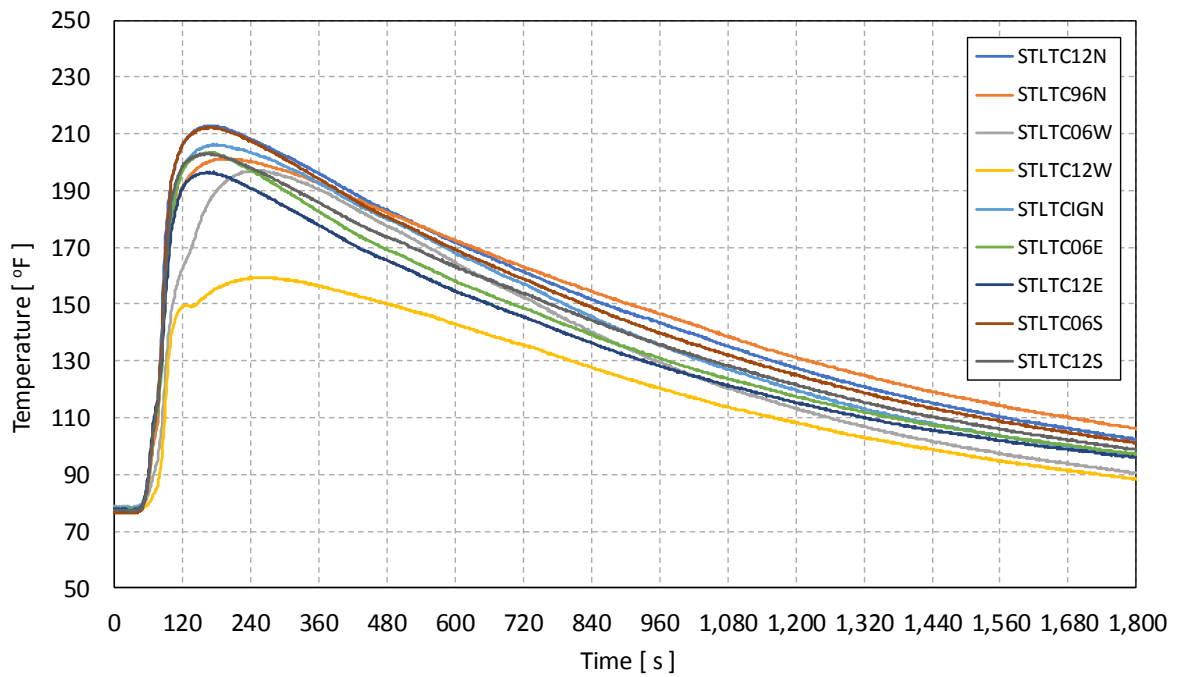


Figure 4-16: Temperatures of the ceiling steel angle for Test #3.

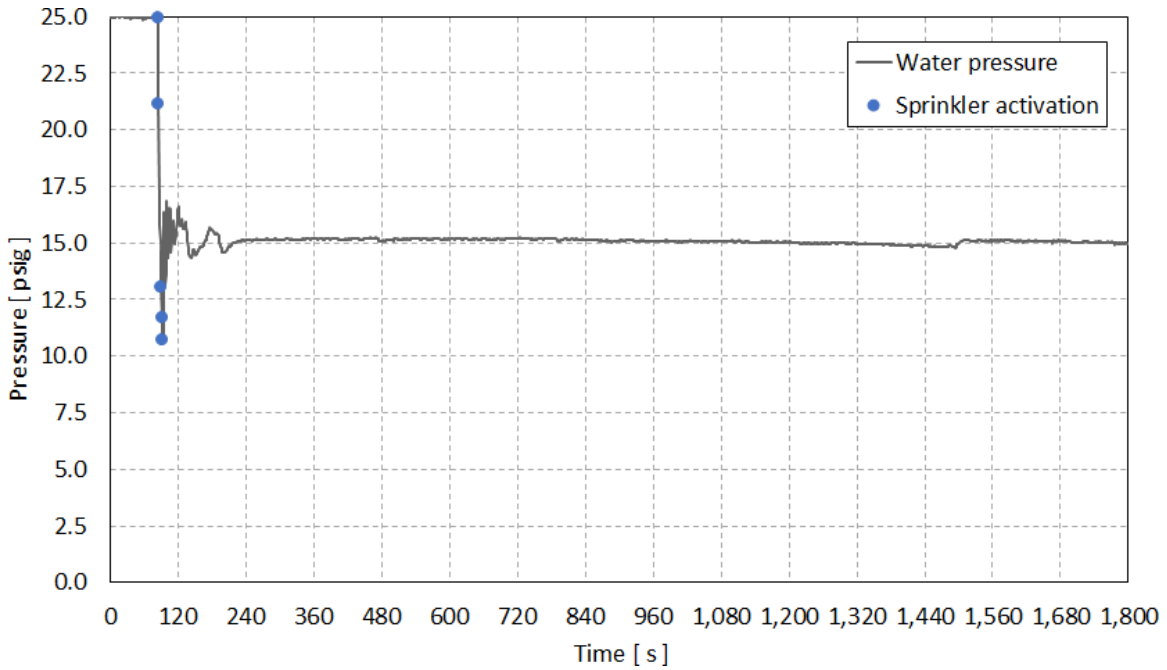


Figure 4-17: Water pressure for Test #3.

4.8 Test #4 Results

Test #4 used the same configuration as Test #3, but the commodity was changed to UUP. The purpose of this test was to evaluate the effect of flow channeling caused by slow-growing fires (see Section 3.2 for numerical modeling details) on the performance of the ceiling sprinklers compared to the baseline UUP test. The purlin depth was kept the same (610 mm or 24 in.) as for Test #3. All other parameters were identical to those in Tests #1–3. As in Test #3, the sprinklers were installed such that the distance between the links and the ceiling was 580 mm (23 in.).

4.8.1 Highlights

A detailed description of fire chronology and a few selected photographs from the test are provided in Sections A.4 and B.4 of Appendix A and Appendix B, respectively. The flames reached the ceiling level 5 min 47 s after ignition. The first sprinkler operated at 6 min 30 s. By 6 min 36 s, flames were reduced to below the third tier, but the fire grew again, and flames were visible on the east face of the fourth tier at 6 min 49 s. Between 7 min 34 s and 7 min 51 s, six additional sprinklers operated including two perimeter sprinklers. White smoke descended to the floor partially obscuring the array at 8 min. Five additional sprinklers operated between 8 min 16 s and 9 min 31 s. After 8 min 30 s, visibility of the main test array was obscured by smoke. The fire gradually became less intense and ceiling temperatures decreased to 93°C (200°F) at approximately 15 min 57 s. At 17 min 59 s and 20 min 23 s, two additional sprinkler operations occurred. The ceiling temperature increased again and after 25 min, peak ceiling temperatures were below 200°C (400°F). The test was terminated at 30 min.

4.8.2 Results and Damage Assessment

Figure 4-18 shows the sprinkler operation pattern and the plan view of the damage assessment. A total of fourteen sprinklers operated during the test including two perimeter operations. The fire neither reached the ends of the main array nor the target arrays. Figure 4-19 shows the damage to the east and west faces of the main array. The peak steel temperature was 216°C (421°F) and was within acceptable limits (see Figure 4-20 for details). Water pressure in the sprinkler pipes was maintained within acceptable bounds as shown in Figure 4-21. The presence of 610 mm (24 in.) deep purlins caused the ceiling jet to be confined within the central purlin channels, which resulted in nine (9) sprinkler operations in the purlin channel adjacent to the channel below which ignition took place. Due to the early perimeter sprinkler operations, Test #4 failed to satisfy one test evaluation criterion. Additionally, the skewed operation pattern along the purlin channels, and early perimeter operations before sprinklers closer to the ignition region operated, are of concern for protection design.

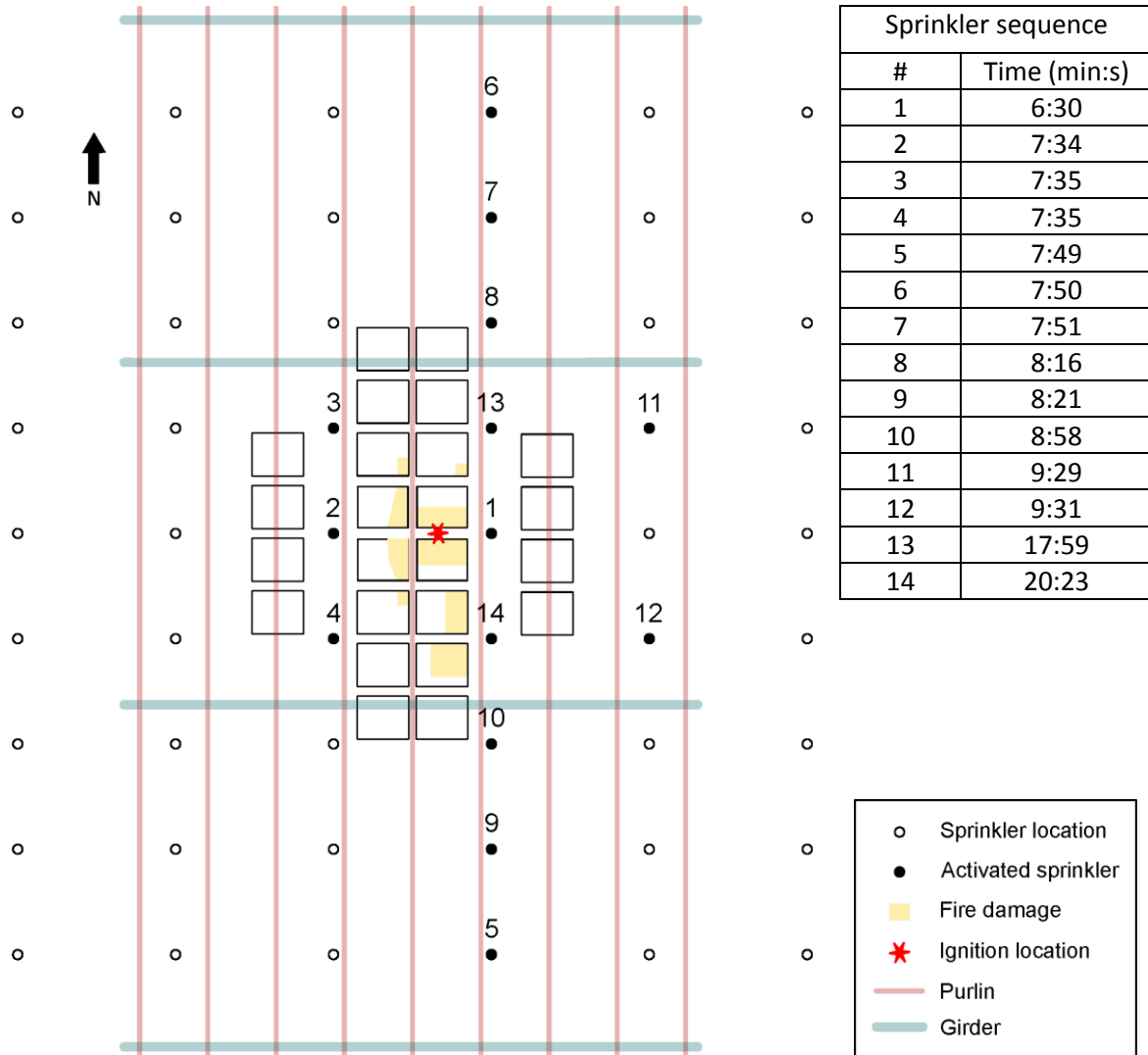


Figure 4-18: Sprinkler operation pattern and top view of damage assessment for Test #4.

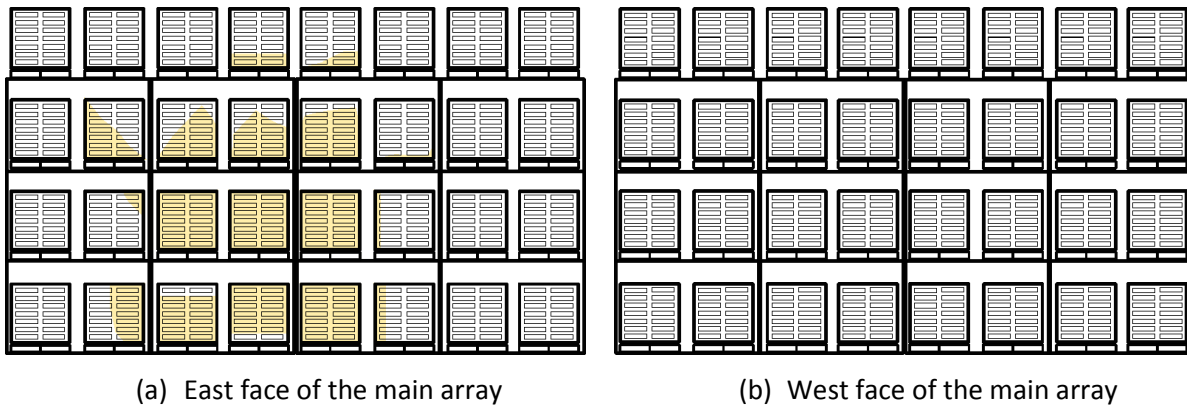


Figure 4-19: Damage assessment on the main array for Test #4.

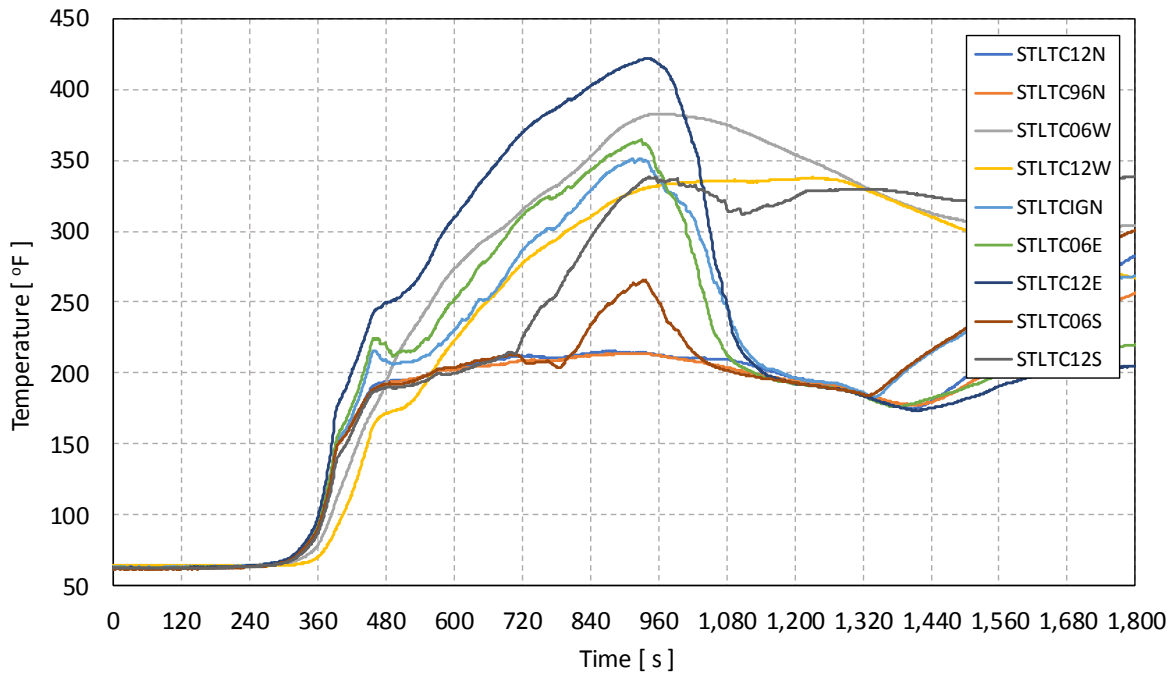


Figure 4-20: Temperatures of the ceiling steel angle for Test #4.

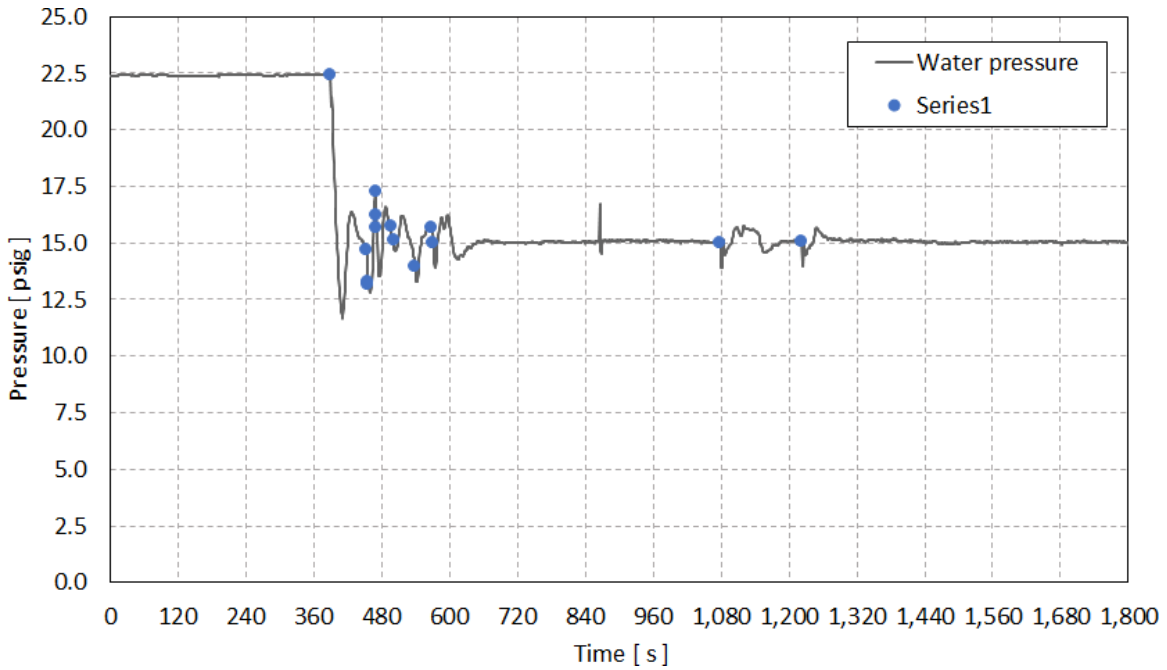


Figure 4-21: Water pressure for Test #4.

4.9 Ceiling Level Gas Temperatures

During Test #1, ceiling level gas temperatures reached a maximum value of 650°C (1200°F) at 1 min 34 s after ignition. As shown in Figure 4-22, the ceiling jet developed initially along the purlin channels, but at 75 s, the temperature contours can also be seen developing in the perpendicular-to-the-purlin direction (east-west). At 105 s, due to five sprinkler operations, the ceiling jet temperature began to decrease, as is evident from Figure 4-22(e). The temperatures continued to decrease until the end of the test and the temperature contours became more symmetric.

In Test #2, a peak ceiling temperature of 870°C (1600°F) occurred at 1 min 34 s. Ceiling jet development was like that in Test #1, with temperature contours developing along the purlin channels, as shown in Figure 4-23. At 90 s, the spread of the ceiling jet in the direction perpendicular to the purlins was more restricted as compared to Test #1. This was caused by greater flow channeling along the 460 mm (18 in.) deep purlin channels (Test #1 had 300 mm or 12 in. deep purlins). The ceiling jet remained hotter for a longer time, as seen in Figure 4-23(e); however, temperatures continued to decrease rapidly until the end of the test. The temperature contours, compared to those of Test #1, remained more asymmetric and biased toward the north-south direction (along the purlin channels).

In Test #3, a peak ceiling temperature of 870°C (1600°F) was reached at 1 min 27 s, around the same time as in Tests #1 and 2. Although the ceiling jet temperature contours were stretched along the purlin channels, enough flow reached adjacent channels to cause five sprinkler operations around the ignition region, as can be observed in Figure 4-24. After the sprinklers operated, the ceiling jet temperatures were brought down quite rapidly. For the deepest purlins tested, 610 mm (24 in.), and for the 4-tier CUP array, the purlins did not adequately affect the ceiling jet temperatures to cause a biased sprinkler activation pattern.

Test #4 was conducted with UUP and the ceiling jet temperatures took longer to reach high values due to the slow growing fire. A peak ceiling temperature of 590°C (1100°F) was only reached at 6 min 30 s. Unlike Tests #1–3 conducted with the CUP commodity (rapid fire growth comparatively), Test #4 ceiling temperature contours remained biased along the purlin channels, as shown in Figure 4-25. Even beyond 720 s, the temperature profiles continued to remain stretched along the two central purlin channels. This biased development of the ceiling jet caused several activations adjacent to and along the central purlin channels.

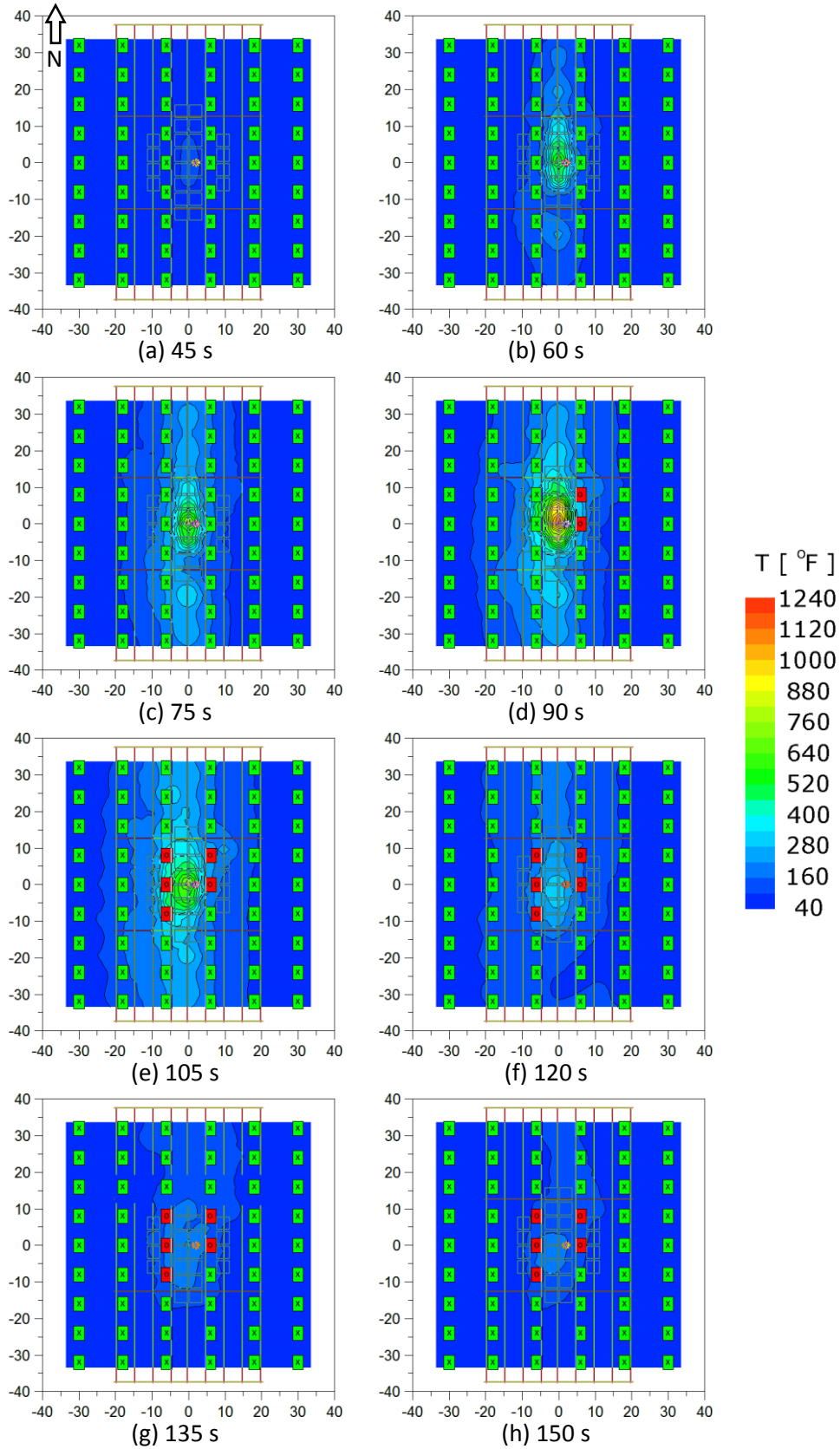


Figure 4-22: Test #1 ceiling temperature contours shown in 15 s increments.

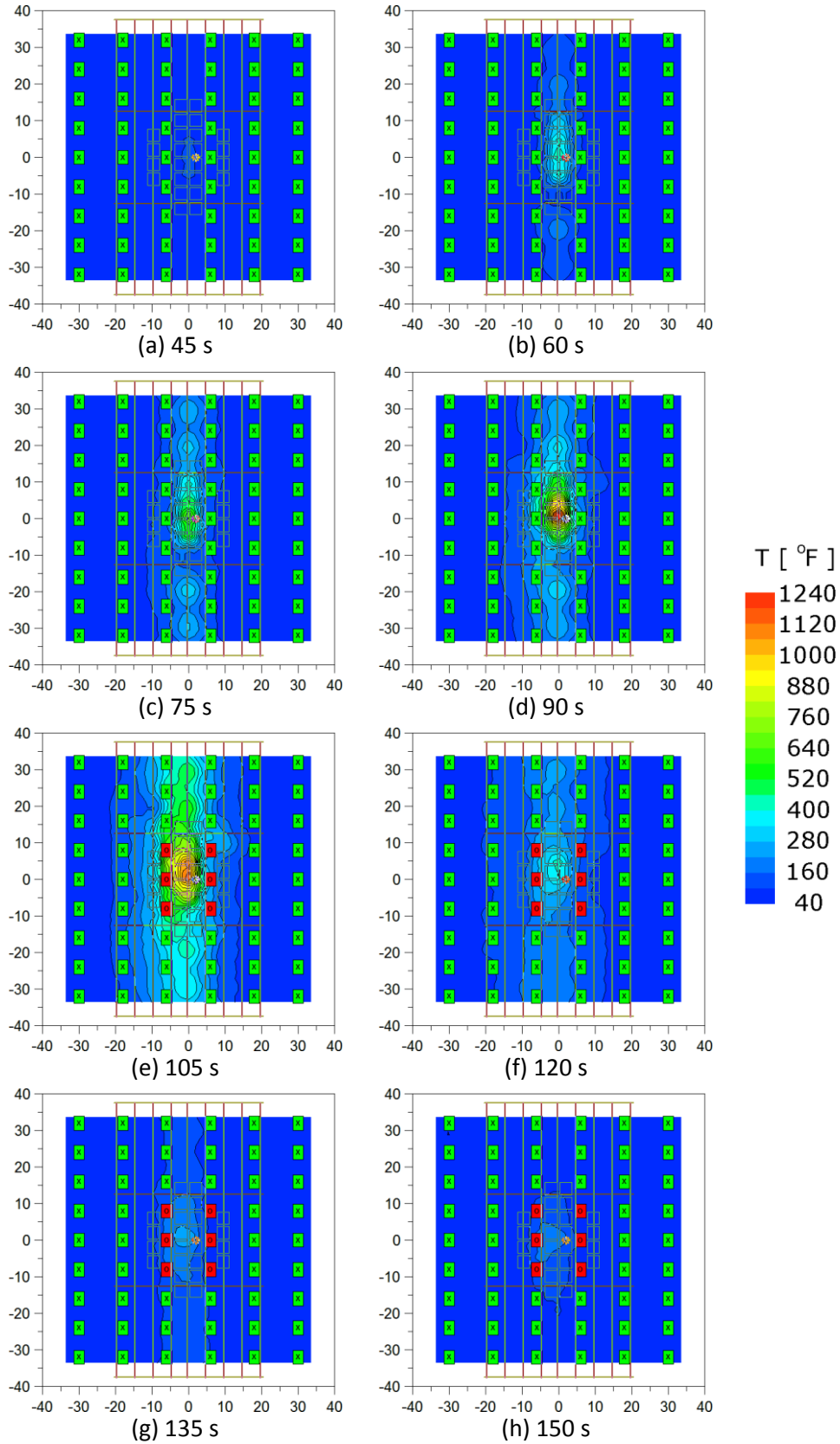


Figure 4-23: Test #2 ceiling temperature contours shown in 15 s increments.

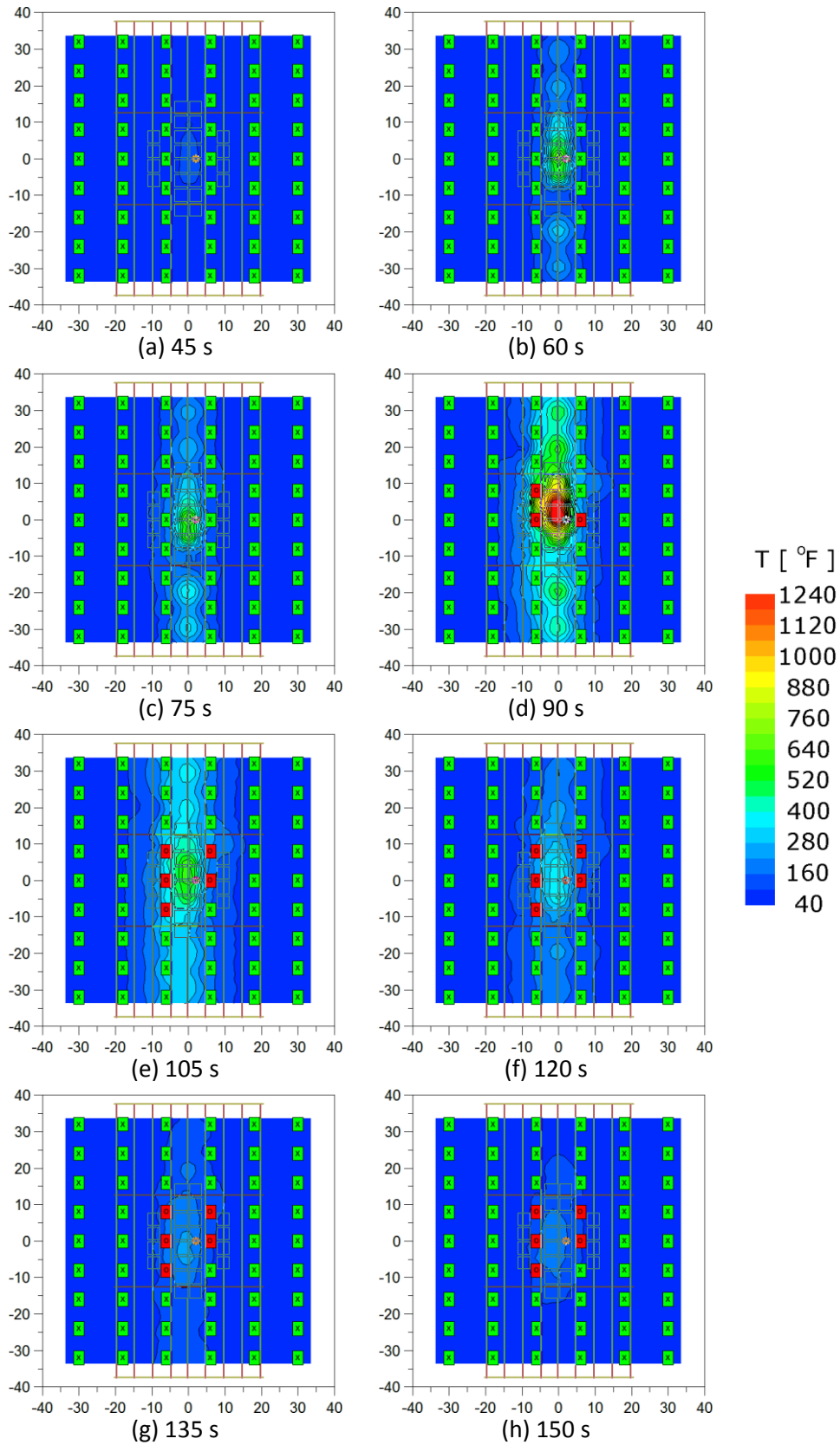


Figure 4-24: Test #3 ceiling temperature contours shown in 15 s increments.

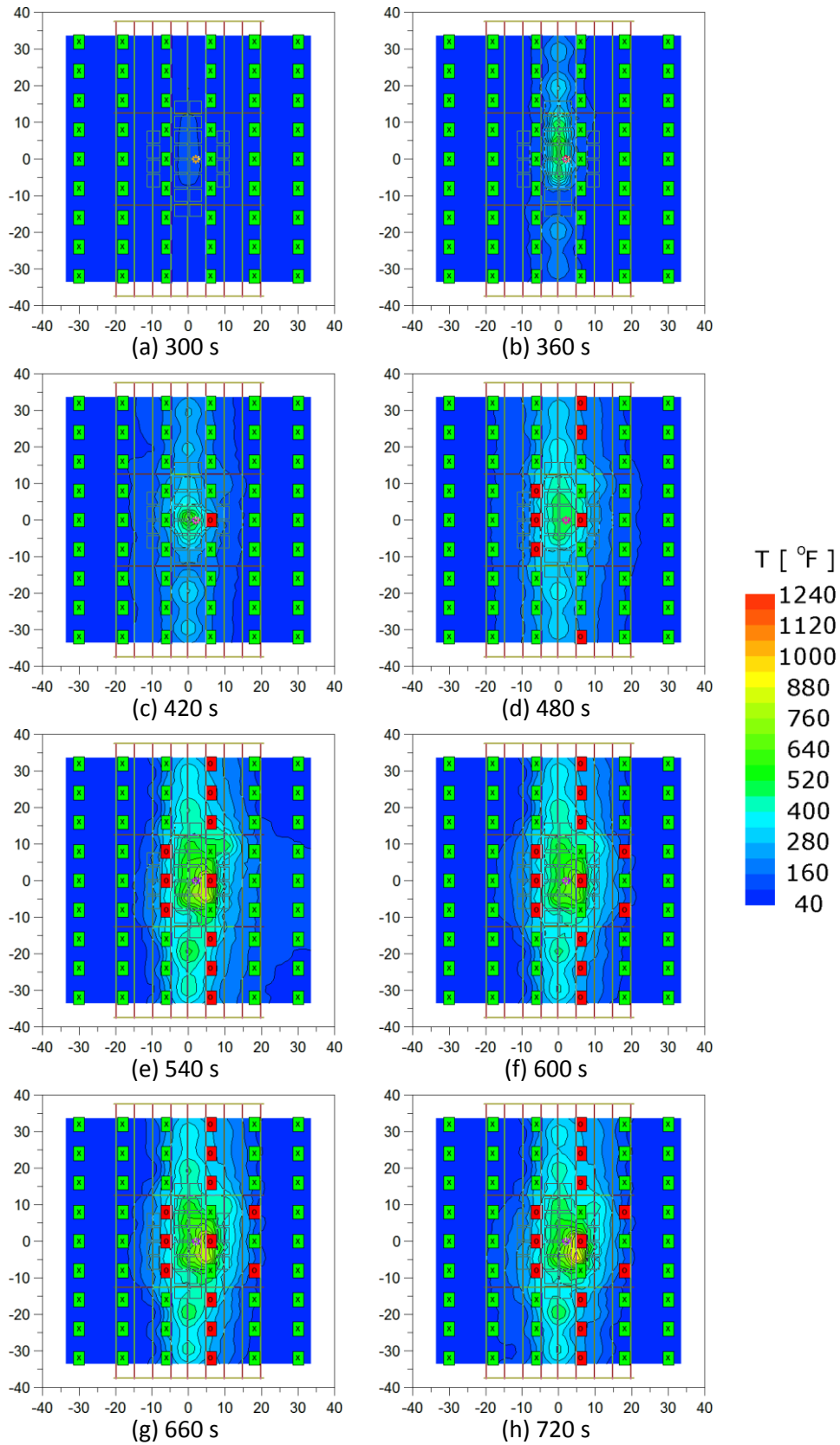


Figure 4-25: Test #4 ceiling temperature contours shown in 60 s increments.

4.10 Comparison against Baseline Test Results

Comparing Tests #1–3 against the baseline test (in the absence of obstructed ceiling construction) conducted earlier, all four evaluation criteria were generally satisfied. Performance parameters of the three tests against the baseline test are summarized in Table 4-4. Between five and six sprinkler operations took place in Tests #1–3, compared to four in the baseline test. The number of activations were between 25 and 50% greater than the baseline test, but this variation is within the observed testing variability. Additionally, no perimeter sprinkler operations occurred. The fire damage was confined to a smaller part of the main test array compared to the observed damage in the baseline test. Ceiling steel peak temperatures in the three tests remained 538°C (1000°F), which was also the case in the baseline test. In terms of the rate of sprinkler operations, the performance of the three obstructed ceiling construction tests were mostly similar to those of the baseline test. The rate of sprinkler operation can be observed to be constant for the three tests, as shown by the plot of activation time versus the number of activations shown in Figure 4-26(a). Except for the delay of the last sprinkler operation in the baseline test, the rate of sprinkler operations was found to be similar with the three obstructed ceiling construction tests.

Table 4-4: Test performance comparison between baseline and obstructed ceiling construction tests (#1–3) for the CUP commodity.

Test Number	Number of Sprinklers Activated	Perimeter Activations	Extent of Damage	Steel Temperature
Baseline (CUP)	4	No	Acceptable	115°C (239°F)
1 (300 mm purlins)	5	No	Acceptable	83°C (182°F)
2 (460 mm purlins)	6	No	Acceptable	99°C (211°F)
3 (610 mm purlins)	5	No	Acceptable	100°C (212°F)

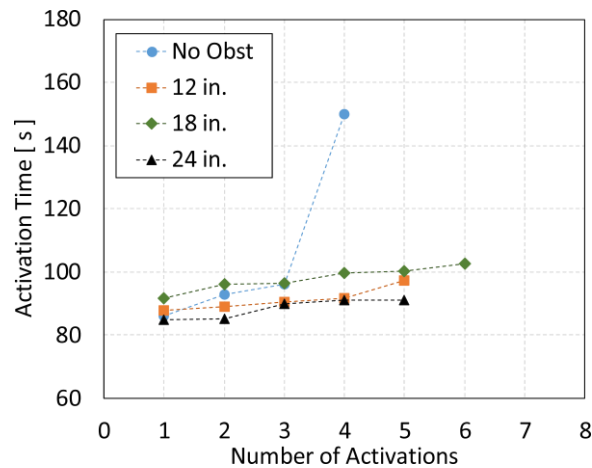
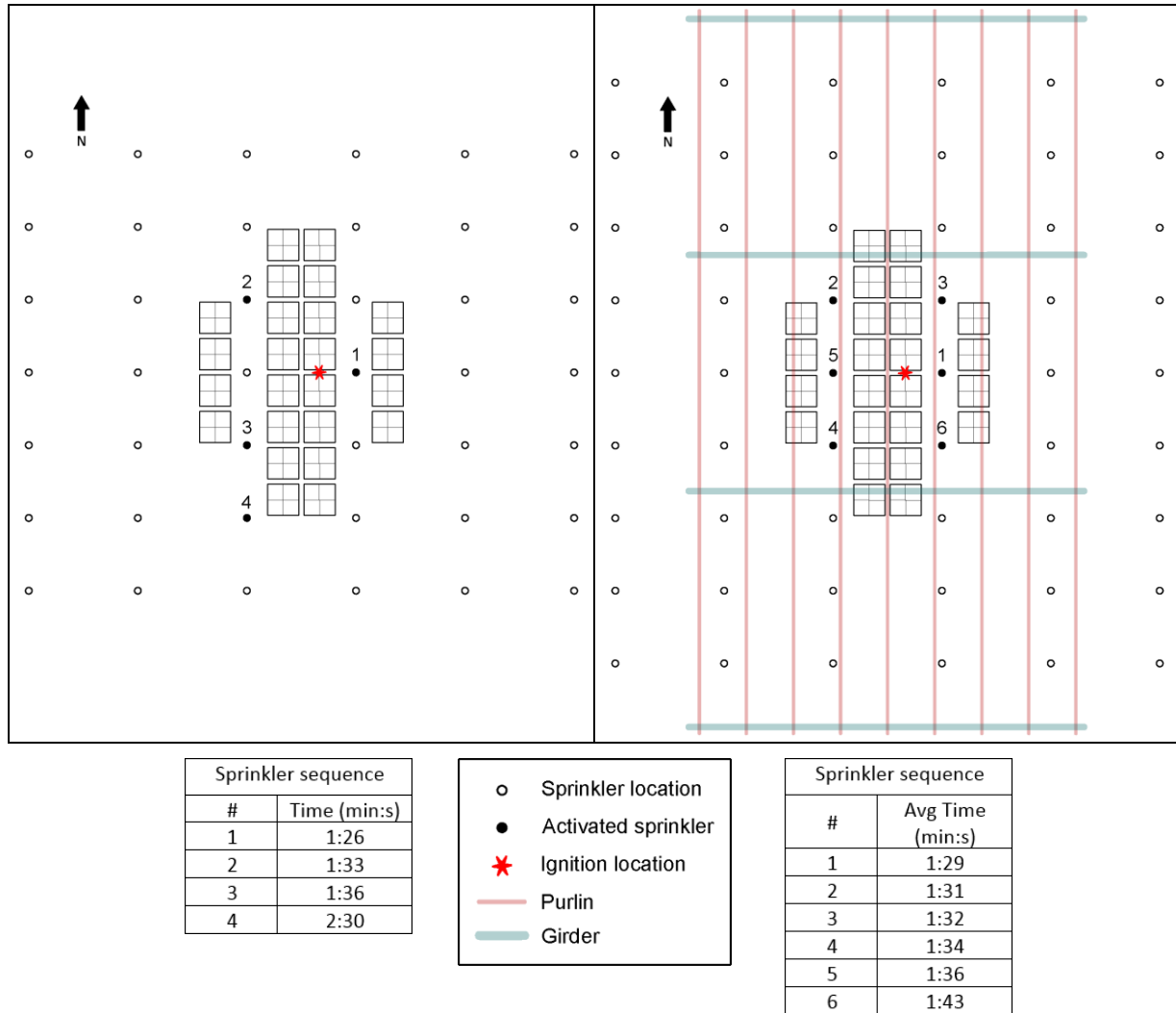


Figure 4-26: Activation times plotted as functions of number of activations for tests with and without obstructed ceiling construction for the CUP tests.

The average activation times for Tests #1–3 are shown alongside the activation times for the baseline test in Figure 4-27. In the baseline test, the first three sprinklers to activate were close to the ignition location, as shown in Figure 4-27 (a). On average, the sprinkler operation patterns for the three obstructed ceiling tests were identical, with a symmetric activation pattern around the ignition location as can be observed in Figure 4-27 (b). Overall, it can be concluded that, for the 4-tier CUP rack storage array tested, the effect of the obstructed ceiling construction on sprinkler protection design was minimal for purlin depths up to 610 mm (24 in.). Less sprinkler skipping, and significantly reduced commodity damage were also observed in all three tests.



(a) Unobstructed ceiling

(b) Obstructed ceiling

Figure 4-27: Comparison of sprinkler operation patterns for tests conducted with (a) unobstructed ceiling, and (b) obstructed ceiling (average activation times for Tests #1–3: purlin depths were between 300–610 mm or 12–24 in.). The commodity was CUP and the storage arrangements were identical in all tests.

Test #4 results are compared against those of the baseline test for the UUP commodity. The performance of Test #4 against the baseline test is summarized in Table 4-5. In Test #4, fourteen sprinklers operated as compared to fifteen operations in the baseline test. However, two perimeter sprinkler activations occurred. The perimeter activations occurred earlier than the following eight additional activations. Earlier perimeter activations were caused by the accumulation of hot ceiling jet gases near the outer girders causing the ceiling jet to thicken rapidly resulting in activations before the interior sprinklers activated. This phenomenon was also observed to occur in the UUP simulations (see Figures 3-20 to 3-23 in Section 3.2.2 for details). However, the extent of fire damage was restricted to a small region on the main test array, a performance that mirrors the observed extent of damage in the baseline test. The ceiling steel temperatures were also found to be within acceptable limits.

Table 4-5: Test performance comparison between baseline and the obstructed ceiling construction test (#4) for the UUP commodity.

Test Number	Number of Sprinklers Activated	Perimeter Activations	Extent of Damage	Steel Temperature
Baseline (UUP)	15	Yes (1) ^v	Acceptable	104°C (220°F)
4 (610 mm purlins)	14	Yes (2)	Acceptable	216°C (421°F)

The rate of sprinkler activations in Test #4 was found to match the rate observed in the baseline test, as indicated by the activation time plot shown in Figure 4-28, except for the two delayed activations after the 12th sprinkler. The rate of activations, though, does not provide information on the sprinkler operation pattern differences between Test #4 and the baseline test. Figure 4-29 illustrates the difference in operation patterns: due to the confinement of the thin ceiling jet along the central purlins and the resulting accumulation of the hot ceiling jet gases near the girders, the majority of the sprinkler activations in the presence of the 610 mm (24 in.) deep purlins and girders occur along the north-south direction (i.e., along the purlin channels). This is shown in Figure 4-29(b). Comparatively, the baseline test sprinkler activations occur almost symmetrically around the ignition region, as can be observed in Figure 4-29(a). The ceiling jet channeling effect due to the deep purlin channels can be mitigated by closing the purlin channels, i.e., by eliminating the gap at the ceiling level where girders are installed, as described in Section 3.2.2.

^v It should be noted that instead of nine rows of sprinklers as in Test #4 of the present series, the baseline UUP test was conducted with only seven rows of sprinklers. Although one activated sprinkler was identified as a perimeter sprinkler, in reality it was located 7.3 m (24 ft) from the ignition location in the north-south direction as compared to the two activated perimeter sprinklers in Test #4 each located at a 9.8 m (32 ft) distance.

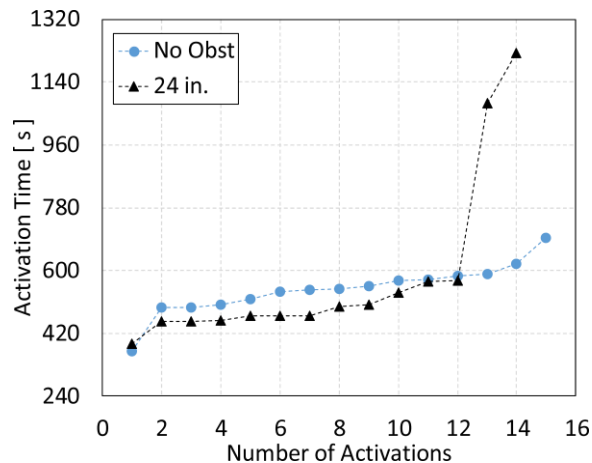
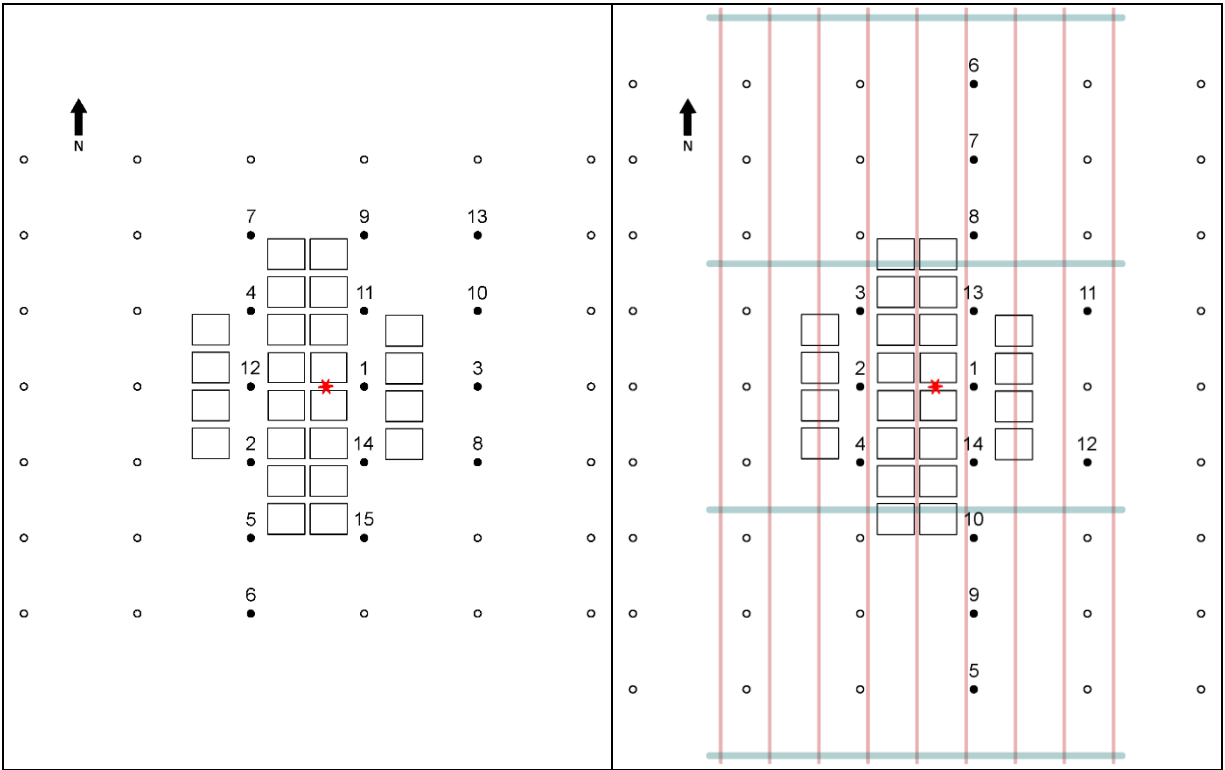


Figure 4-28: Activation times plotted as functions of number of activations for tests with and without obstructed ceiling construction for the UUP tests.

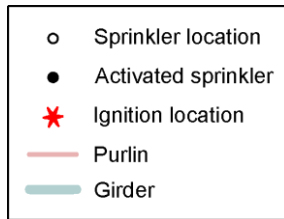
4.11 Summary

From the four large-scale tests conducted and a comparison with the baseline tests conducted in the absence of obstructed ceiling construction, the following can be summarized:

- The protection provided by K360 (K25.2) pendent QR sprinklers operating at 0.97 barg (14 psig) – a discharge density of 41 mm/min (1.0 gpm/ft²) per sprinkler – is adequate to protect CUP commodity stored to a height of 6.1 m (20 ft) under a 7.6 m (25 ft) high ceiling in the presence of obstructed ceiling construction with purlin depths of 300–610 mm (12–24 in.).
- Compared to the four sprinkler activations in the baseline test conducted earlier, five–six activations occurred in the CUP obstructed ceiling tests. All activations in the current series of tests occurred within 6–11 s intervals.
- The presence of obstructed ceiling construction caused symmetric sprinkler activations for the CUP commodity compared to the baseline test and sprinkler skipping did not occur. Considerably less fire damage was also observed.
- Although increasing the purlin depth from 300 mm (12 in.) to 610 mm (24 in.) did not have a significant effect on the sprinkler activation patterns, times, or suppression effectiveness, significant channeling of the ceiling jet was observed when 460 mm (18 in.) and 610 mm (24 in.) purlins were used. Flow channeling along deep central purlin channels also caused a biased sprinkler activation pattern below the central purlin channels in the UUP test. Mitigation of this effect is possible by closing the gap above the girders as demonstrated by numerical modeling (see Section 3.2.2 for details).



Sprinkler sequence	
#	Time (min:s)
1	6:08
2	8:13
3	8:13
4	8:21
5	8:37
6	9:00
7	9:05
8	9:07
9	9:16
10	9:30
11	9:33
12	9:44
13	9:50
14	10:19
15	11:34



Sprinkler sequence	
#	Time (min:s)
1	6:30
2	7:34
3	7:35
4	7:35
5	7:49
6	7:50
7	7:51
8	8:16
9	8:21
10	8:58
11	9:29
12	9:31
13	17:59
14	20:23

(a) Unobstructed ceiling

(b) Obstructed ceiling

Figure 4-29: Comparison of sprinkler operation pattern for tests conducted with (a) unobstructed ceiling, and (b) obstructed ceiling (610 mm or 24 in. deep purlins). The commodity was UUP and the storage arrangements were identical in the two tests.

5. Conclusions and Recommendations

In the present study, FireFOAM simulations were conducted to determine sprinkler activation patterns and times under non-sloped ceilings in the presence of obstructed construction (purlins and girders). A growing fire on a 2 × 2 × 3 CUP rack-storage array with a maximum convective HRR of 15 MW and a slow-growing fire with the UUP commodity were used as plume sources. Developing ceiling jets were investigated and sprinkler activation calculations were made by decoupling activation from other suppression phenomena. Activation times and patterns for non-sloped ceilings with obstructed ceiling construction were compared against similar unobstructed ceiling results. Purlin depths in the range of 100–610 mm (4–24 in.) were considered with a single girder depth of 610 mm (24 in.) used. Purlin separation distances of 1.5 m (5 ft) and 3.0 m (10 ft), girder separation distances of 7.6 m (25 ft) and 12.2 m (40 ft), ceiling clearances from the top of the CUP rack-storage array of 1.5 m (5 ft) and 3.0 m (10 ft), and the link distance from the ceiling were selected as parameters in the study.

Results from the simulations show that the presence of purlins can result in early activation times for the first ring sprinklers, provided the purlins are not very deep. For the deeper purlins (of a depth ≥460 mm or 18 in.), flow confinement results in the ceiling jet developing along the purlin channels, causing skewness in activation patterns.

A series of large-scale tests was designed with input from the numerical simulation results. Four large-scale tests were conducted with the CUP and UUP commodities and purlins of 300–610 mm (12–24 in.) depths separated by 1.5 m (5 ft). The test performances were compared against baseline tests conducted earlier in the absence of obstructed ceiling construction.

5.1 Conclusions

From the range of conditions explored in numerical modeling and large-scale testing, major trends involving the principal parameters are summarized below.

- For the CUP commodity, modeling results showed that activations of the central sprinklers (i.e., ones close to the ignition region) are not adversely affected by the presence of purlins of depth ≤610 mm (24 in.).
- Large-scale tests were conducted using the CUP commodity with the testing parameters developed from modeling results. Purlin depths of 300–610 mm (12–24 in.) were selected based on the modeling input. Compared to the four sprinkler activations in the CUP baseline test conducted earlier with an unobstructed ceiling, five–six central sprinkler activations occurred in the obstructed ceiling tests (all within 6–11 s intervals) and fire spread was successfully controlled. Sprinkler skipping did not occur unlike in the baseline test and considerably less commodity damage was observed in all three tests.
- To overcome the potential of spray impingement when sprinklers are placed inside deep channels formed by purlins, modeling and testing results recommended lowering the sprinkler links from a DS 2-0 maximum permissible depth of 430 mm (17 in.) for QR/OT sprinklers

installed below unobstructed ceilings [1] to a maximum of 760 mm (30 in.) for 610 mm (24 in.) deep purlins (i.e., 150 mm or 6 in. below the bottom edge of the purlins). For the 760 mm (30 in.) link distance, the average activation times were found to be earlier than in the case of sprinklers located 430 mm (17 in.) under unobstructed ceilings. A similar observation was also made for the SR/HT sprinklers. Therefore, for purlin depths >430 mm (17 in.) for QR/OT sprinklers and >330 mm (13 in.) for SR/HT sprinklers, a general recommendation was made for the sprinkler links to be placed on a plane below the bottom of the purlins, up to a distance of 150 mm (6 in.).

Both the modeling results and large-scale tests showed that purlin depths ≤ 300 mm (12 in.) do not adversely affect the activation times of the central sprinklers for the CUP commodity, which involves fast fire growth rates. No significant biased sprinkler activation patterns due to flow confinement in the purlin channels was observed. Flow channeling was, however, observed in the modeling results and in tests conducted with purlin depths of 460 mm (18 in.) and 610 mm (24 in.), which could have an adverse effect on the sprinkler activation pattern away from the fire source. This is of concern for conditions when the central sprinklers are unable to arrest fire spread.

- For the UUP commodity, which involves an initially slow fire growth rate, modeling showed that the flow channeling effect caused biased activation patterns to develop below the central purlin channels and early perimeter sprinkler activations also occurred due to hot gas accumulation near the outside girders. Flow channeling and early perimeter sprinkler activations were also observed in a large-scale test involving the UUP commodity and 610 mm (24 in.) purlins.
- For purlin depths >300 mm (12 in.), modeling using the UUP commodity showed that closing the purlin channel gaps above the girder locations reduces the flow channeling effect and symmetric activation patterns occur.

5.2 Recommendations

Analyzing the results from the large-scale tests and the modeling study, the following general recommendations are made toward an update of the DS 2-0 [1] sprinkler protection designs for non-sloped ceilings in the presence of obstructed ceiling construction:

1. A ceiling with purlins of ≤ 300 mm (12 in.) depth can be considered an unobstructed type compared to the existing guidance of 100 mm (4 in.) in DS 2-0 [1].
2. For purlin depths > 430 mm (17 in.) in case of QR/OT sprinklers or > 330 mm (13 in.) for SR/HT sprinklers, links could be placed on a plane at a maximum distance of 150 mm (6 in.) below the bottom edge of the purlins. This recommendation is valid for a maximum purlin depth of 610 mm (24 in.).
3. For purlin depths ≤ 610 mm (24 in.), sprinklers need not be installed in every purlin channel in contrast to the current guidelines provided in DS 2-0 [1]. Due to the strong channeling effect observed in the modeling results and the tests for purlin depths of ≥ 460 mm (18 in.), it is recommended that vertical barriers be installed to close the purlin channels in order to reduce biased sprinkler activation patterns. Based on modeling results, a maximum closed purlin channel length of 7.6 m (25 ft) is recommended.

References

1. "FM Global Data Sheet 2-0, Installation Guidelines for Automatic Sprinklers," FM Global, January 2014.
2. "NFPA 13: Standard for the Installation of Sprinkler Systems," National Fire Protection Association, 2016.
3. roman023. (December 12, 2016) View from below on painted pillar with steel joints - Stock image, <https://www.istockphoto.com/photo/view-from-below-on-painted-pillar-with-steel-joints-gm623266960-109242747> (Retrieved February 21, 2018).
4. ansonmiao. (February 06, 2016) Inside a large empty new warehouse - Stock image, <http://www.istockphoto.com/photo/inside-a-large-empty-new-warehouse-gm507493310-84758497> (Retrieved February 7, 2018).
5. Jacek_Sopotnicki. (December 5, 2013) Modern, Brand New Storehouse - Stock image, <https://www.istockphoto.com/photo/modern-brand-new-storehouse-gm454173711-25894842> (Retrieved February 21, 2018).
6. H.-Z. Yu, D. B. Pounder, and M. Fischer, "Fire Performance Evaluation of a K-16.8 Suppression-mode Upright Sprinkler," *Journal of Fire Protection Engineering*, vol. 14, no. 2, pp. 101-124, 2004.
7. Internal correspondence.
8. M. A. Delichatsios, "The Flow of Fire Gases Under a Beamed Ceiling," *Combustion and Flame*, vol. 43, pp. 1-10, 1981.
9. R. G. Bill, H.-C. Kung, W. R. Brown, and E. E. Hill, "Effects of Cathedral and Beamed Ceiling Construction on Residential Sprinkler Performance," *Fire Safety Science*, pp. 643-653, 1988.
10. P. Chatterjee and J. A. Geiman, "Numerical Simulations of Sprinkler Activations and Spray Transport under Obstructed, Sloped Ceilings," FM Global, Technical Report 3059743, 2017.
11. FireFOAM. [Online]. <http://www.fmglobal.com/modeling>
12. "OpenFOAM: The Open Source CFD Toolbox, User Guide, Version 2.2.0," February 22, 2013.
13. OpenFOAM v3 User Guide: 5.4 Mesh generation with snappyHexMesh. [Online]. <https://cfd.direct/openfoam/user-guide/v3-snappyHexMesh>

14. Y. Wang, P. Chatterjee, and J. L. de Ris, "Large Eddy Simulation of Fire Plumes," *Proceedings of the Combustion Institute*, vol. 33, no. 2, pp. 2473-2480, 2011.
15. G. Agarwal, A. Gupta, M. Chaos, K. V. Meredith, and Y. Wang, "An Experimental and Modeling Approach to Investigate the Burning Behavior of Cartoned Unexpanded Plastic Commodity," in *9th U.S. National Combustion Meeting*, Cincinnati, OH, 2015.
16. P. Chatterjee, J. L. de Ris, Y. Wang, and S. B. Dorofeev, "A Model for Soot Radiation in Buoyant Diffusion Flames," *Proceedings of the Combustion Institute*, vol. 33, no. 2, pp. 2665-2671, 2011.
17. P. Chatterjee and K. V. Meredith, "Numerical Modeling of Sprinkler Activations and Spray Transport Under Sloped Ceilings," FM Global, Technical Report 3055093, 2015.
18. P. Chatterjee, K. V. Meredith, and Y. Wang, "Temperature and Velocity Distributions from Numerical Simulations of Ceiling Jets Under Unconfined, Inclined Ceilings," *Fire Safety Journal*, vol. 91, pp. 461-470, July 2017.
19. P. Chatterjee, K. V. Meredith, B. Ditch, H.-Z. Yu, Y. Wang, and F. Tamanini, "Numerical Simulations of Strong-Plume Driven Ceiling Flows," *Fire Safety Science*, vol. 11, pp. 458-471, 2014.
20. Y. Wang, K. V. Meredith, X. Zhou, P. Chatterjee, Y. Xin, M. Chaos, N. Ren, and S. B. Dorofeev, "Numerical Simulation of Sprinkler Suppression of Rack Storage Fires," *Fire Safety Science*, vol. 11, pp. 1170-1183, 2014.
21. K. V. Meredith, P. Chatterjee, X. Zhou, Y. Wang, and H.-Z. Yu, "Validation of Spray Water Distribution Patterns for the K11.2 Sprinkler in the Presence of a Rack Storage Fire Plume Generator," *Proceedings of the 13th Fire Science and Engineering Conference (INTERFLAM)*, pp. 307-316, 2013.
22. K. V. Meredith, P. Chatterjee, Y. Wang, and Y. Xin, "Simulating Sprinkler Based Rack Storage Fire Suppression under Uniform Water Distribution," *Proceedings of the Seventh International Seminar on Fire & Explosion Hazards*, pp. 511-520, 2013.
23. A. Gupta, K. V. Meredith, G. Agarwal, S. Thumuluru, Y. Xin, M. Chaos, and Y. Wang, "Development of a CFD Model for Large-Scale Rack-Storage Fires of Cartoned Unexpanded Plastic Commodity," in *2nd European Symposium of Fire Safety Science*, Nicosia, Cyprus, 2015.
24. "FM Global Data Sheet 8-9, Storage of Class 1, 2, 3, 4 and Plastic Commodities," FM Global, June 2015.

Appendix A. Fire Chronology

A.1 Test #1

Time (min:s)	Observations
0:00	Ignition was achieved
0:16	Flames reached the top of 1 st tier
0:37	Flames reached the top of 2 nd tier
0:42	Flames reached the top of 3 rd tier
0:47	Flames reached the top of the array
0:53	Flame impingement on the ceiling observed
1:28	First sprinkler activation was observed
1:34	Ceiling temperature over the ignition briefly reached 650°C (1200°F)
1:29 – 1:37	Four additional sprinklers activated
1:47	Flames were reduced to below the 3 rd tier. White smoke descended to the floor partially obscuring the array
2:16	Visibility of the main test array completely obscured by smoke
3:00 – 6:15	Peak ceiling temperatures were below 93°C (200°F)
7:00 – 30:00	Peak ceiling temperatures were below 38°C (100°F)
30:00	Test was terminated

A.2 Test #2

Time (min:s)	Observations
0:00	Ignition was achieved
0:17	Flames reached the top of 1 st tier
0:34	Flames reached the top of 2 nd tier
0:41	Flames reached the top of 3 rd tier
0:46	Flames reached the top of the array
0:59	Flame impingement on the ceiling observed
1:32	First sprinkler activation was observed
1:34	Ceiling temperature over the ignition briefly reached 870°C (1600°F)
1:36 – 1:43	Five additional sprinklers activated
1:49	Flames were reduced to below the third tier. White smoke descended to the floor partially obscuring the array
2:15	Visibility of the main test array completely obscured by smoke
2:40 – 3:30	Peak ceiling temperatures were between 66 and 93°C (150 and 200°F)
4:10 – 30:00	Peak ceiling temperatures were below 38°C (100°F)
30:00	Test was terminated

A.3 Test #3

Time (min:s)	Observations
0:00	Ignition was achieved
0:15	Flames reached the top of 1 st tier
0:34	Flames reached the top of 2 nd tier
0:40	Flames reached the top of 3 rd tier
0:46	Flames reached the top of the array
0:51	Flame impingement on the ceiling observed
1:25	Two sprinkler activations were observed
1:27	Ceiling temperature over the ignition briefly reached 870°C (1600°F)
1:30 – 1:31	Three additional sprinklers activated
1:46	Flames were reduced to below the third tier. White smoke descended to the floor partially obscuring the array
2:02	Visibility of the main test array completely obscured by smoke
2:27 – 2:57	Peak ceiling temperatures were between 66 and 93°C (150 and 200°F)
8:50 – 30:00	Peak ceiling temperatures were below 38°C (100°F)
30:00	Test was terminated

A.4 Test #4

Time (min:s)	Observations
0:00	Ignition was achieved
3:10	Flames reached the top of 1 st tier
4:51	Flames reached the top of 2 nd tier
5:06	Flames reached the top of 3 rd tier
5:18	Flames reached the top of the array
5:47	Flame impingement on the ceiling observed
6:30	First sprinkler activations were observed. Ceiling temperature over the ignition briefly reached 590°C (1100°F)
6:36	Flames were reduced to below the third tier
6:49	Flames visible on east face at the 4 th tier
7:34 – 7:35	Three additional sprinklers activated
7:49 – 7:51	Three additional sprinklers activated including two perimeter activations
8:00	Flames visible on east face above the fourth tier. White smoke descended to the floor partially obscuring the array
8:15 – 15:20	Peak ceiling temperatures were between 230 and 370°C (450 and 700°F)
8:16 – 9:31	Five additional sprinklers activated
8:30	Visibility of the main test array completely obscured by smoke
15:57 – 22:20	Peak ceiling temperatures stayed around at 93°C (200°F)
17:59 – 20:23	Two additional sprinklers activated
25:00 – 30:00	Peak ceiling temperatures increased and stayed constant at ~200°C (400°F)
30:00	Test was terminated

Appendix B. Selected Testing Photographs

B.1 Test #1



Figure B-1: Test #1 array at 1 min after ignition.



Figure B-2: Test #1 array at 1 min 15 s after ignition.



Figure B-3: Test #1 array at 1 min 30 s after ignition.



Figure B-4: Test #1 array at 1 min 45 s after ignition.

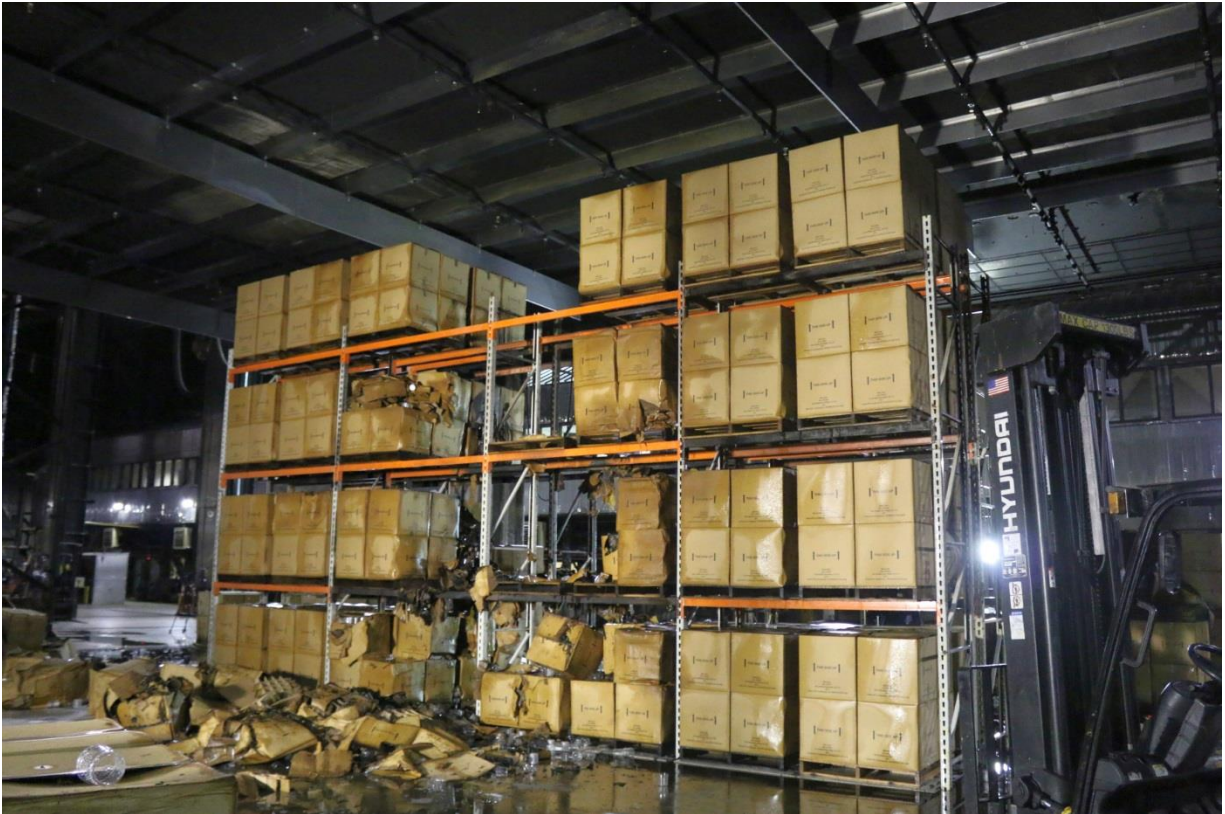


Figure B-5: Test #1 post-test photograph of the east face of the main array showing fire damage.

B.2 Test #2



Figure B-6: Test #2 array at 1 min after ignition.



Figure B-7: Test #2 array at 1 min 15 s after ignition.



Figure B-8: Test #2 array at 1 min 30 s after ignition.



Figure B-9: Test #2 array at 1 min 45 s after ignition.

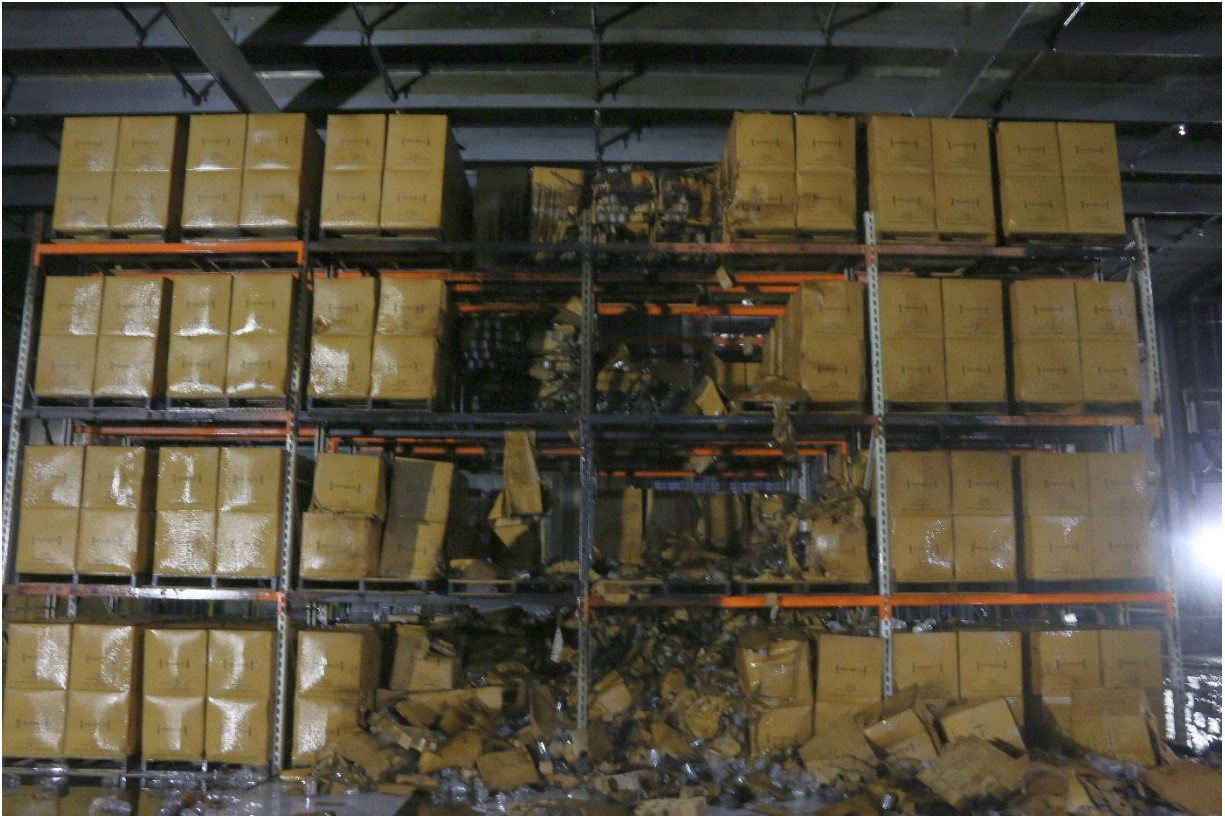


Figure B-10: Test #2 post-test photograph of the east face of the main array showing fire damage.

B.3 Test #3



Figure B-11: Test #3 array at 1 min after ignition.



Figure B-12: Test #3 array at 1 min 15 s after ignition.



Figure B-13: Test #3 array at 1 min 30 s after ignition.



Figure B-14: Test #3 array at 1 min 45 s after ignition.



Figure B-15: Test #3 post-test photograph of the east face of the main array showing fire damage.

B.4 Test #4



Figure B-16: Test #4 array at 5 min after ignition.



Figure B-17: Test #4 array at 6 min after ignition.



Figure B-18: Test #4 array at 7 min after ignition.



Figure B-19: Test #4 array at 8 min after ignition.



Figure B-20: Test #4 post-test photograph of the east face of the main array showing fire damage. Close-up of the damage area is shown in the inset.

Appendix C. FireFOAM Modeling Details

The current study is based on the 2.2.x version of OpenFOAM with a git commit SHA-1 hash ID of 1f35a0ff2a58105bbfce2259a74df47334a0fa53, from Sun Jan 4 14:34:56 2015. The FireFOAM git commit SHA-1 hash ID was 73e0bd30a861d546eb8c23a3f5b3498eb7229fbd, from Wed Sep 28 10:20:31 2016. The case files are archived under the branch in `fireFoam-2.2.x/archives/chatterjeep/obstructedCeilings/2016`.



Printed in USA © 2018 FM Global
All rights reserved.
fmglobal.com/researchreports

FM Insurance Company Limited
1 Windsor Dials, Windsor, Berkshire, SL4 1RS
Authorized by the Prudential Regulation Authority and regulated by the Financial Conduct
Authority and the Prudential Regulation Authority.